



저작자표시-비영리-변경금지 2.0 대한민국

이용자는 아래의 조건을 따르는 경우에 한하여 자유롭게

- 이 저작물을 복제, 배포, 전송, 전시, 공연 및 방송할 수 있습니다.

다음과 같은 조건을 따라야 합니다:



저작자표시. 귀하는 원저작자를 표시하여야 합니다.



비영리. 귀하는 이 저작물을 영리 목적으로 이용할 수 없습니다.



변경금지. 귀하는 이 저작물을 개작, 변형 또는 가공할 수 없습니다.

- 귀하는, 이 저작물의 재이용이나 배포의 경우, 이 저작물에 적용된 이용허락조건을 명확하게 나타내어야 합니다.
- 저작권자로부터 별도의 허가를 받으면 이러한 조건들은 적용되지 않습니다.

저작권법에 따른 이용자의 권리는 위의 내용에 의하여 영향을 받지 않습니다.

이것은 [이용허락규약\(Legal Code\)](#)을 이해하기 쉽게 요약한 것입니다.

[Disclaimer](#)

Master's Thesis of Engineering

**Material Properties of
Ultra-High Performance Concrete with
Carbon Nanotubes and Ozone Water**

오존수와 탄소나노튜브를 이용하여
제작한 초고성능 콘크리트의 재료특성 연구

February 2021

Graduate School of Engineering
Seoul National University
Architecture and Architectural Engineering

Dongwook Kim

Material Properties of Ultra-High Performance Concrete with Carbon Nanotubes and Ozone Water

Advisor: Sung-Gul Hong

Submitting a Master's thesis of
Architecture and Architectural Engineering

October 2020

Graduate School of Engineering
Seoul National University
Architecture and Architectural Engineering

Dongwook Kim

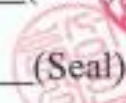
Confirming the Master's thesis written by
Dongwook Kim

December 2020

Chair _____ Hong-Gun Park _____ (Seal)

Vice Chair _____ Sung-Gul Hong _____ (Seal)

Examiner _____ Cheol-Ho Lee _____ (Seal)



Abstract

Ozone water is active in its own chemical reaction and have an effect in dispersing Carbon Nanotubes (CNTs). Due to the dispersion, CNTs can give additional self-detection capability of ultra-high performance concrete (UHPC) and improve mechanical properties. Focusing on these performance, this paper aimed to establish the overall material properties of O3-UHPC and UHPC produced by adding CNTs.

In order to achieve the purpose of this study, changed physical and chemical properties of O3-UHPC made from ozone water at specific concentrations were identified using specially designed ozone water generators. and machine learning techniques were applied to the results of the compressive strength experiments to analyze the compression strength trends of O3-UHPC according to the concentration of ozone water.

As a result, the compression strength test confirmed that if the concentration of ozone water exceeds 0.55 g/ml, compressive strength of UHPC may have no effect or reduced. Also, O3-UHPC have slightly more fluidity when concentration of ozone is below than 0.03 g/ml.

As shown by the hydration reaction test, X-ray diffraction (XRD) and Thermogravimetric analysis (TG) results, O3-UHPC specimens that have been over a few minutes can be confirmed that the effects of ozone water have disappeared and have almost the same chemical composition as general UHPC.

In case of CNTs, mechanical and chemical properties of each UHPC-CNT composite produced by mixing a certain percentage of CNTs are summarized, and suitable CNTs mixing rate were proposed to facilitate the performance of the UHPC-CNT composite and on-site construction ability.

Result of applying machine learning technique to the experimental results of compressive strength of UHPC mixed with CNTs, it can be confirmed that the physical performance of composite materials significantly decreases when CNTs is mixed with more than 0.1% of cement weight. The chemical composition of the composite material also shows that the properties of the cementitious material do not work well if CNT is mixed above a certain concentration.

Lastly, to ensure the positive effects of ozone water and CNTs on UHPC at the same time, experiments were conducted by setting up additional groups of experiments to make a difference between the concentration of ozone and the rate of CNTs.

As a result of compressive strength mapping of UHPC produced by setting the concentration of ozone water and CNTs mixing ratio as variables in three dimensions, if the concentration of ozone water is 0.4 g/ml, and CNTs mixing ratio is 0.2% by weight of cement, the compressive strength resulting in higher performance than using either CNTs or ozone water.

This suggests that when UHPC composites are produced at a rate of specific ozone concentrations and CNTs with steam curing, it can give a variety of additional performance, including electromagnetic shielding by CNTs, while expressing similar mechanical performance than general UHPC.

Keyword : Ultra-high performance concrete (UHPC), Ozone Water, O₃-UHPC, Machine Learning, Carbon Nanotubes, UHPC-CNT Composite

Student Number : 2019-22286

Contents

Abstract.....	i
Contents.....	iii
List of Tables.....	vi
List of Figures.....	vii
List of Abbreviations.....	x
Chapter 1. Introduction.....	1
1.1 General.....	1
1.1.1 The latest issues of Ultra-High Performance concrete.....	1
1.1.2 Ozone Water.....	3
1.1.3 Carbon Nanotubes.....	4
1.2 Scope and Objectives.....	6
1.3 Organization of the Dissertation.....	8
Chapter 2. Preliminary Study.....	10
2.1 Literature Review.....	10
2.1.1 Development and Application of UHPC.....	10
2.1.2 Ozone Treatment Technology and Effect.....	15
2.1.3 Compatibility between UHPC and CNTs.....	19
2.2 Materials used in this study.....	21

Contents

2.3 Microstructure analysis used in this study.....	22
2.3.1 Isothermal Calorimetry.....	22
2.3.2 X-ray Diffraction (XRD) Method.....	23
2.3.3 Thermogravimetric (TG) Analysis.....	24
2.4 Machine learning techniques in this study.....	25
2.4.1 Polynomial Regression.....	27
2.4.2 <i>k</i> -Nearest Neighbor (<i>k</i> -NN) Regression.....	28
2.4.3 Decision Tree.....	30

Chapter 3. Effect of Ozone Water on UHPC Performance. **32**

3.1 Introduction.....	33
3.2 Parameters of Study.....	33
3.3 Material Properties.....	35
3.4 Fabrication of Specimens.....	37
3.5 Test Set-up and Instrumentation.....	39
3.5.1 Test Conditions.....	39
3.5.2 Compressive Strength Test.....	39
3.5.3 Flow Test.....	40
3.5.4 Hydration Reaction Test.....	41
3.5.5 X-ray Diffraction (XRD).....	42
3.5.6 Thermogravimetric (TG) Analysis.....	42
3.6 Test Results.....	43
3.6.1 Compressive Strength.....	43
3.6.1.1 Processed Data by Machine Learning.....	44
3.6.2 Cement Paste Fluidity	52
3.6.3 Hydration Reaction at Initial Period.....	54
3.6.4 Chemical Component Analysis.....	56
3.6.4.1 XRD Results.....	57
3.6.4.2 TG Analysis.....	58
3.7 Summary.....	59

Chapter 4. Advisable UHPC-CNT Composite material Production Method	60
4.1 Introduction.....	61
4.2 Parameters of Study.....	61
4.3 Material Properties.....	62
4.4 Fabrication of Specimens.....	63
4.5 Test Set-up and Instrumentation.....	65
4.5.1 Test Conditions.....	65
4.5.2 Compressive Strength Test.....	65
4.5.3 Flow Test.....	66
4.5.4 Hydration Reaction Test.....	66
4.5.5 X-ray Diffraction (XRD), Thermogravimetric (TG) Analysis.....	66
4.6 Test Results.....	67
4.6.1 Compressive Strength.....	67
4.6.1.1 Processed Data by Machine Learning.....	68
4.6.2 Cement Paste Fluidity	83
4.6.3 Hydration Reaction at Initial Period.....	84
4.6.4 Chemical Component Analysis.....	87
4.6.4.1 XRD Results.....	87
4.6.4.2 TG Analysis.....	88
4.7 Summary.....	90
 Chapter 5. Concluding Remarks.....	 91
 References.....	 94
 Appendix.....	 97
 초 록.....	 122

List of Tables

Table 1-1. Two possible UHPC mixture proportions by mass.....	2
Table 2-1. Mixture proportions by weight with performance.....	12
Table 2-2. Material properties of OPC and white cement.....	12
Table 2-3. Mixture proportion of UHPC with changes in QS amount.....	13
Table 2-4. Resistivity and compressive strength of 3 experimental group.....	18
Table 2-5. Mechanical and chemical properties of white cement.....	21
Table 2-6. Ranges of input features of concrete component (variables).....	26
Table 3-1. Properties of ozone water generator.....	35
Table 3-2. Mix proportion of each experimental group.....	37
Table 3-3. Number of compressive strength test data.....	39
Table 3-4. 2 θ angle of cement compounds by XRD analysis.....	42
Table 3-5. Number of additional compressive strength data.....	44
Table 3-6. Flow test result and comparison with general UHPC.....	53
Table 3-7. Numerical values from heat curve of experimental groups.....	56
Table 4-1. Properties of multi-wall CNTs.....	63
Table 4-2. Mix proportion of UHPC-CNT composite experimental group.....	63
Table 4-3. Number of compressive strength test data.....	65
Table 4-4. Flow test result and comparison with general UHPC.....	83
Table 4-5. Numerical values from heat curve of experimental groups.....	86

List of Figures

Fig. 1-1. Typical composition of UHPC by Ductal®.....	1
Fig. 1-2. Water treatment plant exposed to ozone environment.....	3
Fig. 1-3. Schematic representation of SWCNT and MWCNT.....	4
Fig. 1-4. Schematic representation of EMI shielding mechanism.....	5
Fig. 2-1. Trend of compressive strength of UHPC according to water-cement ratio (C : SF : SP = 1: 0.25 : 0.016).....	11
Fig. 2-2. CO ₂ emission of the UHPC with different content of rock dust and compressive at 28 days.....	14
Fig. 2-3. Experimental settings for absorption breakthrough and ozonated water regeneration of activated carbon bed.....	15
Fig. 2-4. TEM micrographs of (a) original CNTs, (b) Ozone treated CNTs with 30 minutes.....	17
Fig. 2-5. Experimental setup for mechanical strength test.....	18
Fig. 2-6. Schematic diagram of self-healing by electronic device...	19
Fig. 2-7. Optical microscope images of (a) damaged, (b) healed sample.....	20
Fig. 2-8. Typical result of cement isothermal calorimetry result.....	22
Fig. 2-9. Schematic representation of X-ray diffraction by Bragg's law.....	23
Fig. 2-10. Scatter plots target versus input variables.....	26
Fig. 2-11. Example of polynomial regression.....	27
Fig. 2-12. Example of k-NN Regression.....	29
Fig. 2-13. Example of model prediction by decision tree regression.	31

List of Figures

Fig. 3-1. Graphical abstract of chapter 3.....	34
Fig. 3-2. Ozone water generator.....	35
Fig. 3-3. Schematic representation of ozone water production.....	36
Fig. 3-4. Experiment samples after curing.....	37
Fig. 3-5. Fabrication and specimens of hydration reaction test.....	38
Fig. 3-6. Experiment samples for XRD, TG analysis.....	38
Fig. 3-7. Schematic representation of flow test instruments.....	40
Fig. 3-8. Verification of reproducibility of hydration reaction test.....	41
Fig. 3-9. Mean compressive strength of each experimental groups.....	44
Fig. 3-10. Distribution of compressive strength of O ₃ -UHPC for each experimental group.....	45
Fig. 3-11. Polynomial regression results of O ₃ -UHPC compressive strength.....	46
Fig. 3-12. k-NN regression results of O ₃ -UHPC compressive strength.....	48
Fig. 3-13. Decision tree results of O ₃ -UHPC compressive strength..	50
Fig. 3-14. Results of flow test of general, O ₃ -UHPC.....	53
Fig. 3-15. Cumulative heat and heat flow curve comparison (O ₃)....	54
Fig. 3-16. XRD Results of hydration suspended samples after 28 days..	57
Fig. 3-17. TG analysis of hydration suspended samples after 28 days..	58
Fig. 4-1. Graphical abstract of chapter 4.....	62
Fig. 4-2. Powder type multi-wall CNTs.....	62
Fig. 4-3. Experiment samples after curing.....	64
Fig. 4-4. Mean compressive strength of each experimental groups...	68

Fig. 4-5. Distribution of compressive strength data of each experimental group..... 69

Fig. 4-6. Polynomial regression results of UHPC-CNT composite compressive strength..... 71

Fig. 4-7. Regression planes of O3-CNT composite compressive strength..... 73

Fig. 4-8. Each regression plane and variable(theta) for separated experimental data..... 74

Fig. 4-9. *k*-NN regression results of UHPC-CNT composite compressive strength..... 79

Fig. 4-10. Decision tree results of UHPC-CNT composite..... 81

Fig. 4-11. Results of flow test of general, UHPC-CNT composite... 84

Fig. 4-12. Cumulative heat and heat flow curve comparison (CNTs, O3-CNT)..... 85

Fig. 4-13. XRD Results of hydration suspended samples after 28 days..... 87

Fig. 4-14. TG analysis of hydration suspended samples after 1 day.. 89

List of Abbreviations

ANN	Artificial Neural Network
ASTM	American Society for Testing and Materials
C	Cement
CNTs	Carbon Nanotubes
C.S	Compressive Strength
C-S-H	Calcium-Silicate-Hydrate
C₃A	Tricalcium Aluminate
C₂S	Dicalcium Silicate (Belite)
C₃S	Tricalcium Silicate (Alite)
C₄AF	Tetra Calcium Aluminoferrite
DTG	Derivative Thermogravimetry
EMI	Electromagnetic Interference
FA	Fly Ash
Fig.	Figure
GAC	Granular Activated Carbon
<i>k</i>-NN	<i>k</i> -Nearest Neighbor
ML	Machine Learning
MSE	Mean Squared Error
MWCNT	Multi-walled Carbon Nanotubes
NOM	Natural Organic Matters
OPC	Original Portland Cement
O₃-UHPC	Ozone-UHPC
PCE	Poly-carboxylic Ether
QS	Quartz Sand
RD	Rock Dust
RH	Relative Humidity
SF	Silica Fume

List of Abbreviations

SP	Superplasticizer
SWCNT	Single-walled Carbon Nanotubes
TEM	Transmission electron microscopy
TG	Thermogravimetric
UHPC	Ultra-High Performance Concrete
UFPC	Ultra-high Performance Fiber Concrete
UTM	Universal Testing Machine
XRD	X-ray Diffraction

Chapter 1. Introduction

1.1 General

To this day, active research is being carried out on the structure and materials that make up the building to ensure the safety and performance of the building economically. In particular, high-performance concrete with several times higher strength and ductility is frequently used by using less materials than ordinary concrete to reduce construction and its cost of high-rise buildings. Therefore, research and commercialization of ultra-high-performance concrete(UHPC) made using silica fume and silica powder is being carried out instead of thick aggregate, research on the mixing ratio of materials used in making UHPC, and development of composite materials produced by adding various compounds to UHPC.

1.1.1 The latest issues of ultra-high performance concrete

The UHPC developed in the late 1990s was studied for the purpose of improving its strength over ordinary concrete, and in early 2000, it was actively used in infrastructure construction such as bridge construction.

Since then, studies has been conducted to reduce production cost by finely adjusting the mixing ratio of materials used in UHPC production, while successfully improving the mechanical properties of UHPC by inventing UHPFC with steel fiber to secure tensile strength and ductile behavior in addition to the strength [1].

Material	lb/yd³	kg/m³	Percentage by Weight
Portland Cement	1,200	712	28.5
Fine Sand	1,720	1,020	40.8
Silica Fume	390	231	9.3
Ground Quartz	355	211	8.4
HRWR	51.8	30.7	1.2
Accelerator	50.5	30.0	1.2
Steel Fibers	263	156	6.2
Water	184	109	4.4

Figure 1-1. Typical composition of Ductal®

The materials used for the manufacture and production of UHPC do not differ much from the materials required to manufacture general concrete. However, adding silica powder and silica fume with fine-sized particles reduces the empty space of discontinuous pore structures that depend more on the behavior of fine materials, enabling high structural performance. **Table 1-1** describes the two representative mixture ratios for UHPC and can see how mass ratios can vary depending on particle size.

Table 1-1. Two possible UHPC mixture proportions by mass

UHPC components	Mixture proportion 1	Mixture proportion 2
Cement	1	1
Silica fume	0.325	0.389
Sand	1.432	0.967
Quartz powder / silica flour	0.300	0.277
High-range water-reducing admixture	0.027	0.017
Water	0.280	0.208
Steel fibers	0.200	0.310

In addition, the UHPC mixing process, as well as the materials needed to make UHPC, should be considered important. Unlike general concrete production processes, UHPC requires the injection of additional mixed energy to disperse the mixture through the mixing process and overcome the low internal mixing action, thereby improving the physical properties of UHPC by replacing the thick aggregates responsible for the strength of ordinary concrete. Through this mixture proportion and mixing process, UHPC cement paste can be obtained with ideal workability while maintaining the original strength of UHPC [2].

Ch. 1. Introduction

1.1.2. Ozone Water

Water, which is an essential element for concrete fabrication as well as UHPC, can change the mechanical properties of concrete produced according to the degree of composition. Due to this effect, various functional waters using chemical compounds or electrolysis in water are being invented and studied. Among them, ozone water, which is effective in purifying water quality, is being commercialized in early 2000 [3].

In facility construction, studies are currently underway on the production of high-water treatment concrete structures through ozone treatment or concrete surfaces with ozone treatment due to the disinfection performance of ozone. This is part of an advanced water purification research process using ozone instead of conventional methods of treating water purification with chlorine sterilization, and the main purpose is to prevent erosion of waterproof or corrosion-resistant materials applied to concrete surfaces [4].

However, since the above study uses panels or chemicals that are highly resistant to ozone rather than securing corrosion resistance by changing the characteristics of concrete structures that make up buildings, no studies have been conducted on concrete produced using ozone water itself. Therefore, although the analysis and study of concrete according to the water cement ratio is being conducted in the study on the relationship between UHPC and ozone water, there is currently a lack of research on UHPC properties using the ozone water itself.



Figure 1-2. Water treatment plant exposed to ozone environment

1.1.3. Carbon Nanotubes

Carbon nanotubes(CNTs) refer to the isotopes of carbon with cylindrical or spiral structures, and are nanomaterials used in various fields such as nanotechnology, electrical and materials engineering to date, starting with the discovery of fullerene, the isotope of carbon, in the late 20th century [5].

CNTs are commonly referred to as single-walled carbon nanotubes (SWCNT) and multi-walled carbon nanotubes (MWCNT). SWCNT are one of the allotropes of carbon, substance in the middle of fullerene and flat graphene. Also, it can be idealized by a cutout of a two-dimensional hexagonal lattice of carbon atoms rolled along one of the Bravais lattice vectors of the hexagonal lattice to form an empty cylinder. Similarly, MWCNTs consisting of nested single-wall carbon nanotubes weakly bound together by van der Waals interactions in a tree ring-like structure [6-7].

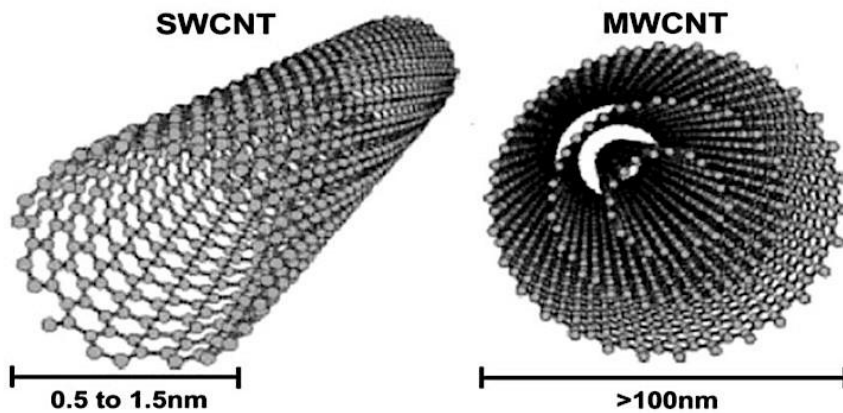


Figure 1-3. Schematic representation of SWCNT and MWCNT

Ch. 1. Introduction

CNTs show several times higher thermal conductivity than copper with superior thermal conductivity and exert high mechanical strength due to shared bonds formed between carbon atoms. Due to these properties, high-strength materials such as nano-epoxy resin and composite polymer fiber made by chemically combining carbon nanotubes can be secured, and are used in various plastic products such as wind turbines and marine paints [8].

In particular, MWCNTs is a nanomaterial capable of absorbing microwave frequencies detected by the radar, so painting them on the surface of the aircraft can reduce the cross-sectional area detected by the radar. In order to further apply these CNTs for electromagnetic interference (EMI) shielding functions to buildings, the addition of CNTs to UHPC in the field of building materials can be used as an effective conductive filling material for developing conductive cement materials [9].

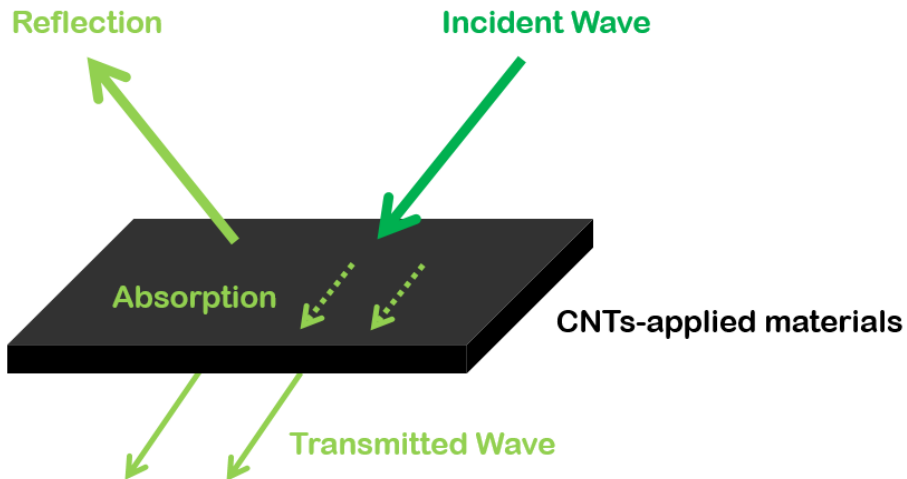


Figure 1-4. Schematic representation of EMI shielding mechanism

Therefore, this paper confirmed changes in mechanical properties of UHPC-CNT composite by varying the mixing rate and check physical behavior of cementitious material by applying variables of ozone water concentration and mixing rate of CNTs simultaneously to identify correlation with ozone water and CNTs.

1.2 Scope and Objectives

The purpose of this research can be divided into two objectives, and main purpose is to identify the effects of UHPC and UHPC-based composite materials on ozone water.

1. Comparing the physical and chemical properties of ozone-UHPC (O3-UHPC) and general UHPC by functional water produced by dissolved ozone. The main purpose of this comparison is to identify and differentiate the changed properties of UHPC produced with ozone water and to establish the overall material characteristics from the production to usability.

When carrying out this research, it is necessary to pay attention about properties of ozone water itself. the longer the temperature of the cement paste increases, the vaporization of ozone dissolved in the mixed water may cause O3-UHPC to become the same as general UHPC. To prevent this, the methods of producing general UHPC and O3-UHPC are analyzed by subdividing into two processes, taking into account the degree of mixing of ingredients mixed together.

In addition, use machine learning techniques to analyze big data of compressive strength of UHPC and O3-UHPC to predict O3-UHPC according to the concentration of ozone water to identify the period (concentration) where performance is maximized.

Ch. 1. Introduction

2. Proposing an effective CNTs proportion of UHPC-CNT composite produced by mixing powder-type MWCNTs in UHPC. A number of studies have mainly aimed at identifying chemical or physical properties of the UHPC-CNT composite produced by mixing a certain percentage of CNTs into the UHPC. But this study further analyzed the properties of UHPC-CNT composite produced by dissolving ozone into them using machine learning methods.

Through this comprehensively analyze, the distribution of the compressive strength of composite materials according to ozone concentration and CNTs mixing rate determines how the ozone water and CNTs mixing rate affect composite materials.

1.3 Organization of the Dissertation

This paper dealt with various experimental results, including machine learning technique, to identify the material properties of O3-UHPC and UHPC-CNT composite materials. In addition, the focus of this paper is introducing the overall material properties of O3-UHPC and UHPC-CNT composite and the process and results of checking the performance changes of general UHPCs are introduced in the following order.

Chapter 2 contains preliminary research on the previous UHPC-related material test results, as well as the study of ozone treatment technology and applicability of UHPC and CNTs. Based on information about the materials used to produce the samples used in this study, this paper briefly mentioned how the XRD and TG tests were planned and carried out, and finally introduced the three machine learning techniques used to analyze the results of the compression strength experiment.

Starting with **Chapter 3**, derive the results of physical and chemical experiments of O3-UHPC. In particular, machine running is used to predict the compressive strength of O3-UHPC according to ozone concentrations in the results of the compression strength test, which has a large amount of data. And after the flow test, hydration reaction test, XRD and TG experiment, the results obtained are schemed and analyzed to identify the overall material characteristics of O3-UHPC.

Ch. 1. Introduction

In **Chapter 4**, experimental data are collected and schematized equally in the results of experiments with UHPC-CNT composite as shown in Chapter 3, to identify how the ozone concentration of the mixed water used in the composite materials affected.

Chapter 5 summarizes the material properties of O3-UHPC and UHPC-CNT composite introduced in Chapter 3 and 4, and concludes the paper by mentioning the limitations and potential for development of the research carried out in each chapter.

Chapter 2. Preliminary Study

2.1 Literature Review

The contents covered in this chapter introduces the research cases referenced for writing this paper, and summarizes some of the research results contained in this paper among the highlights of each research field. Starting with the UHPC development and application, this paper handled material properties of building materials added with CNTs and method and application case of ozone treatment technology. In addition, XRD, TG tests were briefly described to analyze the microstructure of the samples and machine learning techniques were introduced to analyze the results of the compression strength tests,

2.1.1 Development and Application of UHPC

UHPC can exert high strength without aggregates is because of the proper mix of cement, silica fume and powder. JJ Park et al. reported fixed silica fume ratio and reduced filling powder can reduce water-cement ratio and increase compressive strength. The UHPC currently manufactured can basically use 180 MPa if it contains steel fiber by contain certain ratio and 150 MPa only made by cement paste without steel fiber. **Figure 2-1** shows the change of compressive strengths with various water-cement ratio when other component (cement(C), silica fume(SF), superplasticizer(SP)) ratios are fixed. [10]

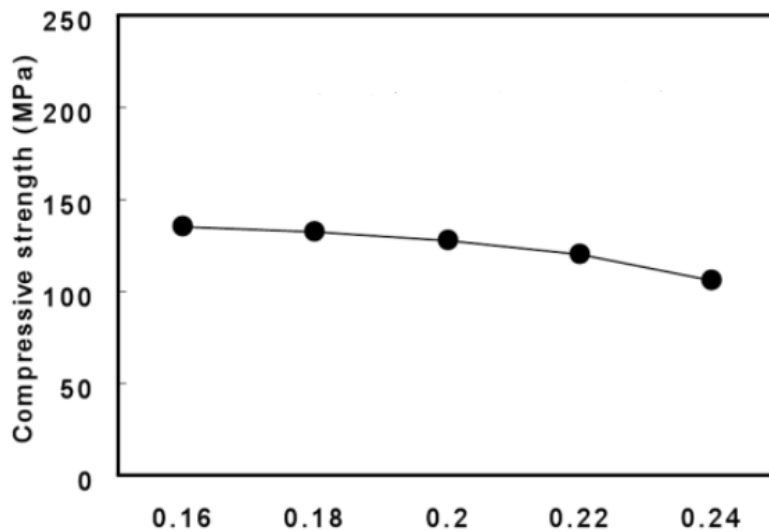


Figure 2-1. Trend of compressive strength of UHPC according to water-cement ratio (C : SF : SP = 1 : 0.25 : 0.016)

The result of compressive strength test showed that compression strength increases as the water cement ratio decreases. Through this, using filling powder or fine component should be considered for increase the intensity of UHPC. Therefore, fine silica fume and silica powder were used to exert sufficient compressive strength by cement paste without steel fiber and white cement was used to make UHPC samples instead of plain cement to increase productivity at the same time.

S EI-Tawil et al. compared the compression and tensile strength of UHPC specimens made from original Portland cement(OPC) and white cement. Cube specimens were poured at once into 50.8mm cubed molds. Mix table of the UHPC component used with the cube specimens manufactured for the compression strength (C.S) test result and OPC, white cement properties as follows [11].

Table 2-1. Mixture proportions by weight with performance

Specimen	White Cement(W) / OPC(P)	Silica fume	Silica powder	C.S (MPa)
W-25-25	1	0.25	0.25	192.7
W-25-15			0.15	192.7
W-25-00			0.00	173.8
P-25-25			0.25	190.0
P-25-15			0.15	183.1
P-25-00			0.00	174

Table 2-2. Material properties of OPC and white cement

Type	C_3S (%)	C_2S (%)	C_3A (%)	C_4AF (%)	Blaine(m^2/kg)
OPC	74	13	5	1	395
White Cement	59	17	4	15	430

As shown in **Table 2-1**, it is possible to see the difference in compression strength by type of cement as well as the mixing ratio of silica powder, and UHPC samples produced using white cement displayed higher compression strength than OPC. Also, the difference of cement compounds between the OPC and white cement which were used in compressive strength test is shown in **Table 2-2**. To reduce colouring effect that occurs in OPC, limestone with relatively low chromium, manganese and iron ratios are used. This confirms that the hydration of white cement is slightly slower than OPC but can increase its strength slightly.

Ch. 2. Preliminary Study

In a similar direction, studies are being conducted to produce UHPC with eco-friendly materials based on the replacement of existing components with other materials to improve the performance.

R Yang et al. use quartz sand (QS) made by recycled rock to utilize UHPC production and reduce environmental risk. At present, QS are normally used in UHPC as aggregates, which account for 40 ~ 65% in total volume. However, due to the relatively high price and environmental problems of production, Research on QS has recently been underway to reduce production costs and environment burden. Therefore, they replaced some quantities of QS with rock dust and then produced UHPC to compare their respective compressive strength of each, and the result is as follows [12].

Table 2-3. Mixture proportions of UHPC with changes in QS amount

Mixture	C	FA	SF	QS	RD	W	PCE
QS100	780	220	190	1030	0	205	50
QS80				824	206		
QS60				618	412		
QS40				412	618		
QS20				206	824		
QS0				0	1030		

(C: cement, FA: fly ash, SF: silica fume, QS: quartz sand, RD: rock dust, W: water, PCE : water-reducer of polycarboxylic-ether based)

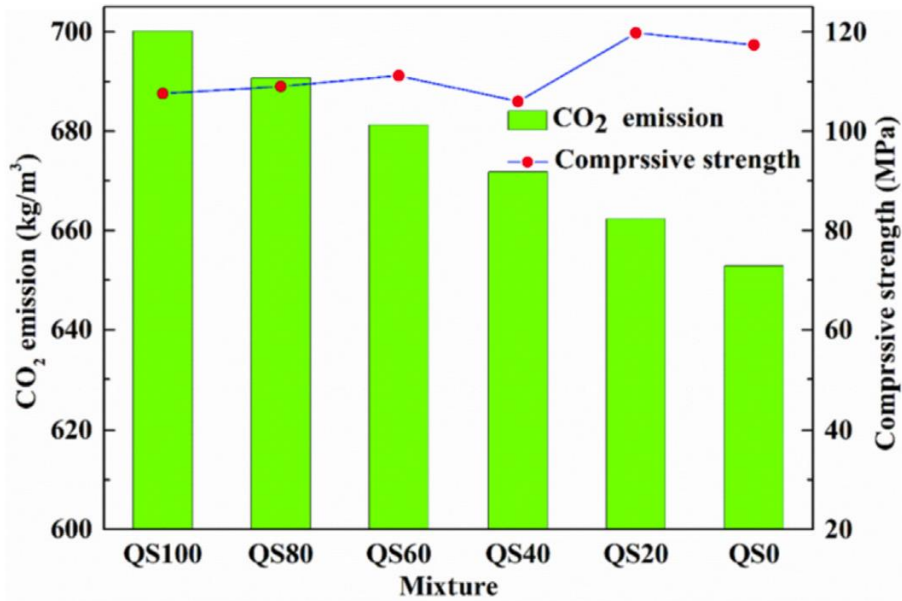


Figure 2-2. CO₂ emission of the UHPC with different content of rock dust and compressive strength at 28 days.

(QS100: reference; QS80, QS60, QS40, QS20 and QS0: experimental group).

As shown in **Figure 2-2**, by replacing part or all of QS with rock dust (RD), it can be confirmed that the UHPC's production unit price can be reduced and the compressive strength can be improved at the same time. Recently, over 10 million tons of rock dust are created annually in China. As a kind of non-biodegradable solid waste, such a lot of rock dust would timelessly occupy a large area of land for processing and seriously endangering the ecology, hydrology form and fertility of soil. Also, air-suspended portion can arouse skin disorders, respiratory and visual. This can be used actively in UHPC production to solve overall environmental problems.

Thus, this paper aims to promote the improvement of UHPC-related architectural technology as the research related to partially replaced UHPC component and environmental friendly UHPC as mentioned.

Ch. 2. Preliminary Study

2.1.2 Ozone Treatment Technology and Effect

Gas-state ozone can block ultraviolet rays when present in molecular states in the stratosphere, and ozone present on the ground is usually used to disinfect bacteria and viruses present in the material by melting or surface treatment. Taking this effect into account, representative technologies related to ozone can be classified into two main categories.

On ozone water, research is being conducted on improving the process of adsorption of activated carbon during the water purification process by oxidizing ozone water. During the water treatment process, the active carbon adsorption process is responsible for removing organic substances that have not been removed by biological treatment, and recently, ozone water is used to purify water with high concentrations of odor-causing or natural organic matters (NOM). To identify the change in adsorption efficiency of activated carbon due to contact with ozone water, adsorption failure experiment and on-site regeneration experiment using ozone water were performed, and the experimental process and device composition were shown in **Figure 2-3**.

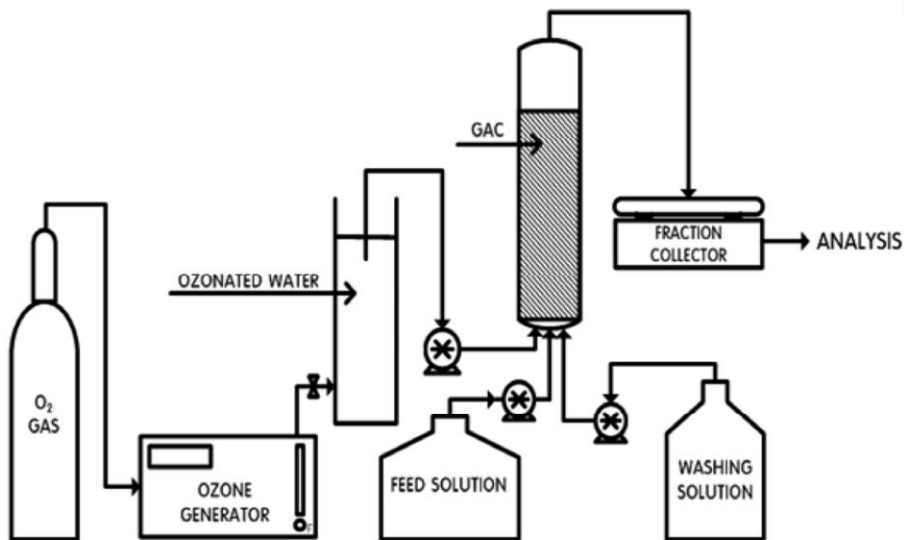
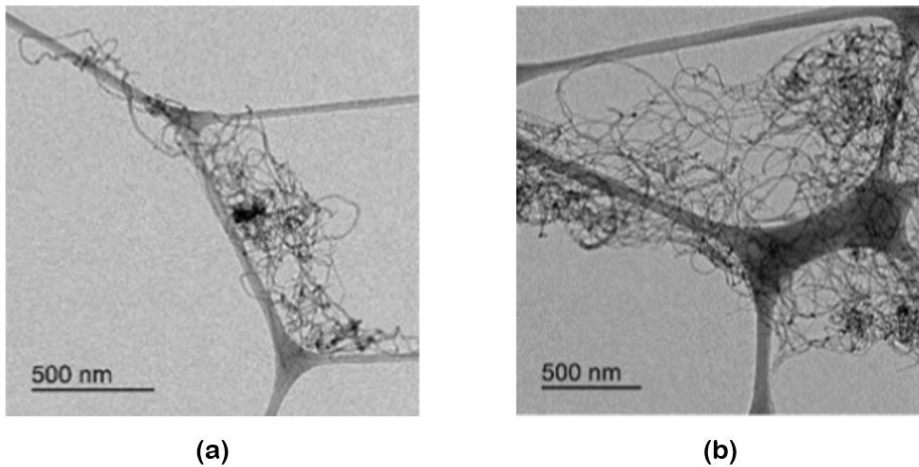


Figure 2-3. Experimental settings for adsorption breakthrough and ozonated water regeneration of activated carbon bed.
(GAC: granular activated carbon)

The above study shows that proper control of the time spent in contact with activated carbon and ozone water in the water treatment process can reduce the loss of activated carbon compared to conventional charcoal regeneration methods. In other words, ozone water can be used to operate the water treatment process economically [13].

Similarly, studies are being conducted to improve the mechanical strength and electrical conductivity of the cement paste mixture mixed with CNT using gas-state ozone. B. Del Moral et al. treated ozone gas on the surface of carbon nanotubes to determine the mechanical properties of cement paste containing CNT by ozone and its effect on deformation detection functions.

When making concrete by mixing carbon nanotubes with cement, the mechanical and electrical properties of concrete are improved but tend to be concentrated due to hydrophobic properties, which can produce uneven performance of concrete. To prevent this, the surface of carbon nanotubes can be ozone-treated to reduce the hydrophobic nature of carbon nanotubes. Ozone treatment on carbon nanotubes in this prior study, a quantity of 1 g CNTs were subjected to an O₃ atmosphere for different times (30 and 60 min) in a rotating reactor using an air flow of 0.5 L/min and 95% intensity. The surface modification was carried out at room temperature and at 160 °C. The TEM microscope picture comparing the resulting CNTs concentration changes is shown in **Figure 2-4**.



**Figure 2-4. TEM micrographs of (a) original CNTs,
(b) Ozone treated CNTs with 30 minutes.**

The left TEM micrograph in **Figure 2-4** shows that the CNTs are agglomerated with each other after mixing CNTs in cement matrix, while the right TEM micrograph shows that the CNTs are dispersed due to ozone treatment on the CNTs surface. This shows that ozone treatment can uniformly demonstrate the performance of concrete made of CNT mixed cement paste.

The above conclusions can also be identified by the variation in the compressive strength and electrical resistance of the cement complex mixed with CNT. The reason for mixing CNTs into cement matrix is not only to improve the ductility, tensile and flexural strength of concrete but also to monitor internal structural conditions caused by piezoelectric resistance. In this prior study, compressive strength test and the electrical resistance measurement and deformation detection test were performed as shown in **figure 2-5**, and results are shown in **Table 2-4**. Compressive strength test was conducted according to EN 196-1:2005.

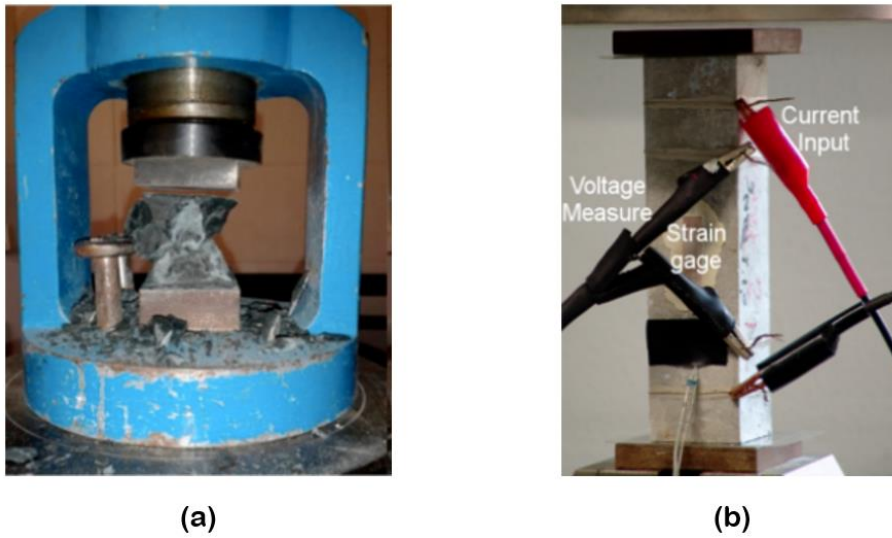


Figure 2-5. Experimental setup for mechanical strength test
 ((a) Compressive strength, (b) Electrical resistivity and strain sensing tests.)

Table 2-4. Resistivity and compressive strength of 3 experimental group

CNT (%) - Treatment	Resistivity (Ω -cm) 28 Days	Resistivity (Ω -cm) 90 Days	Compressive Strength (MPa) 28 Days
0% - N/A	1716	40,107	51.0
1% - None	1513	29,103	45.0
1% - Ozone (30 min)	1414	12,696	51.5

(Cement paste cured for 28 days at 100% RH, and then until 90 days at 60% RH.)

Table 2-4 indicates ozone treatment can reduce resistivity of cement paste mixed with CNTs. While the compressive strength of a CNT mixed without ozone treatment was lower than that of the control group, ozone-treated subjects can be seen to perform the physical performance of the test without loss of strength. Consequently, Ozone treatment technology allows the performance of building materials mixed with CNT to be displayed without loss [14].

Ch. 2. Preliminary Study

Therefore, the purpose of this paper is identifying the generality of O3-UHPC by using ozone dissolved in mixed water and checking the changed material properties.

2.1.3 Compatibility between UHPC and CNTs

As mentioned in previous chapter, UHPC composed of fine materials to increase packing density. For this reason, the mechanical properties of UHPC is improved, but hot steam curing is essential, and is vulnerable to explosive spalling and self-shrinkage [15].

Research that uses CNT to give self-detection or self-recovery performance to micro-structure is still active, and examples are that carbon nanotubes are mixed into polyurethane composite to improve mechanical properties of the composite, as well as to detect cracks and treat damaged parts on their own. The schematic diagram and the results of self-recovery are as follows,

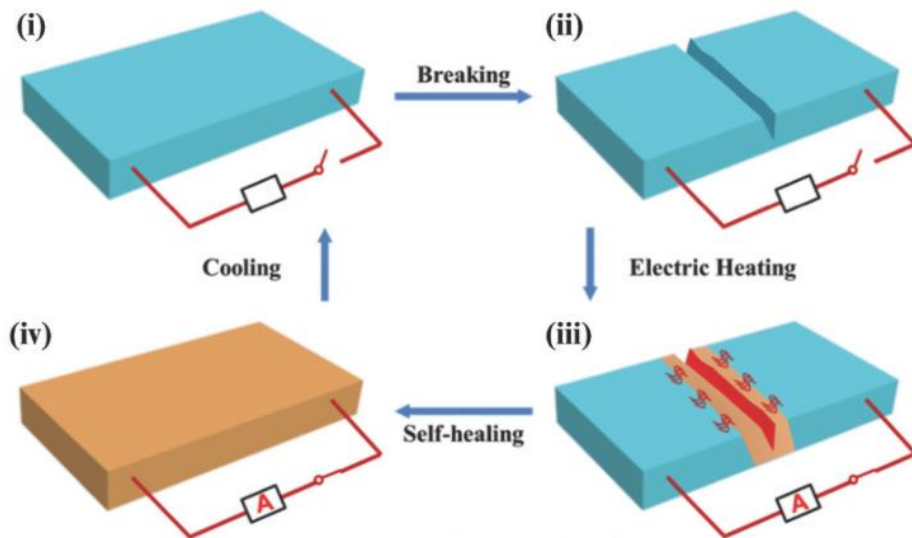


Figure 2-6. Schematic diagram of self-healing by electronic device

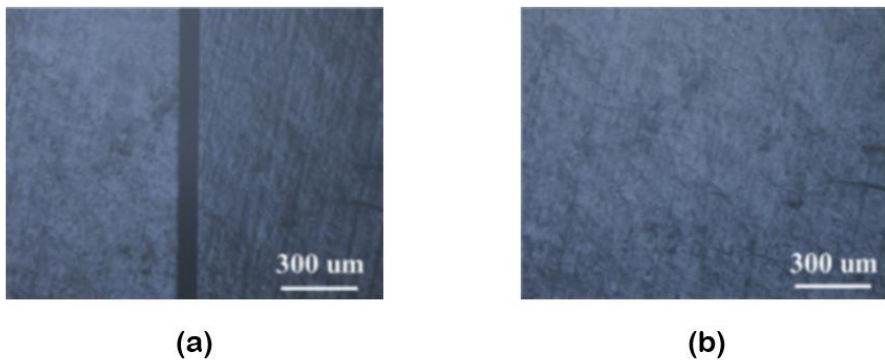


Figure 2-7. Optical microscope images of (a) damaged, (b) healed sample

In the same context, mixing CNT and UHPC for self-recovery can prevent the collapse of microstructure. Specifically, when CNTs mixed in cement paste and water, it partially absorbs on the surfaces of CNTs evaporates. Due to this state, CNTs act as a support for the micro-collapse occurring inside the UHPC, enabling self-recovery of the internal structure [16].

According to M jung et al, it can be found that the UHPC autogenous shrinkage could be reduced if the dispersion was well achieved after the CNT was mixed with UHPC. Also, dispersed CNTs can physically interconnect hydration products (i.e., calcium silicate hydrate) and fill the pore structure of UHPC. By this reaction, CNTs could stiffen the matrix and densified pore solution, it makes UHPC could reduce autogenous shrinkage [16].

Although mixing CNTs in UHPC can gain the advantages mentioned above, it is not only ineffective but also degrade UHPC's own performance if proper dispersion of CNTs is not achieved. Therefore, the study on how to disperse CNTs in the compound is currently underway, and in this paper, the importance of CNT dispersion is to be highlighted by comparing the property differences of UHPC according to whether or not CNT disperses.

2.2 Materials used in this study

The raw materials for manufacturing UHPC were Type I ordinary Portland cement (OPC, Union Cement Co., Ltd., Korea), silica fume (Grade 940U, Elkem, Norway), silica powder (S-SIL 10, SAC, Korea, mean particle size of 4.2 μm) and silica sand (Saeron Co., Ltd., Korea) with particle diameter in range of 0.2–0.3 mm. The chemical composition and mechanical properties of white OPC are shown in the **Table 2-5**. Cement and silica fume were used as binders, and silica powder and silica sand were used as physical filler and fine aggregate.

Table 2-5. Mechanical and chemical properties of white cement

Properties		KSL 5204 OPC	White OPC
Chemical composition	ferric oxide (Fe_2O_3) (%)	Under 0.5	0.31
	Magnesium oxide (MgO) (%)	Under 5.0	1.85
	Sulfur trioxide (SO_3) (%)	Under 3.5	2.7
	Loss of Ignition (LOI) (%)	Under 3.0	2.5
Mechanical properties	Insoluble Residue (%)	Under 0.75	0.57
	Fineness (cm^2/g)	Upper 3,000	3,400
	Stability (%)	Under 0.8	0.46
	Whiteness Index	Upper 89	90.0

(Compared in accordance with the cement standard KS L 5204.)

Mixing steel fibers in UHPC increases ductility, such as tensile and flexural strength, then compressive strength of concrete. In this paper, compressive strength results of UHPC under various experimental conditions were intensively compared to identifying the mechanical properties of UHPC produced using ozone water and CNTs, so the mixing of steel fibers was not considered. In subsequent chapters, the UHPC's mix table was introduced for experimental purposes.

2.3 Microstructure analysis used in this study

2.3.1 Isothermal Calorimetry

When cementitious material reacts with water, it produces a hydration product (i.e., calcium hydroxide, C-S-H) and at the same time it hardens, releasing heat due to cement hydration. Hydration heat can identify the time when hardening of cement material begins while checking and comparing the time of occurrence, and it can be determined that hydration has occurred actively by comparing the cumulative heat amount.

The typical result of isothermal cement calorimetry result is shown in **Figure 2-8**. Generally, hydration reaction process of Portland cement subdivided into five stages and generate hydration product for each step [17].

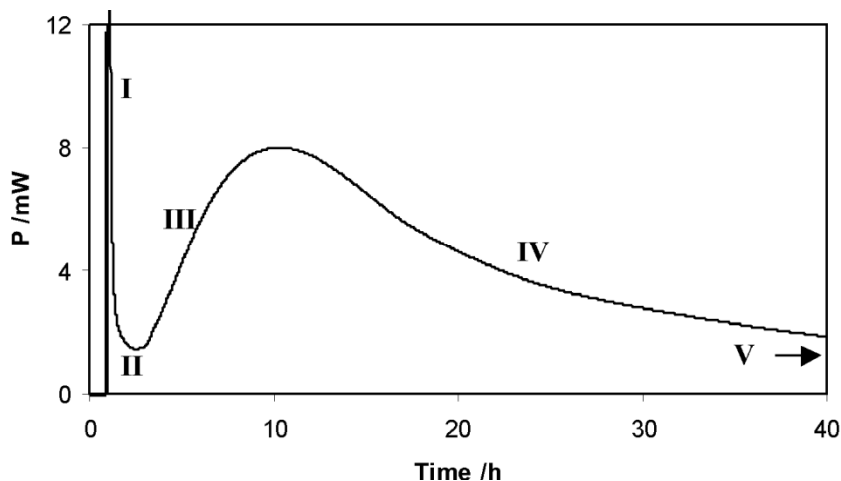


Figure 2-8. Typical result of cement isothermal calorimetry result (I. Rapid initial processes, II. Dormant period, III. Acceleration period, IV. Retardation period, V. Long term reactions)

On the same basis, isothermal calorimeter (TAM Air Thermostat with 8-channel Calorimeter) was used in this paper to identify the thermal flow of cementitious materials. In particular, hydration reaction test was performed with firm control of temperature to facilitate the comparison between the experimental groups.

2.3.2 X-ray Diffraction (XRD) Method

X-ray Diffraction (XRD), one of the fields of X-ray crystallography, is the method of analyzing the atomic and molecular structure of crystals. Major concept is measuring the angle and intensity of electron by diffracted X-ray beam. In studies related to building materials, XRD is a method mainly used for fine-grained materials such as cement or silica fume etc.

Specifically, when X-ray reach electrons in the crystal structure, electron produces spherical waves, which is illustrated in **Figure 2-9**. Some waves are cancelled by interference but constructive interference occurred in a few determined directions in accordance with Bragg's law:

$$2d \sin \theta = n\lambda \quad (2.1)$$

Where d is spacing between diffracting planes, θ is incident angle, n is any integer, and λ is beam wavelength.

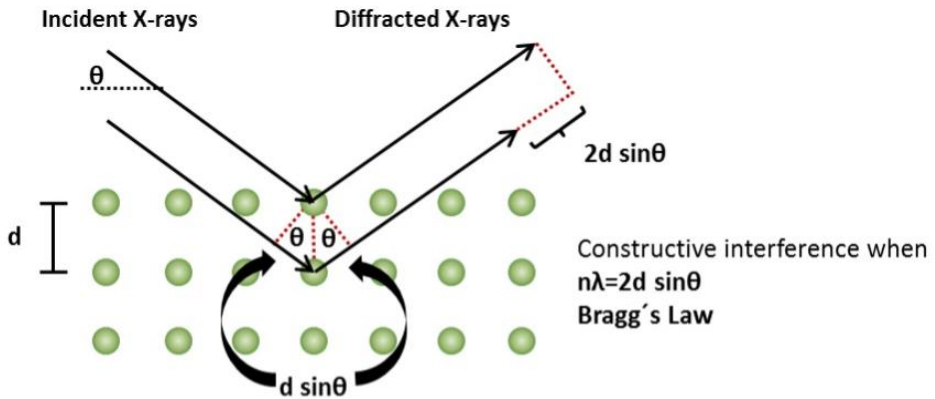


Figure 2-9. Schematic representation of X-ray diffraction by Bragg's law

In other words, part of incident X-ray is deflected by an angle 2θ and producing a reflection spot in diffraction pattern. Therefore, using diffraction pattern can analyze the microstructure of fine-grained material.

2.3.3 Thermogravimetric (TG) Analysis

Thermogravimetric (TG) analysis is a quantitative analysis of changes in the weight of organic or inorganic materials depending on the temperature of the samples to be measured. It is often used for analyzing cement compound due to supplementary cementitious materials (i.e., silica fume, fly ash) present in cement material reacts with OPC and contained water, causing changes in sample weight.

TG analysis is able to identify monosulphate (i.e., $\text{Al}_2\text{O}_3\text{-Fe}_2\text{O}_3\text{-mono}$ phase, AFm) or calcium-silicate-hydrates (C-S-H). Those hydration products can undergo several thermal reactions and these processes occur at certain temperatures [15].

After analysis process is completed, collected thermogravimetric data from a thermal reaction is compiled into plotting (referred to as a TG curve) of percentage of initial mass or mass itself on y axis versus temperature on the x-axis. In particular, an inflection point can be determined through the first derivative of the TG curve, and the amount of hydration product can be predicted according to y-value of the inflection point.

When TG analysis is performed on cement materials, the locations of the three inflection points and each y-values are mainly checked, and the hydration products for which each point means C-S-H and ettringite (near 100°C), portlandite (between 400 and 500°C) and calcite (between 700 and 800°C) in order of temperature [18].

2.4 Machine learning techniques in this study

With the invention of construction materials (i.e., Portland cement), mankind was able to construct a building that could exert high intensity and serviceability for decades. Entering 21st century, research activities are not limited to each specific field but are being carried out in convergence with information and communication technology to affect all research areas, including economy and industry.

As computers began to spread to the public, various architecture-related studies were conducted using big data statistical analysis. Using machine learning (ML) algorithm, P Ziolkowski et al. predicted the pattern of concrete strength according to mixing method which is difficult to recognize by human cognitive ability, and proposed an equation of concrete compressive strength that can be applied in construction site using data mining and artificial neural network (ANN). The range of input data (variables) for each concrete component (i.e., cement, water, fine aggregate, coarse aggregate) used to form an ANN is shown in **Table 2-6** and output data for each variable is shown in **Figure 2-10** [19].

Refer to this research, this paper applied three machine learning algorithms to predict compressive strength of UHPC with added ozone water or CNT by specific concentrations and definitions and examples of each ML algorithm were briefly introduced.

Table 2-6. Ranges of input features of concrete component (variables)

Input Features	Minimum (kg/m ³)	Maximum (kg/m ³)	Average (kg/m ³)
Cement	86.00	540.00	278.00
Water	121.80	247.00	182.42
Fine aggregate (sand 0-2mm)	372.00	1329.00	768.55
Coarse aggregate (aggregate above 2mm)	597.00	1490.00	969.08

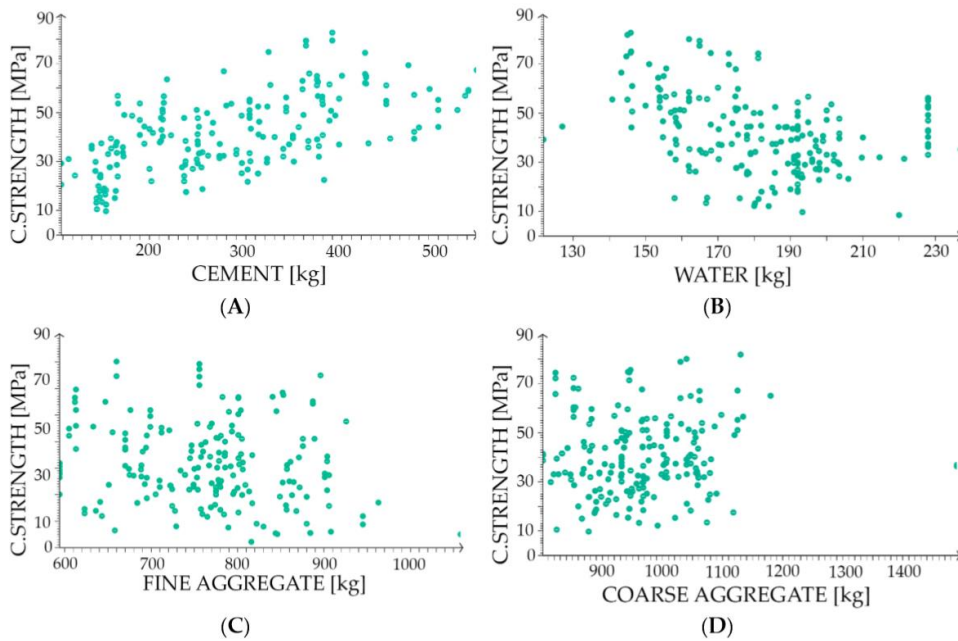


Figure 2-10. Scatter plots target versus input variables

(a) Cement, (b) Water, (c) Fine Aggregate, (d) Coarse Aggregate

To model the experimental results, this paper was analyzed using Python programming language introduced in scikit-learn and the main science library of Python. JupyterLab and Google Colab are mainly used to operate Python and all Python codes were compiled in the appendix of this paper except for examples to introduce ML techniques.

2.4.1 Polynomial Regression

Model-based learning should be performed based on a number of experimental results to apply ML. For specific example, compiled results are shown in **Figure 2-11**, a series of processes modelling the results of the experiment into one or more model parameters are called regression.

Polynomial regression is a technique that predicts the experimental data held in a linear and nonlinear manner. This provides a more ideal model for training data than linear regression, and the higher the model's order, the more likely it is to be to over-fit the experimental data. Therefore, a model that is about to occur is used to predict the distribution that is a precondition for the data.

Thus, this paper produced the model of the compressive strength results of various UHPCs through data mining and then performed a polynomial regression to predict the compressive strength of UHPC according to the concentration of ozone water or CNTs.

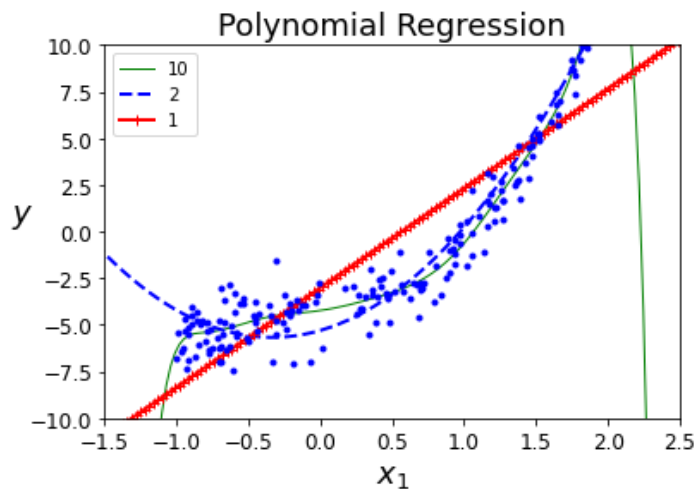


Figure 2-11. Example of polynomial regression
(Example data and codes are contained in the appendix)

2.4.2 *k*-Nearest Neighbor (*k*-NN) Regression

k-Nearest Neighbor (*k*-NN) algorithm is method to learn by utilizing the dataset itself, rather than learning about functions for prediction of specific values, such as polynomial regression. The key of this method is identifying the distribution of data at a distance (weight) to the *k*-th from one data and classify it into specific class, using *KNeighborsClassifier()* method for classifying dataset and *KNeighborsRegressor()* for predicting additional data.

In case of O₃-UHPC, UHPC-CNTs composite, when applying *k*-NN regression method to datasets that are focused on a specific interval (concentration), the smaller the number of peripheral data considered, the more biased the prediction results for some data than for the whole. **Figure 2-12** shows an example of applying *k*-NN regression, and it can be seen that the predicted result depends on the number of peripheral data to be considered (number of `n_neighbors`).

In this paper, *k*-NN regression methods were used to predict the compressive strength of O₃-UHPC and UHPC-CNTs composite, which is difficult to generate and maintain ozone concentration and limited experimental data.

Parameters for applying *k*-NN regression are as follows:

- ♦ `p = 2`: calculating the distance between data, apply the Euclidean distance to determine the weight between samples.
- ♦ `n_neighbors = 10`: Number of peripheral data to consider when predicting new data.
- ♦ `weight = 'distance'`: Weight points by the inverse of their distance.

In this case, closer neighbors of query point will have greater influence than neighbors which are further away.

Ch. 2. Preliminary Study

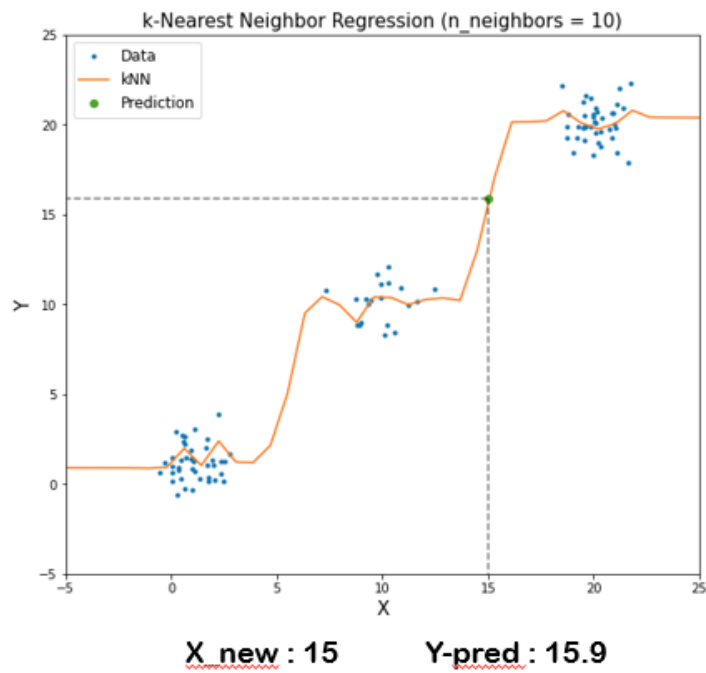
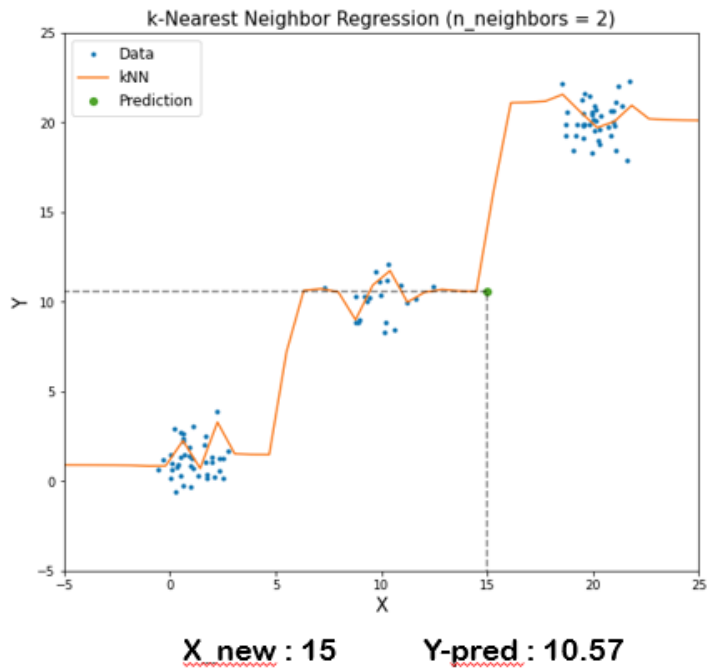


Figure 2-12. Example of k-NN Regression
(Example data and codes are contained in the appendix)

2.4.3 Decision Tree

When classifying data into dichotomically, the decision tree method is a frequently used ML technique because it provides visualization of classification results and criteria. Decision tree classifies the data at the root node according to specific criteria until it finally completes the creation of the leaf node.

To apply this method, data can be classified up to the maximum depth of the decision tree when mean square error (MSE) is calculated on each nodes. The MSE expression for evaluating a series of samples by applying the system's predictive function is as follows:

$$\text{MSE}(\mathbf{X}, h) = \frac{1}{m} \sum_{i=1}^m (h(\mathbf{x}^{(i)}) - y^{(i)})^2 \quad (2.2)$$

Where m is number of samples in dataset.

\mathbf{X} is a matrix that contains all feature values of all samples in the dataset,

h is a predictive function of the system (=hypothesis)

$\mathbf{x}^{(i)}$ is the vector of all feature value of the i -th sample in the dataset, and

$y^{(i)}$ is the expected output of the sample.

The result of applying decision tree regression to the dataset example are shown in **Figure 2-13**. If the depth of the decision tree is larger than certain size, a lot of leaf node MSEs are become zero, which means regression model has been overfitted. Therefore, appropriate depth of tree should be created.

According to this technique, this paper applied the decision tree regression to the compressive strength data of UHPC for ozone water concentration of CNTs to derive the period in which certain strength is expressed, and confirming the mechanical property distribution for the UHPC.

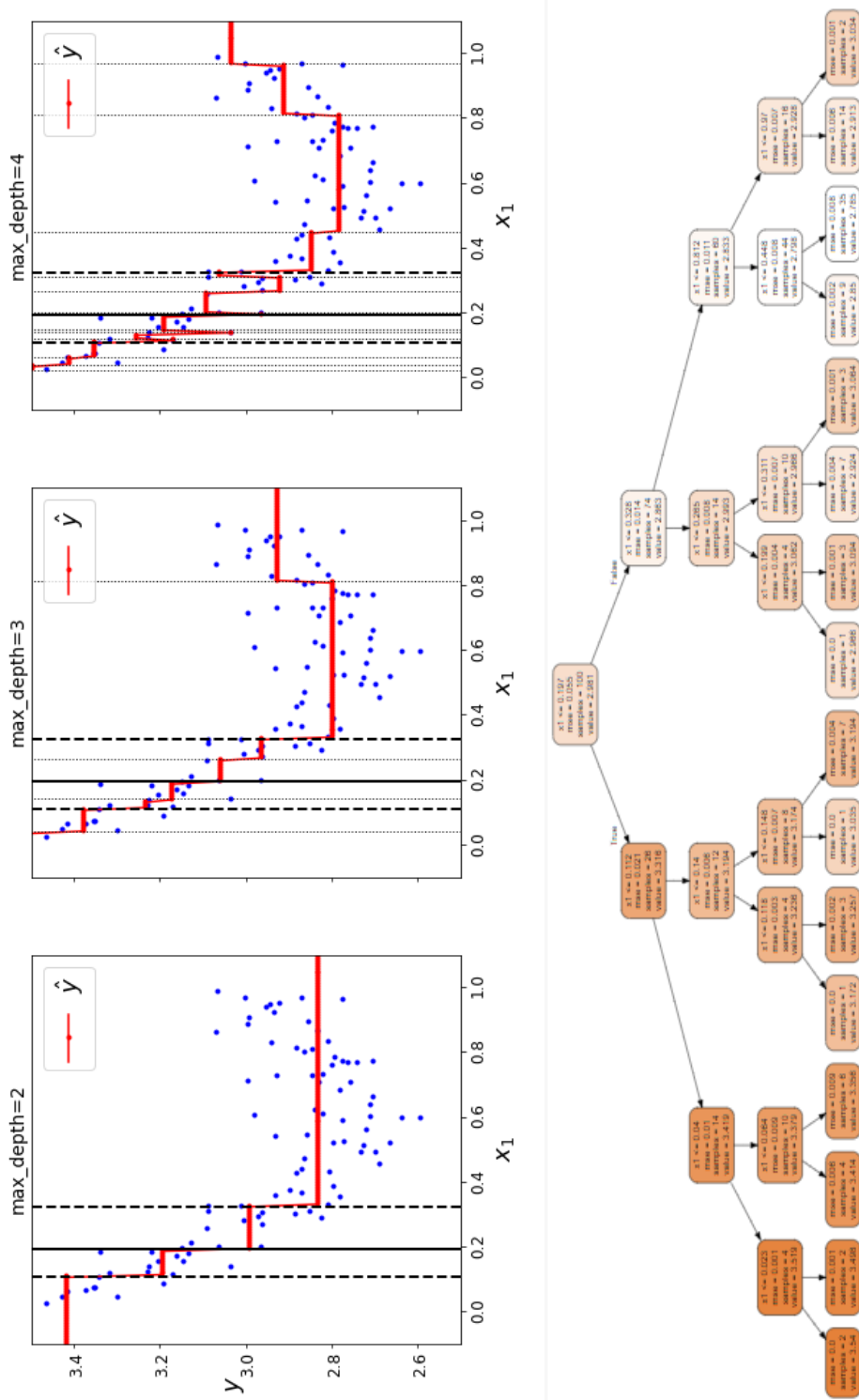


Figure 2-13. Example of model prediction by decision tree regression
 (Example data and codes are contained in the appendix)

Chapter 3. Effect of Ozone Water on UHPC Performance

The research carried out in this chapter is largely aimed at identifying the effects of ozone water on UHPC by comparing material properties. Specifically, mechanical properties, including compressive strength and flow of cement paste produced by ozone water, and chemical properties of O₃-UHPC using isothermal calorimetry, XRD and TG results were compared with the general UHPC.

As a result of compressive strength experiments show that the compressive strength of UHPC has increased slightly due to concentration of ozone in O₃-UHPC. Also, the flow rate of UHPC cement paste produced by mixing ozone water is improved than general UHPC.

However, unlike physical changes, it can be seen that the timing of hydration reaction and the chemical structure of the paste are not very clear by ozone water mixing. This can be inferred from ozone dissolved in ozone water is vaporized by the generated heat during the mixing process, resulting in ozone water having the same properties as the common mixture.

3.1 Introduction

In this chapter, plasma generator used to produce O3-UHPC, test specimen's properties were introduced. After the overall composition of experiment, mechanical and chemical properties of O3-UHPC are mainly compared with general UHPC.

In particular, after data mining the compressive strength test, the polynomial regression, k -NN regression and decision tree techniques were performed to identify appropriate ozone concentration period that can maximize the mechanical properties of O3-UHPC. Python codes to implement ML techniques are introduced in appendix.

3.2 Parameters of Study

In this paper, to identify the mechanical properties of UHPC specimens, not only determine compressive strength of UHPC and O3-UHPC but also measured the state mechanical properties, both cement paste was casted on the cubic mold and carried room temperature curing at 20 °C and relative humidity (RH) of 60% in a chamber. In addition, high temperature steam curing was performed for 48 hours with 90 °C and RH of 99% for developing the required strength in a short period of time. After that, natural drying was performed for one day in an environment with the same temperature and RH as room temperature curing. Lastly, to check the flow of the UHPC specimen, flow test was conducted immediately after the completion of cement paste mixing.

Ch. 3. Effect of Ozone Water on UHPC Performance

For samples used in hydration reaction test, XRD, TG analysis to identify the chemical properties of the specimen, the curing conditions mentioned above are the same instead, but are mixed except silica sands. To carry out chemical experiments, test specimens were produced under this condition was stopped 1 and 28 days after the mixing was completed to check the chemical composition of the specimen at certain times.

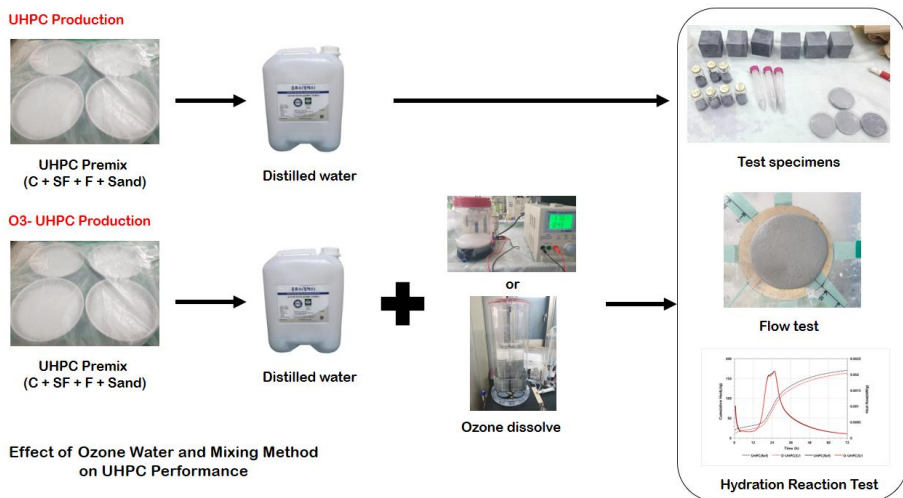


Figure 3-1. Graphical abstract of chapter 3

3.3 Material Properties

The UHPC components used in this study are as mentioned in Chapter 2.2. This chapter introduces the ozone water generator used in O₃-UHPC production. The ozone water with certain concentration was produced using two devices and is shown **Figure 3-2** and **Table 3-1**. Both generators were produced by the Bio Plasma Laboratory (Kwangwoon university, Korea).



(a)



(b)

Figure 3-2. Ozone water generator ((a): Type 1, (b): Type 2)

Table 3-1. Properties of Ozone water generator

Properties \ Generator	Type 1	Type 2
Tank capacity	1500 ml	Inner box: 5000 ml Outer box: 4000 ml
Ozone concentration	0 ~ 0.1 g/ml	0 ~ 1.3 g/ml

When producing ozone water using the above instruments, distilled water was used to exclude the effect on the chemical composition of cement paste by water. The process of producing ozone water using plasma generator is illustrated in **Figure 3-3**.

The concentration of ozone water is determined by the performance of the plasma generator and the temperature of the dissolved water. Also, the greater the size of the plasma generating device (the better the efficiency of replacing the atmosphere with ozone), the closer the temperature of the water is to 4 degrees, the higher the concentration of ozone water.

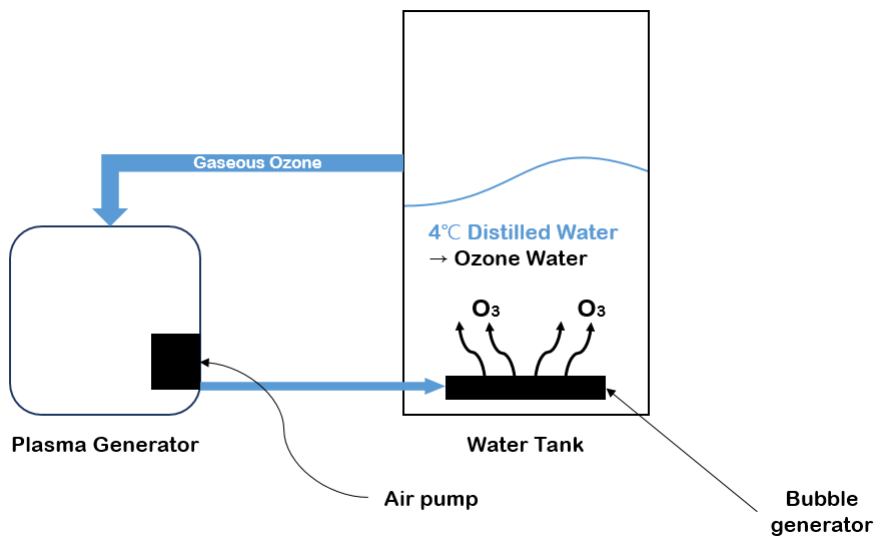


Figure 3-3. Schematic representation of ozone water production

To use ozone water generators, power must be supplied to air pumps and plasma generators, and must be kept dry. Also, containers that produce ozone water must be sealed until the fabrication is complete, otherwise it is difficult for ozone to dissolve in water.

3.4 Fabrication of Specimens

In order to compare the mechanical properties of general UHPC and O3-UHPC, cement paste of experimental group casted a cube mold with a length of 50mm and then cured at 20 °C and RH of 60% in a chamber by one day. The UHPC and O3-UHPC mix proportion table by weight ratio of cement for each experimental group is shown **Table 3-2**.

Table 3-2. Mix proportion of each experimental group

Experimental Group	W (O ₃)	SP	C	SF	F	Sand
UHPC (Reference)	0.23	0.04	1	0.25	0.35	1.1
O-UHPC(S)	0.23					
O-UHPC(L)	0.23					

(W: water, SP: superplastizier, C: white cement, SF: silica Fume, F: silica powder)

By O3-UHPC, two ozone water generators were used as introduced in **Table 3-1**. and O3-UHPC with Type 1 is marked as O-UHPC(S), and O3-UHPC with Type 2 is marked as O-UHPC(L). This distinction is due to different concentrations of ozone water used.



Figure 3-4. Experiment samples after curing

(O-UHPC Vol.1 is O-UHPC(S) and O-UHPC Vol.2 is O-UHPC(L))

Ch. 3. Effect of Ozone Water on UHPC Performance

In contrast, in order to determine the timing of hydration reactions and the chemical composition of cement paste in each experimental group, specimens shall be produced excluding silica sand from the mixing table shown in **Table 3-2**. Then prepare silica-sand filled ampoule to compare the specific heat of specimen before operating calorimeter.

Also, to carry out XRD and TG analysis, test specimens must stop curing at the specified time (Day 1, Day 28) and perform hydration suspension. Hydration suspension treatment was performed by shredding the specimen and removing the remaining water inside the cement system complex using isopropyl alcohol and ethanol.



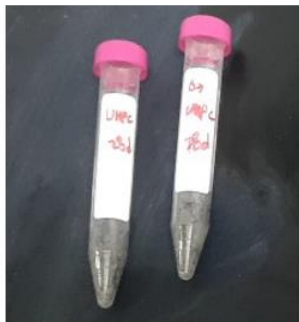
(a)



(b)

Figure 3-5. Fabrication and specimens of hydration reaction test

((a): cement paste before putting it in ampoule, (b) hydration reaction test specimens)



(a)



(b)

Figure 3-6. Experiment samples for XRD, TG analysis

((a): during hydration suspension, (b) after hydration suspension)

3.5 Test Set-up and Instrumentation

3.5.1 Test Conditions

All physical and chemical experiments were classified into control groups, general UHPC, and experimental groups O-UHPC(S) and O-UHPC(L), especially indoors with room temperature maintained at 20 °C when conducting hydration reaction tests.

3.5.2 Compressive Strength Test

For the compressive strength test, a number of cube specimens were produced to apply machine running techniques to the test results and O3-UHPC was produced using ozone water with various concentrations to reduce bias of models produced by the experimental results.

Table 3-3. Number of compressive strength test data

Experimental Group	Ozone Concentration (g/ml)	Number of Data
UHPC (Reference)	0	36
O-UHPC(S)	0.03	27
	0.1	27
O-UHPC(L)	1	18
Total (Day 1, Day 28, Steam Curing)		108

Compressive strength of the samples was measured at day 1, day 28 and day 3(after steam curing) according to American society for testing and materials (ASTM) C109 and ASTM C348-20 [20,21] by universal testing machine (UTM) with a capacity of 2000 tons. Follow equation used for calculate compressive strength of specimens of each experiment groups.

$$\text{Compressive Strength } \sigma = P/A \text{ (MPa)} \quad (3.1)$$

Where P is maximum load (N) and A is surface area of specimen (2500 mm²).

3.5.3 Flow Test

Flow tests were performed in accordance with ASTM C1856 [22] to measure the flow rate of cement paste by each experimental group.

The mold used for flow test is 70 mm diameter on the top and 100 mm in diameter on the bottom, and test was conducted on circular plate with a diameter of 250 mm. Note that the flow test should be carried out immediately after the mixing is completed because curing begins after the cement paste mixing is completed.

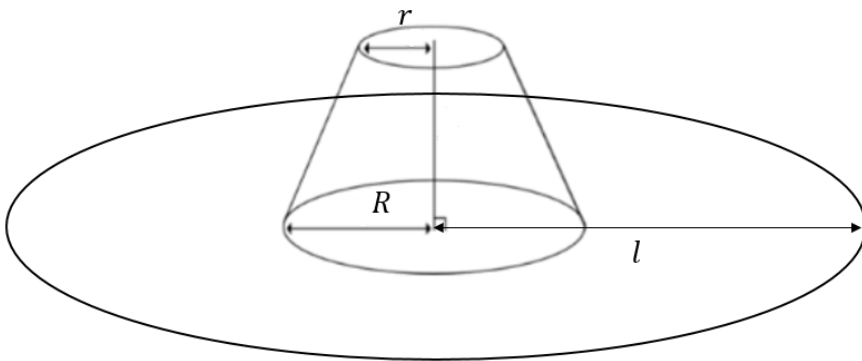


Figure 3-7. Schematic representation of flow test instruments

($r = 70$ mm, $R = 100$ mm, $l = 250$ mm)

3.5.4 Hydration Reaction Test

After the mixing is completed, UHPC cement paste will enter initial set where liquidity decreases within a few days. In this experiment, isothermal calorimetry was measured for 72 hours using a TAM Air system (TA instruments, USA) for check the effect of ozone dissolved in water on the hydration reaction.

Basically, the method of checking the hydration reaction is comparing emitted heat of silica sand which have sum of specific heat occurred by cement and silica fume and the specific heat of 10g of cement paste of experimental group in an isothermal environment of 20 °C.

In case of hydration reaction test of O3-UHPC, two samples were prepared and check reproducibility for each experimental group, as the timing and amount of hydration heat could vary due to a brief time loss.

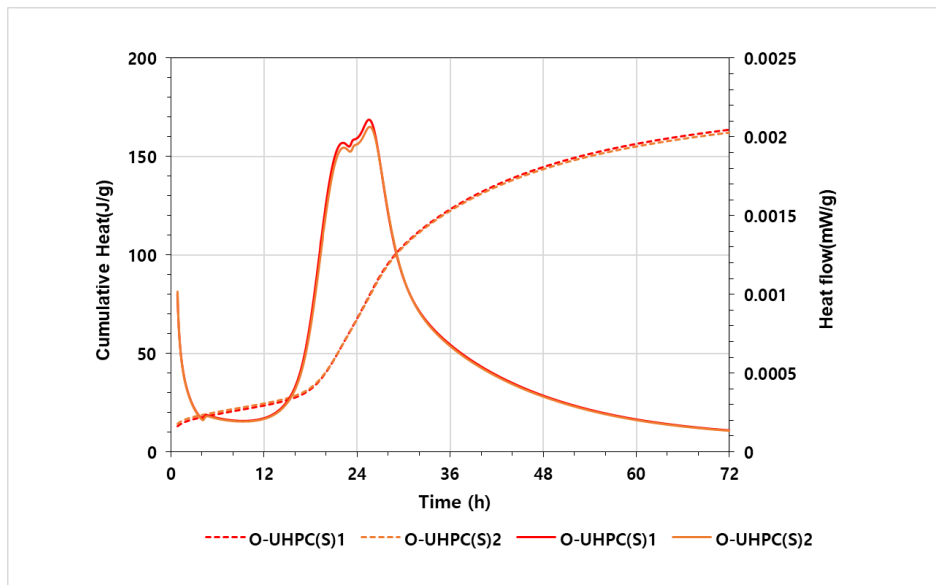


Figure 3-8. Verification of reproducibility of hydration reaction test

3.5.5 X-ray Diffraction (XRD)

XRD diffraction analysis were performed using specimens at day 1 and day 28 of curing with hydration suspension. The device used in analysis is D2 Phaser (Bruker, Germany) with $\text{CuK}\alpha$ ($\lambda = 1.5418 \text{ \AA}$) radiation at 30 kV and 10 mA, a step size of 0.02027° and 2 second per step were employed over a 2θ range of $5\text{--}50^\circ$.

In this research, the amount of compounds presents in cement (belite, alite, gypsum) and produced after the hydration reaction (calcite, ettringite, portlandite) for a certain 2θ angle were measured relatively.

Table 3-4. 2θ angle of cement compounds by XRD analysis

Cement Compound	2θ
Belite (C_2S)	$19^\circ, 32^\circ \sim 33^\circ$
Alite (C_3S)	$29^\circ \sim 30^\circ, 34^\circ \sim 35^\circ$
Gypsum	$11.5^\circ \sim 12^\circ$
Calcite (CaCO_3)	$23.1^\circ, 29.2^\circ, 35.9^\circ$
Ettringite ($\text{Ca}_6\text{Al}_2(\text{SO}_4)_3(\text{OH})_{12}\cdot 26\text{H}_2\text{O}$)	$8^\circ \sim 9^\circ, 15.8^\circ \sim 16^\circ$
Portlandite ($\text{Ca}(\text{OH})_2$)	$17^\circ \sim 18^\circ$

3.5.6 Thermogravimetric (TG) Analysis

TG analysis were conducted using same samples of experimental group used in XRD analysis. Instruments used in analysis is TA instrument Q500 (Bruker, Germany) under N_2 condition at a heating rate of 10 K/min up to 1050°C . Curves generated from TG analysis can help identify continuous weight loss for each experimental group. To identify weight loss of several hydration products (C-S-H, portlandite, calcite), it can be checked through deriving first derivative of the TG curve (DTG).

3.6 Test Results

3.6.1 Compressive Strength

The mean compressive strength of general UHPC, O3-UHPC produced by operating generator type 1 for 4 minutes (0.03 g/ml), 10 minutes (0.1 g/ml) and operating generator type 2 for 2 minutes (1 g/ml) is shown in **Figure 3-10**.

Experiments show that the compressive strength of the 28th day after casting and steam cured specimens did not meet the compression strength criterion (150 MPa or higher). This is the result of making UHPC specimens without mixing steel fibers in the UHPC mixing table.

After one day of curing, the average compressive strength of nine samples in each experimental group tends to decrease if the concentration of ozone is above a certain level. The results can be found to be similar to those for the 28 days of curing. However, in case of steam curing, it can be found that compressive strength of O3-UHPC at all concentrations has been improved.

This result can be inferred from the nature of ozone water itself. If an adequate amount of dissolved water is mixed with cement, ozone can be determined to affect the initial intensity expression by promoting hydration reaction in cement paste. Also, ozone water contributes to the improvement of the compressive strength of UHPC when exposed high temperature and humidity environment.

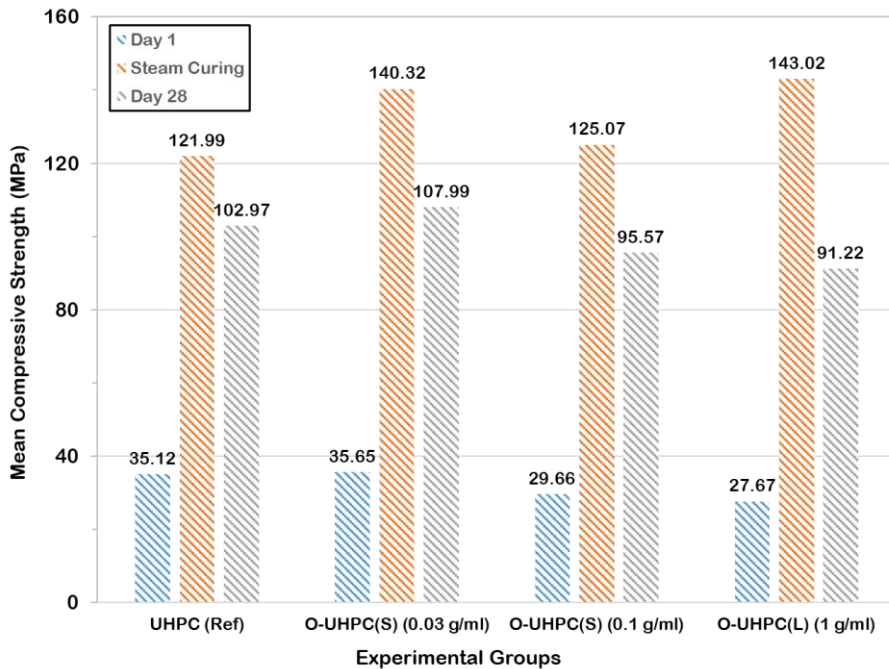


Figure 3-9. Mean Compressive strength of each experimental groups

3.6.1.1 Processed Data by Machine Learning

To more accurately determine the effect of ozone on compression strength, ML techniques were applied based on a number of compressive strength experimental data. Also, additional experimental groups were designated to reduce bias of the predicted compressive strength for newly set concentrations using ML techniques. The distribution of compressive strength of O3-UHPC for each experimental group is shown in Figure 3-11.

Table 3-5. Number of additional compressive strength test data

Experimental Group	Ozone Concentration (g/ml)	Number of Data
O-UHPC(S)	0.05	18
O-UHPC(L)	1.3	27
Total (Day 1, Day 28, Steam Curing)		153 (= 108 + 45)

(0.05 g/ml: operating generator type 2 for 1 minute)

(1.3 g/ml: operating generator type 2 for 4 minutes)

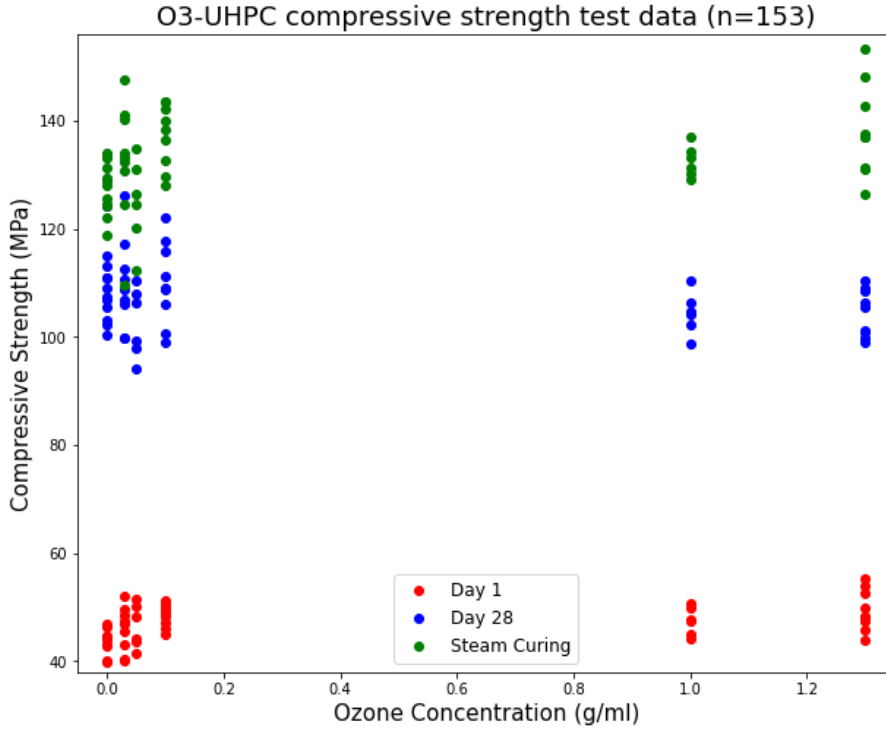


Figure 3-10. Distribution of compressive strength of O3-UHPC for each experimental group

- Polynomial Regression

To determine the overall distribution of compressive strength of O3-UHPC, polynomial regression analysis was conducted for each experimental group. Also, identifying the suitability of the regression model and improvements in the model and data for each experimental group by checking learning curves of linear to 4th-order polynomial regression.

Through this, it is possible to determine the trend of compression strength according to the concentration of ozone water, which is difficult to generate with existing experimental devices. Based on the results of regression from linear to fourth order, the trend of compressive strength is analyzed based on the results of no over-fitting.

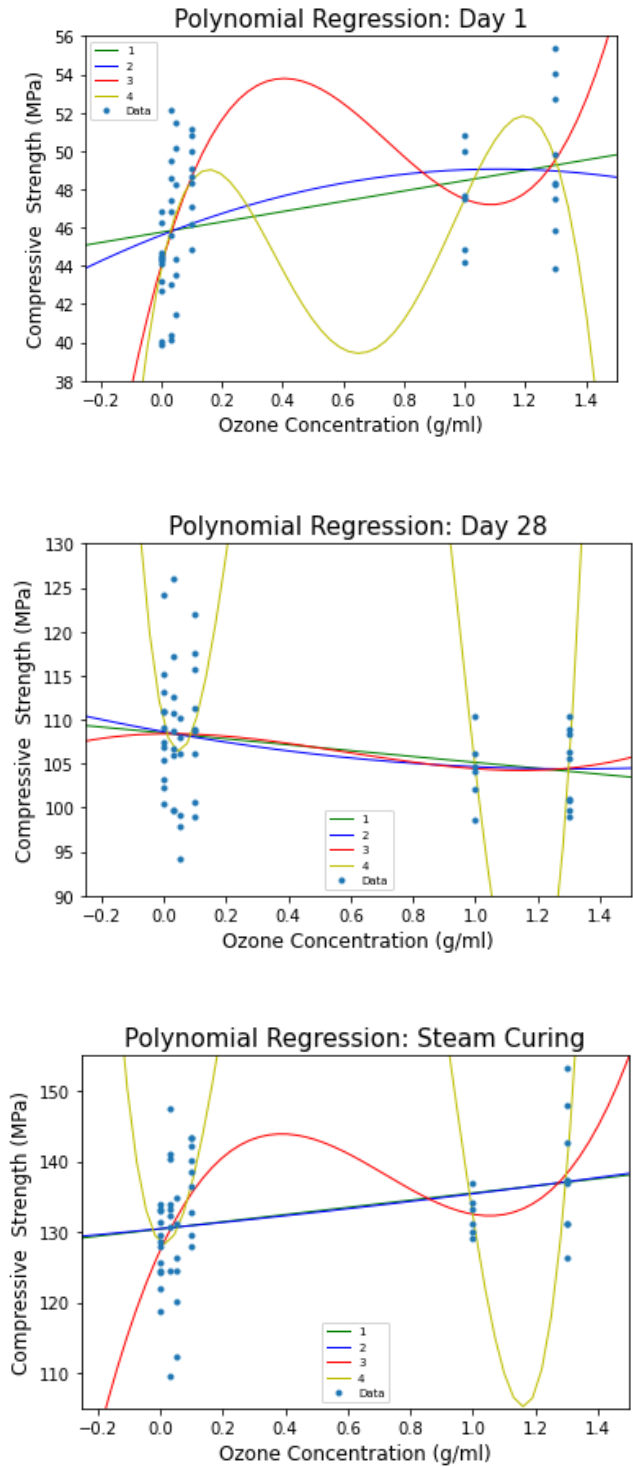


Figure 3-11. Polynomial regression results of O3-UHPC compressive strength

Ch. 3. Effect of Ozone Water on UHPC Performance

As a result of polynomial regression, all experimental groups in O3-UHPC can see that the regression model is over-fitting with the data set if the order of the highest order is greater than or equal to the 4th order. Considering without over-fitting, linear and second order regression suggests that higher the concentration of ozone, the compressive strength of the O3-UHPC which produced after 1 day and steam cured was increased.

On the other hand, for the 28th day experimental group, the higher the ozone concentration, the lower the compression strength is than general UHPC. It can be inferred that this phenomenon caused by difference of curing methods. During room temperature curing, ozone dissolved in ozone water evaporates and bubbles can occur during the process of dropping out of the cement paste, which can affect the cement microstructure.

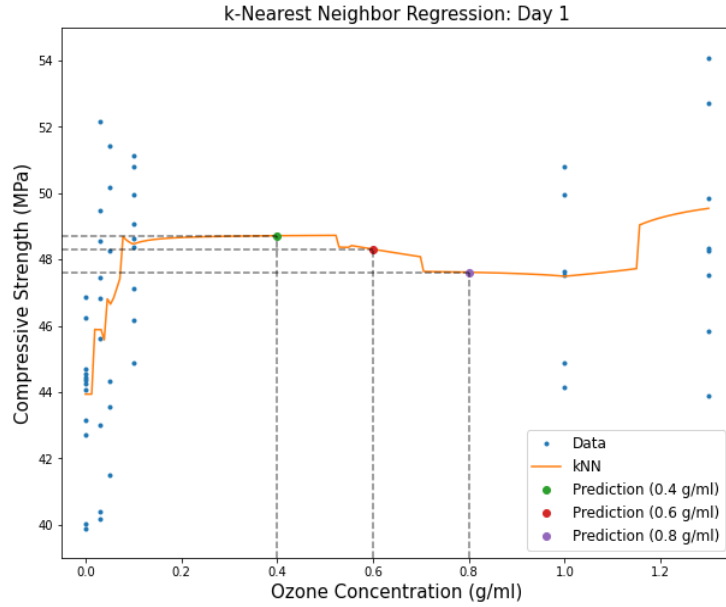
- *k*-NN Regression

To validate the results of the polynomial regression, *k*-NN regression was conducted focusing on the local results of the peripheral data instead of the distribution of the overall data set itself.

To fully reflect the relationship with locally distributed experimental data, 10 neighboring experimental data were set up as populations and then re-analyzed. Based on this analysis, the compressive strength of UHPC produced by ozone water at a specific concentration (0.4, 0.6 and 0.8 g/ml) was predicted.

Ch. 3. Effect of Ozone Water on UHPC Performance

Prediction (0.4 g/ml) = 48.72 MPa
Prediction (0.6 g/ml) = 48.31 MPa
Prediction (0.8 g/ml) = 47.61 MPa



Prediction (0.4 g/ml) = 108.64 MPa
Prediction (0.6 g/ml) = 108.64 MPa
Prediction (0.8 g/ml) = 104.83 MPa

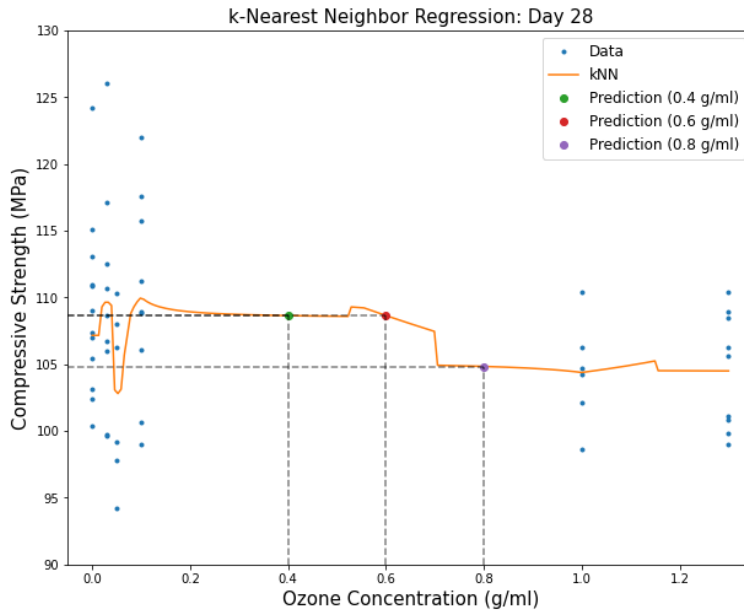


Figure 3-12. *k*-NN regression results of O3-UHPC compressive strength

Ch. 3. Effect of Ozone Water on UHPC Performance

Prediction (0.4 g/ml) = 136.96 MPa
Prediction (0.6 g/ml) = 133.71 MPa
Prediction (0.8 g/ml) = 134.0 MPa

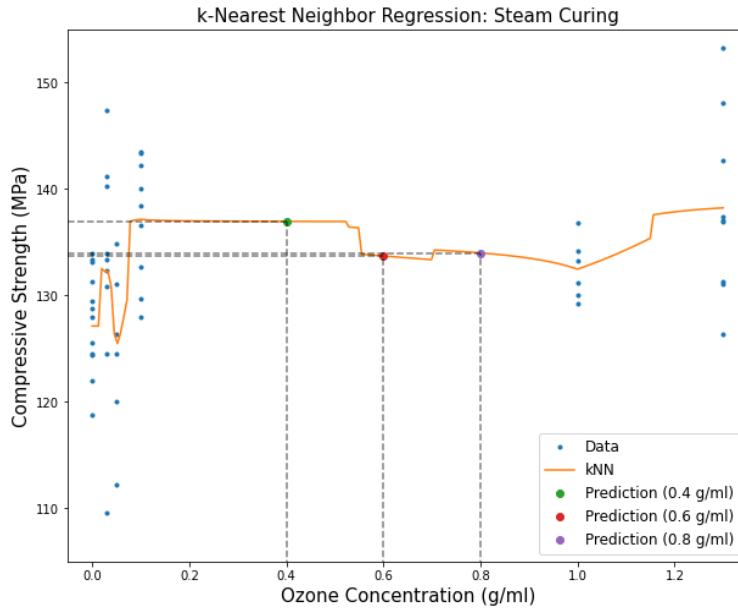


Figure 3-12. (Continued) *k*-NN regression results of O₃-UHPC compressive strength

Interestingly, *k*-NN regression shows that O₃-UHPC in areas without experimental data shows that the higher the concentration of ozone water, regardless of the curing method, the compressive strength unchanged or decreases slightly. In other words, in all three experimental groups, if the concentration of ozone water is greater than 0.55 g/ml, the compression strength is reduced.

- Decision Tree Method

Finally, decision tree method was used to determine expression of compressive strength in certain ozone-concentration period. The index for dividing sections was based on the MSE used in *k*-NN regression, and the ozone concentration section was subdivided in four stages.

For each leaf node produced in the decision tree, the lower the MSE, the more evenly the data can be found to be distributed. On the other hand, high MSE indicates that the experimental data needs to be supplemented because it is an over-fit of the specific data within the interval.

Ch. 3. Effect of Ozone Water on UHPC Performance

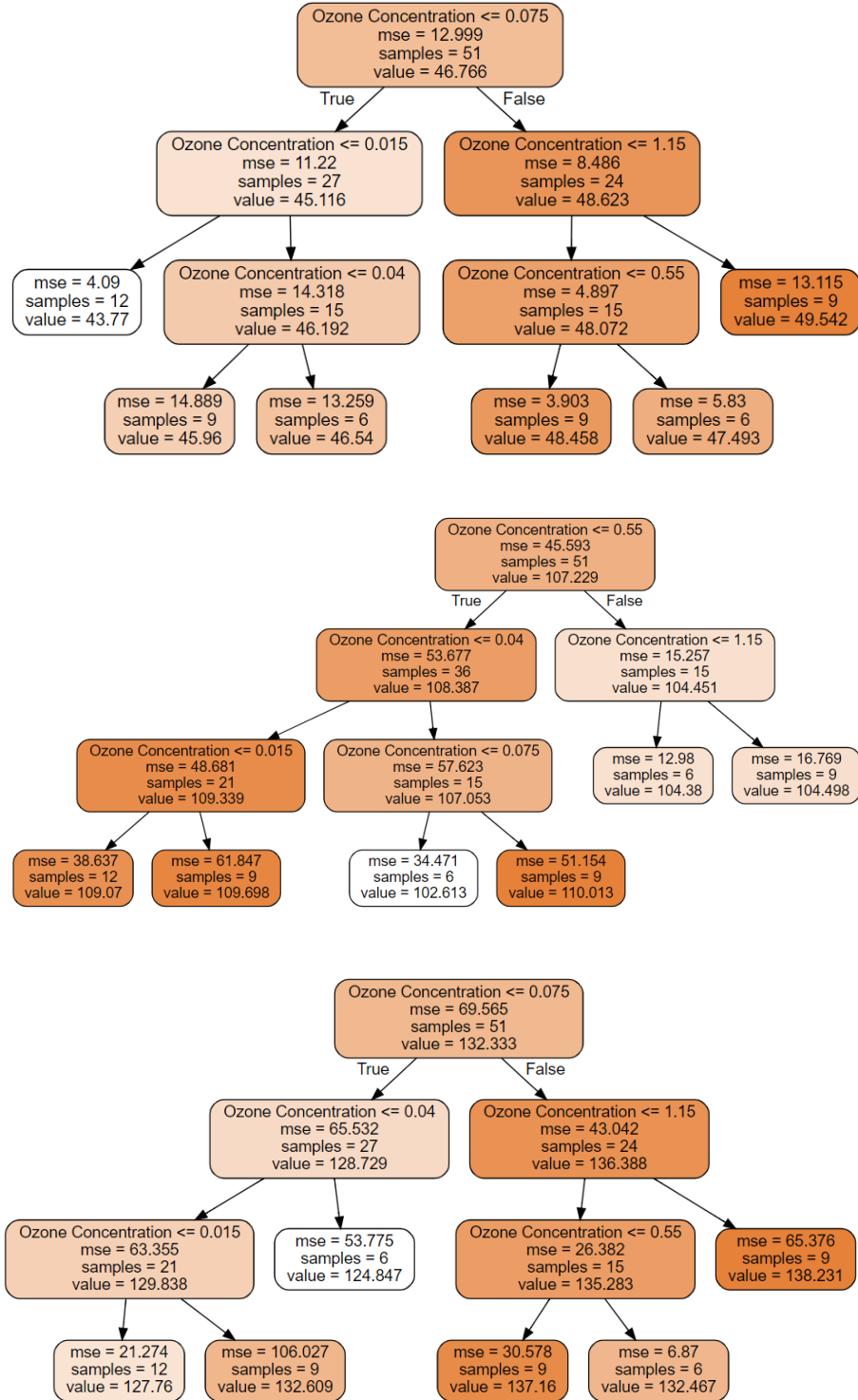


Figure 3-13. Decision tree results of O3-UHPC compressive strength

Ch. 3. Effect of Ozone Water on UHPC Performance

As a result of performing decision tree method, the leaf nodes in the decision tree of all experimental groups represents same group sizes and except room-temperature cured 28 day specimens, it represent similar tree shape.

On the other hand, leaf nodes with MSE greater than half the predicted compressive strength value were created in room-temperature cured in 28 days and steam cured O3-UHPC specimens. This means that the interval included an outlier, which cause MSE to rise significantly. To address this, the data belonging to that section should be classified in a more granular step.

In finalizing the analysis of the compressive strength by ozone concentration of O3-UHPC through three machine learning techniques, the following conclusion can be obtained.

- Polynomial regression suggest that ozone water may increase the initial intensity of UHPC, but that required intensity expression may rather impede intensity expression.
- According to k -NN regression, O3-UHPC may express low compressive strength if the ozone dissolved in ozone is more than 0.55 g/ml. In addition, the intensity of the O3-UHPC will be similar to general UHPC when producing UHPC with ozone concentrations above this level.
- By decision tree method, parameters of each concentration period where compressive strength is expressed can confirmed. Based on this result, if the concentration of ozone water used in the production of O3-UHPC is less than 0.075 g/ml or more than 1.15 g/ml, the compressive strength is more than normal UHPC.

It suggests that the curing method needs to be considered so that the required strength can be displayed in a short period of time, such as hot steam curing, in order to manifest the compressive strength of O3-UHPC.

3.6.2 Cement Paste Fluidity

To easily distinguish the fluidity of cement paste with concentrations of ozone water, O3-UHPC made from ozone water with concentrations of 0.03, 0.1, and 1.3 g/ml were compared. Flow rate of UHPC cement paste for each experimental group is shown in **Table 3-6** and **Figure 3-14**.

In order to compare the fluidity by experimental group with the general UHPC, the length of major and minor axis of ellipse formed by cement paste was measured and area of ellipse was calculated. The equation for calculating the area of ellipse is as follows:

$$A = \pi ab \tag{3.2}$$

Where A is area of ellipse, a is length of ellipse major axis and b is length of ellipse minor axis.

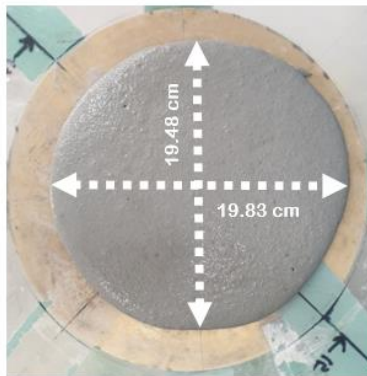
Experiments show that if the concentration of ozone water increases by a certain size, the flow rate of cement paste has increased. However, when the concentration of ozone water reaches 0.1 g/ml, it can be inferred that the greater the concentration of ozone water, it reduces fluidity of cement paste.

In addition, if the concentration of ozone water is significantly improved (1.3 g/ml), the flow rate of cement paste is not significantly different from general UHPC. Therefore, it can be inferred that if concentration of ozone water exceeds a certain number (0.03 g/ml), the compressive strength and fluidity of the UHPC will decrease.

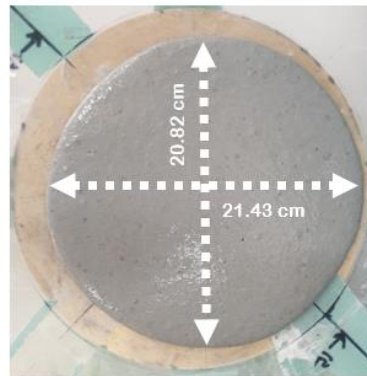
Ch. 3. Effect of Ozone Water on UHPC Performance

Table 3-6. Flow test result and comparison with general UHPC

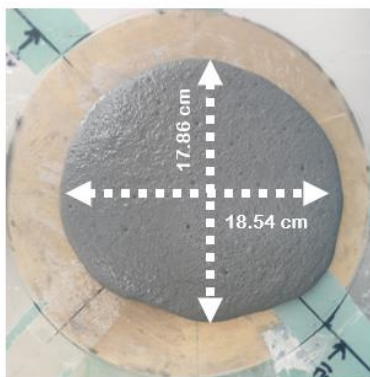
Experimental Group	Major axis length (cm)	Minor axis length (cm)	Area (cm ²)	Relative ratio
UHPC (Ref.)	19.83	19.48	1213.56	1
O3-UHPC (0.03 g/ml)	21.43	20.82	1401.69	1.16
O3-UHPC (0.1 g/ml)	18.54	17.86	1040.26	0.86
O3-UHPC (1.3 g/ml)	20.52	19.36	1248.05	1.03



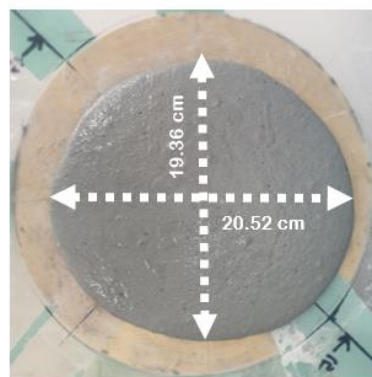
UHPC (0 g/ml) (Ref.)



UHPC (0.03 g/ml)



UHPC (0.1 g/ml)



UHPC (1.3 g/ml)

Figure 3-14. Results of flow test of general, O3-UHPC

3.6.3 Hydration reaction at initial period

The results of isothermal calorimetry and numerical values by heat flow curves are displayed in Fig. 3-15 and Table 3-7.

First, the hydration reactions of general UHPC and O3-UHPC produced with 0.03 g/ml concentrated water show that neither experimental group had significant differences. Also, O3-UHPC, produced from ozone water with a concentration of 1.3 g/ml, also shows almost the same heat flow as a normal UHPC.

This shows that the hydration reaction of the UHPC does not affect the ozone water. The reason for this phenomenon is that the hydration reaction test is performed at a relatively high temperature (20 °C). Due to the nature of ozone water, it can be dissolved in water for longer periods of time at low temperatures (4°C). Therefore, if the experiment continues at room temperature (more than 4°C) for more than a few hours, the material properties of ozone water UHPC can easily disappear.

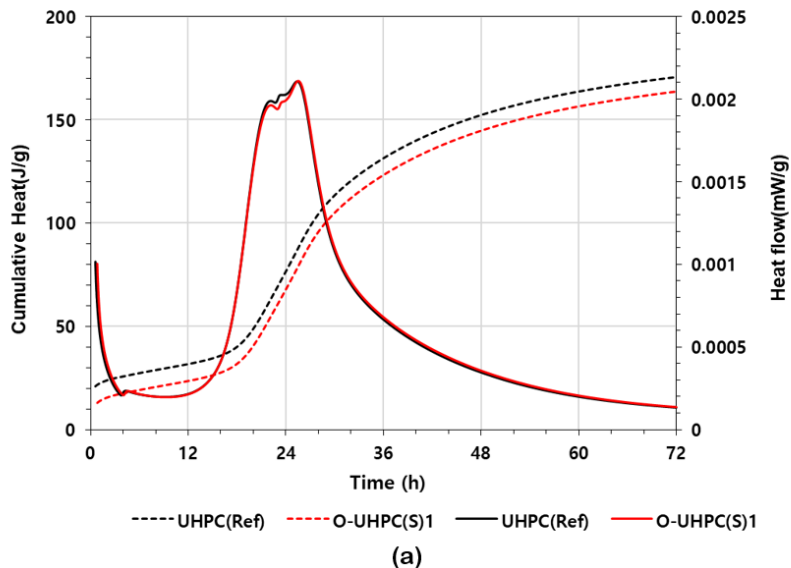


Figure 3-15. Cumulative heat and heat flow curve comparison
 ((a): UHPC with O3-UHPC (0.03 g/ml))

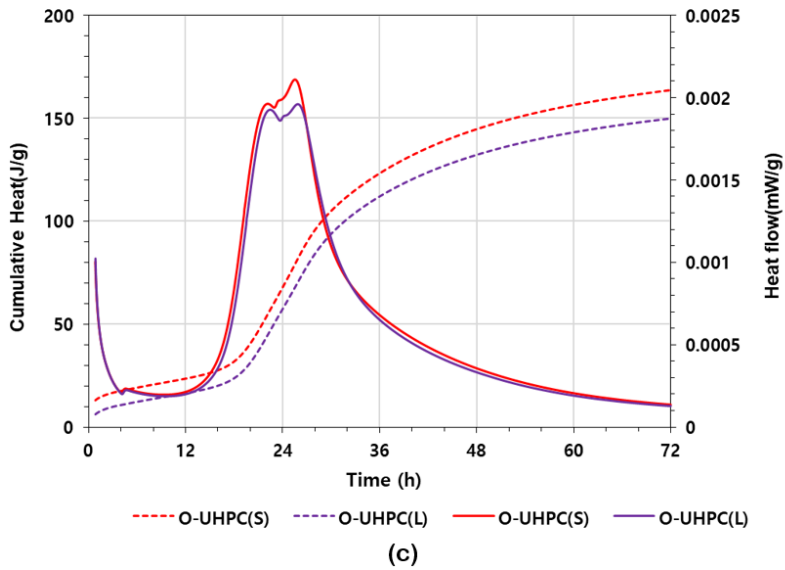
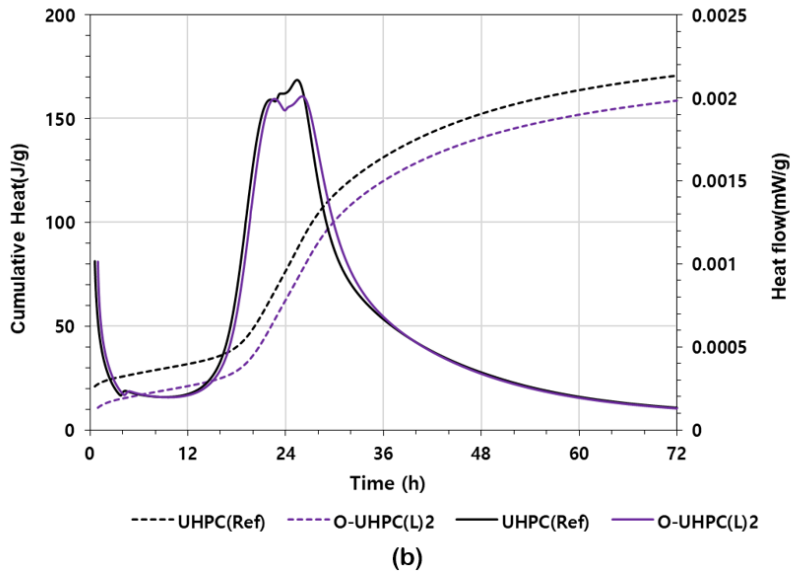


Figure 3-15. Cumulative heat and heat flow curve comparison (O₃)

(Continued) (b): UHPC with O₃-UHPC (1.3 g/ml),

(c): O₃-UHPC with different concentration (0.03, 1.3 g/ml)

Table 3-7. Numerical values from heat curve of experimental groups

Experimental Group	Minimum heat flow (J/g)	Initial period of acceleration (h)	Slope (J/g · h)
UHPC (Ref.)	0.0001978	9.088	2.18×10^{-5}
O3-UHPC (0.03 g/ml)	0.0001965	9.422	2.09×10^{-5}
O3-UHPC (1.3 g/ml)	0.0001962	9.673	2.03×10^{-5}

3.6.4 Chemical Component Analysis

When comparing the chemical properties of cement, for XRD experimental results, the results obtained from the 28th day sample compared to the 1st day sample show a more accurate amount of cement compound, and the more accurate the peak of the XRD experimental results, the more accurate the amount of compounds can be compared.

As TG analysis results only partially (30g) after shredding the suspended samples, many experiments need to be carried out on the same group of subjects to avoid bias in the analysis. In addition, it may be difficult to compare the exact amount of cement compounds if the slope of the curve occurs in the temperature period where there should be no response in the DTG curve results.

3.6.4.1 XRD Results

The result of XRD of each experimental group with suspension of hydration reaction on 28th day after manufacture is shown in **Figure 3-16**. To accurately compare the cement hydration products of each experimental group, experiment was repeated by matching the quartz peak.

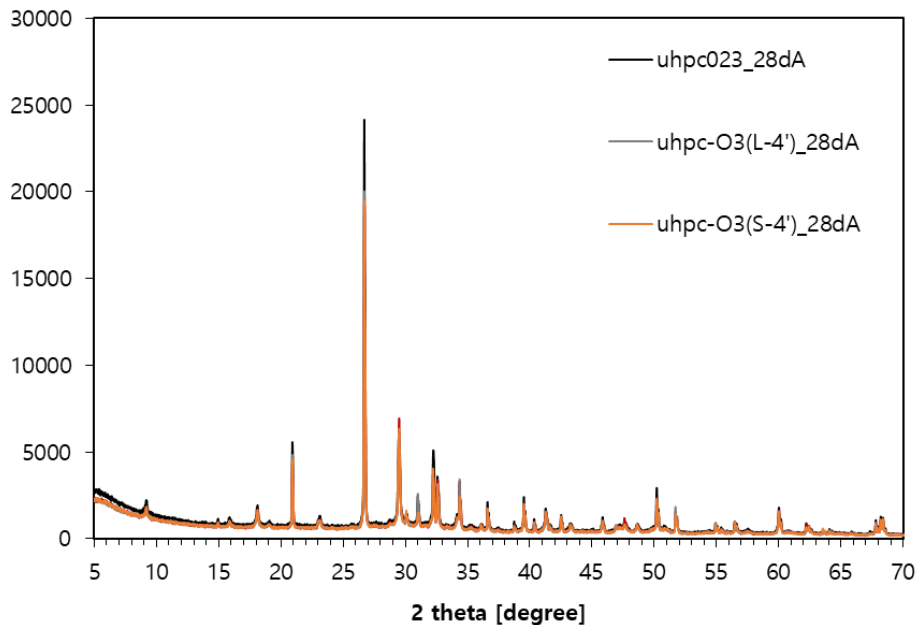


Figure 3-16. XRD Results of hydration suspended samples after 28 days

The analysis on specimen after 28 days shows that the amount of ettringite (at angle 8°) and portlandite (at angle 18°), the cement hydrate, is nearly same regardless of ozone water concentration. Also, checking the ratio of alite to determine whether or not the initial strength of cement compounds is expressed (30°) shows that all experimental groups have similar peaks and Belite to long-term intensity have similar peak to all experimental groups.

Consequently, it can be inferred that ozone has little or no effect on the hydration and pozzolan reactions of cementitious material. In other word, due to the rapid volatility of ozone water itself, the ozone in the cement paste evaporated after being casted. It represents the same chemical composition as the general UHPC.

3.6.4.2 TG Analysis

The result of TG analysis of each experimental group with suspension of hydration reaction on 1st day after manufacture is shown in **Figure 3-17**.

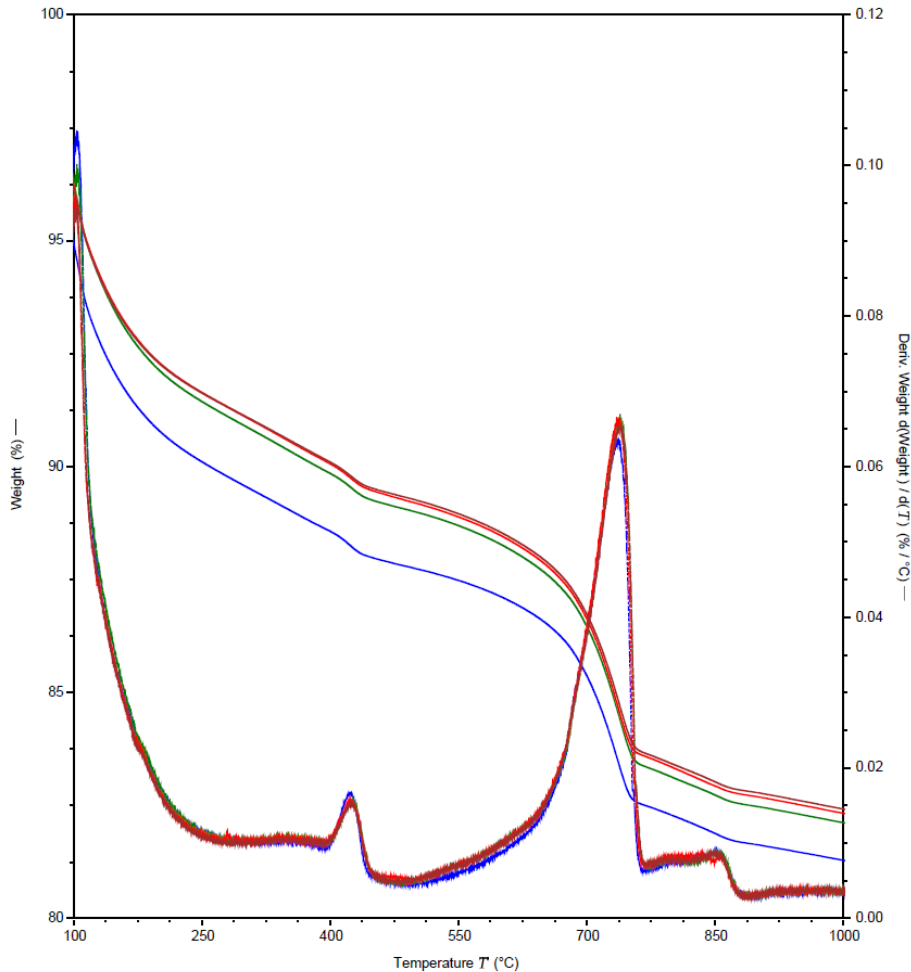


Figure 3-19. TG analysis of hydration suspended samples after 28 days

Note in the graph above is the DTG curve caused by the burning of cement compounds due to high heat. The two peaks represent portlandite and calcite respectively, and it can be seen that the peaks formed in all experimental groups are identical. This is consistent with the results of the XRD experiment and proves that the effects of ozone water disappear after several days of casted.

3.7 Summary

The results of experiments are summarized as follows:

1. The use of ozone water as a mixture of UHPCs may improve physical properties, including initial compressive strength and fluidity.
2. However, the effects of ozone water are lost when exposed to room temperature environments for a long time or when heat is applied to cementitious material.
3. According to the machine learning methods, If O3-UHPC is produced using ozone water with a certain concentration (0.55g/ml), the compressive strength may be less expressed than general UHPC.
4. By hydration reaction test, XRD, and TG analysis, the chemical composition of O3-UHPC, which is 1 and 28 days after casted, confirm that there is no difference from the general UHPC.

When O3-UHPC is applied to the site, it is difficult to achieve effects by vaporizing them within hours when producing UHPCs using ozone water at room temperature. Therefore, it is necessary to slow the vaporization of ozone in the mixed water by cooling the materials needed for making UHPC.

Finally, when producing cement materials using ozone water, it is necessary to prevent the vaporization of ozone present in ozone water. Therefore, it is necessary to develop techniques to maintain the material properties of ozone water itself by keeping the temperature of the surrounding environment low or by producing high concentrations of ozone water initially.

Chapter 4. Advisable UHPC-CNT Composite Material Production Method

This chapter is aimed at identifying the effects of CNTs on general UHPC and ozone water on UHPC-CNT composites by comparing material properties. Specifically, mechanical properties, including compressive strength and flow of cement paste produced by ozone water and CNTs, and chemical properties of UHPC-CNT composite using isothermal calorimetry, XRD and TG results were compared with the general UHPC.

Compressive strength test and machine learning results show that the compressive strength of UHPC has increased slightly due to proportion of CNTs in UHPC-CNT composite. Also, the flow rate of UHPC cement paste produced by using CNTs is improved than general UHPC.

In chemical composition analysis, it can be seen that the timing of hydration reaction and the chemical structure of the paste are clear by mixing CNTs. This can be inferred from CNTs helped accelerate hydration and expressed earlier. In addition, the XRD and TG results show that when manufactured by mixing CNTs into UHPC, it produces a larger amount of cement compounds than a general UHPC.

Finally, when ozone water and CNTs are applied to UHPC at the same time, it can be inferred that highest compression strength is expressed when the concentration of ozone water is 0.4 g/ml and CNTs proportion is 0.2%, and it can be seen that the properties of both compounds are normally expressed.

4.1 Introduction

In this chapter, powder type CNTs used to produce UHPC-CNT composite and properties of experimental group by CNTs proportion specimens and 2 different production process were introduced. After the overall composition of experiment, mechanical and chemical properties of composite materials are mainly compared with general UHPC.

In particular, after data mining the compressive strength test, the polynomial regression, *k*-NN regression and decision tree techniques were performed to identify appropriate CNTs proportion and ozone concentration that can maximize the mechanical properties of UHPC-CNT composite using 3-dimensional regression model. Python codes to implement ML techniques are introduced in appendix.

4.2 Parameters of Study

Identifying the mechanical properties, not only determine compressive strength of UHPC-CNT composite but also measured the state mechanical properties. The conditions of the specimen's placement and curing are the same as those set by O3-UHPC. To check the flow of the UHPC specimen, flow test was conducted immediately after the completion of cement paste mixing.

For samples used in hydration reaction test, XRD, TG analysis to identify the chemical properties of the specimen, the curing conditions are same but are mixed except silica sands. The hydration reaction of samples produced under this condition was stopped 1 and 28 days after the mixing was completed to check the chemical composition of the specimen at certain times.

Chapter 4. Advisable UHPC-CNT Composite Material Production Method

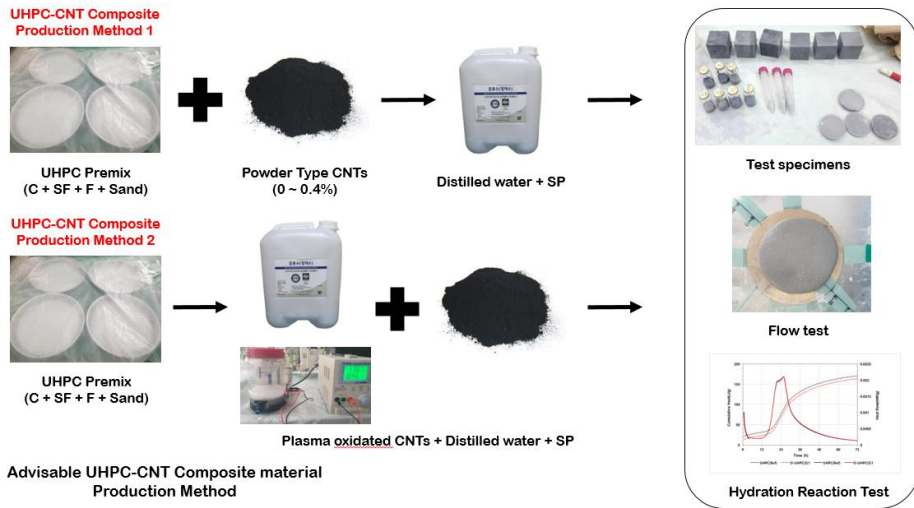


Figure 4-1. Graphical abstract of chapter 4

4.3 Material Properties

In this study, commercially available multi-walled CNTs powder (LUCAN BT1003, LG Chem., Ltd., Korea) produced with chemical vapor deposition (CVD) method were used and their properties are listed in Table 4-1.

Since CNT's own structure were strongly attracted each other and cause cohesion within cement paste [15], it produces composite materials with different timing of adding CNTs and proportion of CNTs should low by weight ratio of cement.



Figure 4-2. Powder type multi-wall CNTs

Table 4-1. Properties of multi-wall CNTs

Avg. length (μm)	Avg. diameter (nm)	Bulk density (g/cm^3)	Purity (wt.%)	Specific surface area (m^2/g)
12	13	0.12	96	186

4.4 Fabrication of Specimens

In order to confirm mechanical properties of UHPC-CNT composite, cement paste of experimental group casted a cube mold with a length of 50mm and then cured at 20 °C and RH of 60% in a chamber by one day. UHPC-CNT composite mix proportion table by weight ratio of cement for each experimental group is shown **Table 4-2**.

Table 4-2. Mix proportion of UHPC-CNT composite experimental group

Experimental Group	W	SP	C	SF	F	Sand	CNTs
UHPC (Reference)	0.23	0.04	1	0.25	0.35	1.1	0
UHPC-CNT 0.05%							0.0005
UHPC-CNT 0.1%							0.001
UHPC-CNT 0.2%							0.002
UHPC-CNT 0.4%							0.004

(W: water, SP: superplasticizer, C: white cement, SF: silica Fume, F: silica powder)

In particular, an additional O3-UHPC experimental group with 0.1% and 0.2% of CNT was established among the experimental groups set up in Table 4-2 to identify the complex effects of ozone water and CNT on UHPC.



Figure 4-3. Experiment samples after curing

Specimens of each experimental group for hydration reaction test, XRD, and TG analysis, were manufactured in the same way as the O3-UHPC experiment. and the experimental group containing ozone water should block contact with the outside air or stop hydration, especially before the ozone vaporization occurs.

4.5 Test Set-up and Instrumentation

4.5.1 Test Conditions

All physical and chemical experiments were classified into control groups, general UHPC, and experimental groups of UHPC-CNT composites with different CNTs proportion, especially indoors with room temperature maintained at 20 °C when conducting hydration reaction tests.

4.5.2 Compressive Strength Test

For the compressive strength test, a number of cube specimens were produced to apply machine running techniques to the test results and UHPC-CNT composites was produced using certain proportion of CNTs to reduce bias of models produced by the experimental results.

Table 4-3. Number of compressive strength test data

Experimental Group	CNTs Proportion (%)	Number of Data
UHPC (Reference)	0	36
UHPC-CNT composite	0.05	27
	0.1	36
	0.2	36
	0.4	27
O3-CNT composite	0.1	27
	0.2	27
Total (Day 1, Day 28, Steam Curing)		216 (= 162+54)

Compressive strength of the samples was measured at day 1, day 28 and day 3(after steam curing). Compressive strengths of each experimental group were calculated with the same guidance as the O3-UHPC experiment.

4.5.3 Flow Test

Flow tests were performed in accordance with same test configuration which established in O3-UHPC experiment. to measure the flow rate of cement paste by each experimental group.

The mold used for flow test is 70 mm diameter on the top and 100 mm diameter on the bottom, and test was conducted on circular plate with a diameter of 250 mm. In particular, when CNT is mixed with cementitious materials at a high rate, it should give attention because it may take long time for the CNT to be poured into the experimental plate by combination with the cement internal microstructure.

4.5.4 Hydration Reaction Test

After the mixing is completed, UHPC cement paste will enter initial set where liquidity decreases within a few days. In this experiment, isothermal calorimetry was measured for 72 hours using same device which used in O3-UHPC experiment.

4.5.5 X-ray Diffraction (XRD), Thermogravimetric (TG) Analysis

For quantitative analysis of the chemical composition of cement compounds, hydration suspension was performed after room temperature curing for a period set in each experimental group. In particular, for XRD experiments, the proportion of quartz was adjusted equally to confirm the changed chemical composition due to CNTs.

In case of TG experiments, test specimens one day after casting were used to check the amount of cement compound due to high heat when creating TG and DTG curves. Specifically, the amount of portlandite and C-S-H and ettringite changed by the CNTs is determined by identifying peak at approximately 140°C and 700°C after the start of experiment.

4.6 Test Results

4.6.1 Compressive Strength

The mean compressive strength of general UHPC, UHPC-CNT composite produced by mixing different proportions of powder type CNTs is shown in **Figure 4-4**.

Unlike O3-UHPC, it can be seen that all experimental groups with CNT mixed together are expressed higher than general UHPC. In particular, proper adjustment of the CNT mixing ratio can be seen to produce compressive strength similar to general UHPC made with steel fibers. In addition, compressive strength of high temperature steam cured UHPC-CNT composite is significantly higher than that of room temperature curing specimens, such as O3-UHPC test results.

It can be inferred from micro-structure of multi-wall CNTs. If an adequate amount of dissolved water is mixed with cement, CNTs become agglomerated to inner structure of cementitious material. Because of this reaction, it can affect the initial intensity expression by promoting hydration reaction in cement paste.

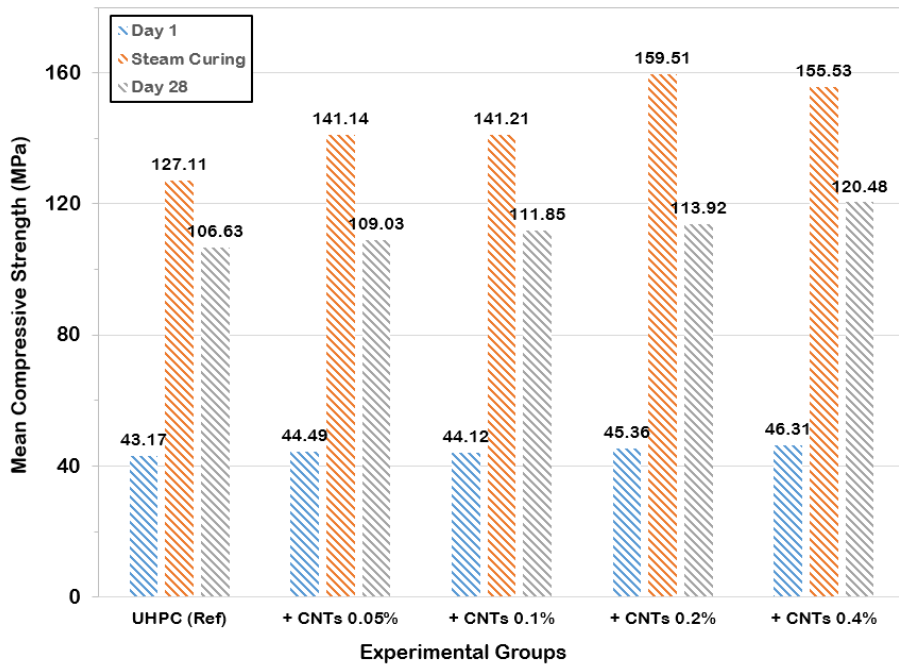
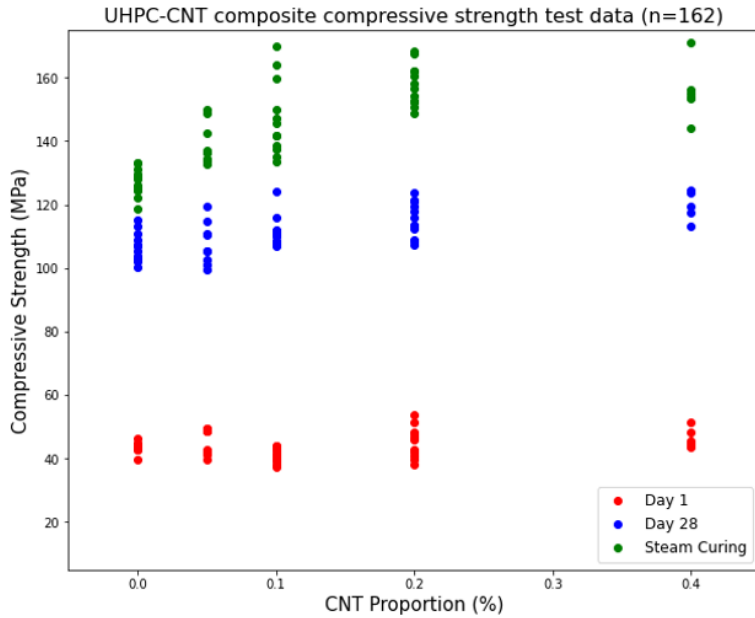


Figure 4-4. Mean Compressive strength of each experimental groups

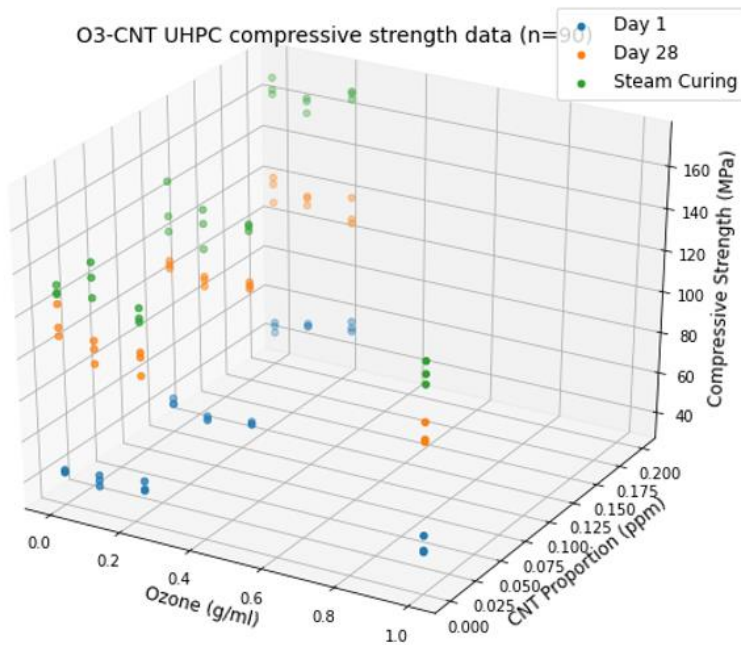
4.6.1.1 Processed Data by Machine Learning

Like applying ML techniques in O3-UHPC test, this experiment applied based on a number of compressive strength experimental data to accurately determine the effect of CNTs on compression strength. Also, 3-dimensional model were designated to find relationships between compressive strength with CNT proportion and ozone concentration. The distribution of compressive strength of O3-UHPC for each experimental group is shown in Figure 4-5.

Ch. 4. Advisable UHPC-CNT Composite Material Production Method



(a)



(b)

Figure 4-5. Distribution of compressive strength data for each experimental group ((a) UHPC-CNT composite and (b) O3-CNT UHPC)

Chapter 4. Advisable UHPC-CNT Composite Material Production Method

- Polynomial Regression

In the same way of O3-UHPC compressive strength analysis, polynomial regression analysis was conducted for each experimental groups in UHPC-CNT composite. Also, identifying the suitability of the regression model and improvements in the model and data for each experimental group by checking learning curves of linear to 4th-order polynomial regression.

In particular, to perform a regression analysis of O3-UHPC dealing with three-dimensional data, it should be represented by a regression plane rather than a regression curve, and the effects of UHPC on two variables can be determined by the sign of the legal line vector in the plane.

Through this, it is possible to determine the trend of compression strength according to the proportion of CNTs, which isn't performed experiment with higher mix proportion. Based on the results of regression from linear to fourth order, the trend of compressive strength is analyzed based on the results of no over-fitting.

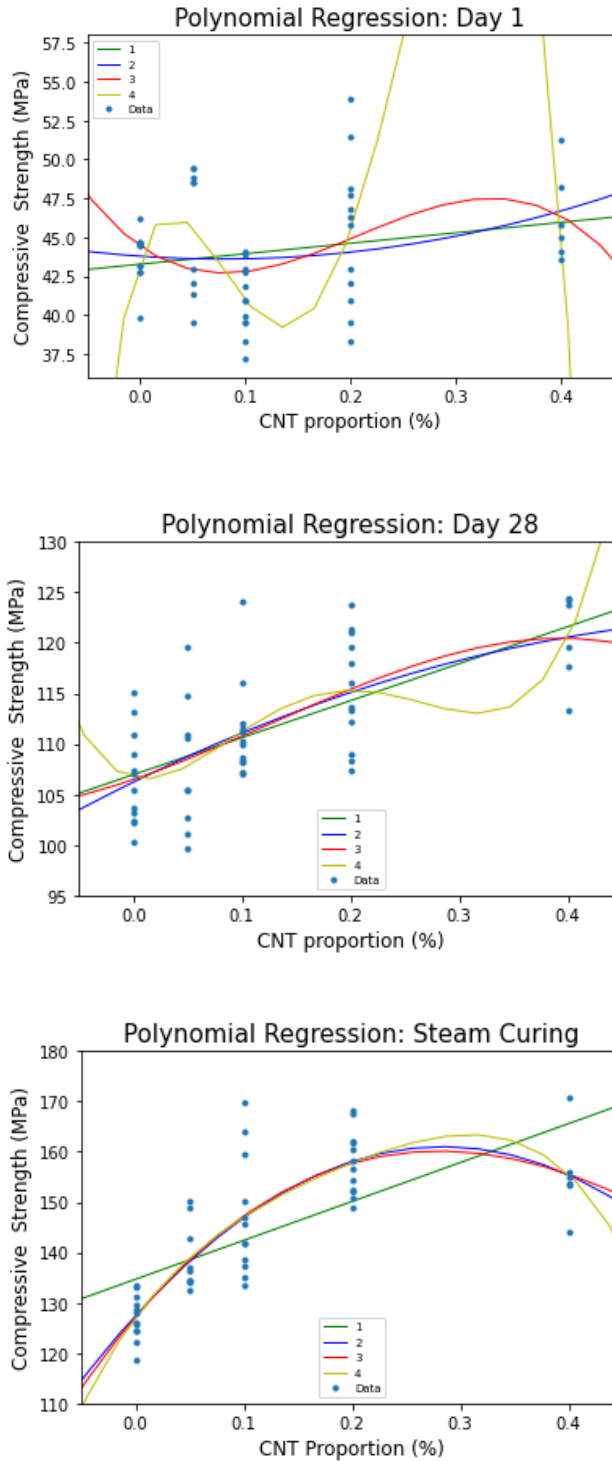


Figure 4-6. Polynomial regression results of UHPC-CNT composite compressive strength

Chapter 4. Advisable UHPC-CNT Composite Material Production Method

As a result of polynomial regression, all experimental groups in UHPC-CNT composite can see that the regression model is over-fitting with the data set if the order of the highest order is greater than or equal to the 4th order. Considering without over-fitting, linear and second order regression suggests that higher the concentration of ozone, the compressive strength of the UHPC-CNT composite which produced after 1 day and steam cured was increased.

It can be inferred that this phenomenon caused by difference of curing methods. During room temperature curing, ozone dissolved in ozone water evaporates and bubbles can occur during the process of dropping out of the cement paste, which can affect the cement microstructure.

- Regression Plane analysis of O3-CNT composite

Unlike previous 2-dimensional analysis, plotting regression plane for three-dimensional experimental data to check the behavior of UHPC compression strength with the mixing rate of ozone water and CNT, dealt with in Chapter 3 and mining additional experimental data. **Figure 4-7** shows the data and regression plane of the O3-CNT composite for each group of experiment.

To determine the concentration of ozone water and mixing rate of CNT's mixture to maximize the compressive strength of O3-CNT composite, divide the experimental data in half and form two different regression planes. After obtaining the parameter equation of the two planes of intersection, apply the configurable constraints on the concentration of ozone water and mixing rate of CNTs to determine the value of both variables when expressing maximum compressive strength.

Ch. 4. Advisable UHPC-CNT Composite Material Production Method

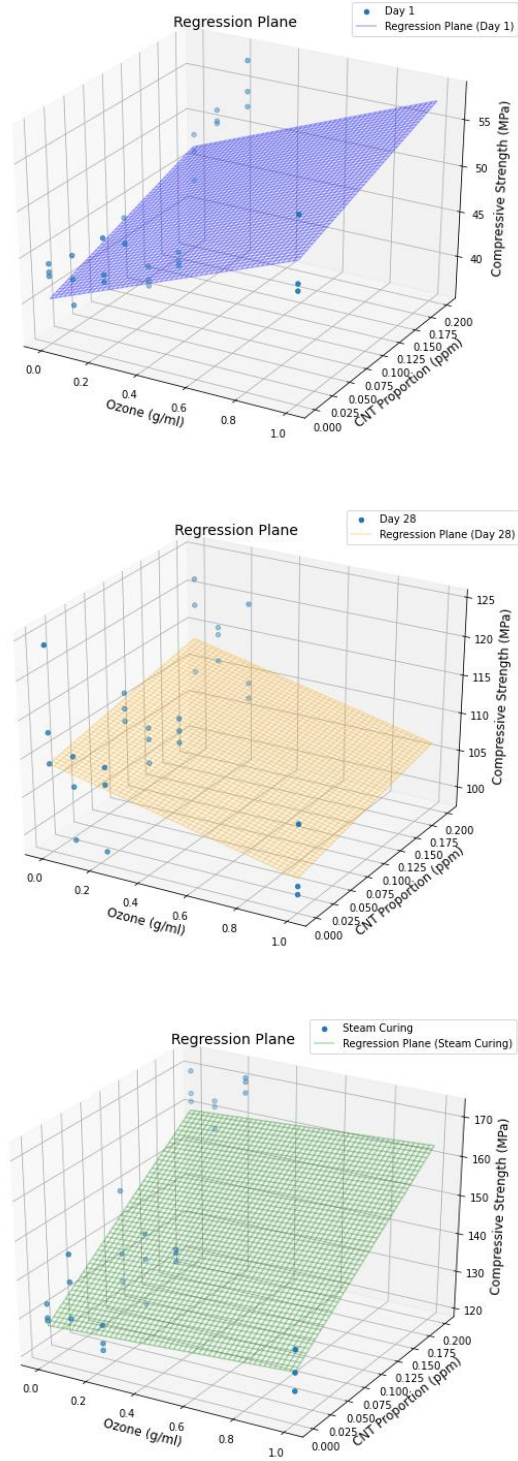


Figure 4-7. Regression planes of O3-CNT composite compressive strength

Chapter 4. Advisable UHPC-CNT Composite Material Production Method

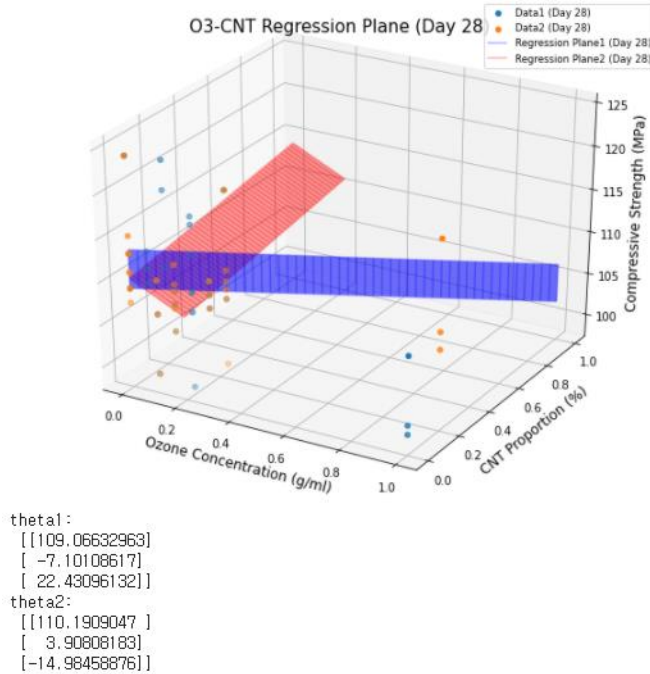
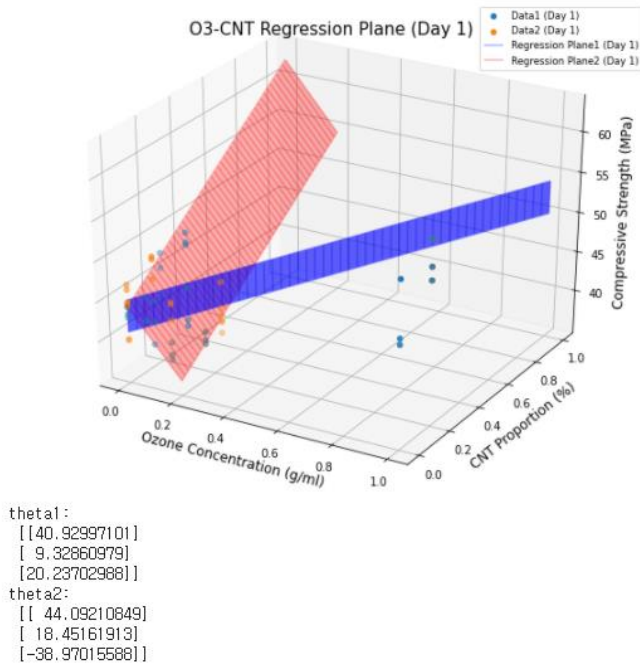
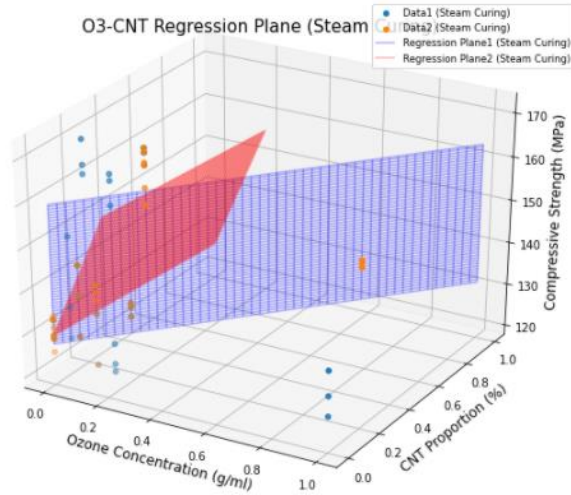


Figure 4-8. Each regression plane and variable(theta) for separated experimental data



```
theta1:
[[127.48642408]
 [ 3.76106679]
 [162.45692922]]
theta2:
[[129.52601665]
 [-3.34950489]
 [151.70223884]]
```

Figure 4-8. (Continued) Each regression plane and variable(theta) for separated experimental data

The equation of the plane calculated from the variables (seta) of the two planes mentioned in **Figure 4-8** is as follows:

Equation of O3-CNT Regression Plane of Day 1:

$$\begin{cases} 9.33x + 20.24y - z + 40.93 = 0 \\ 18.45x - 38.97y - z + 44.09 = 0 \end{cases} \quad (4.1)$$

Equation of O3-CNT Regression Plane of Day 28:

$$\begin{cases} -7.1x + 22.43y - z + 109.07 = 0 \\ 3.91x - 14.98y - z + 110.19 = 0 \end{cases} \quad (4.2)$$

Equation of O3-CNT Regression Plane of Steam curing:

$$\begin{cases} 3.76x + 162.46y - z + 127.49 = 0 \\ -3.35x - 151.7y - z + 129.53 = 0 \end{cases} \quad (4.3)$$

Chapter 4. Advisable UHPC-CNT Composite Material Production Method

From now on, use the two regression planes to calculate the concentration of ozone water and the rate of CNT mixture, which express the maximum compressive strength of O3-CNT composite materials for each experimental group. This chapter covered the computation process for the experimental group of Day 1, and only the results of the same process of Day 28 and steam curing group were introduced.

First, the positional relationship between two regression planes is determined by dot product of each plane's normal vector. Equation (4.4) states that the dot product result of two normal vector is not zero, so the two planes have intersection.

$$(9.33 \times 18.45) - (20.24 \times 38.97) + 1 = -610.1495 \neq 0 \quad (4.4)$$

Second, find point of intersection assume $z = 0$. By solving 1st-order simultaneous equation. Result can be easily obtained by matrix operations.

$$\begin{cases} 9.33x + 20.24y = -40.93 \\ 18.45x - 38.97y = -44.09 \end{cases} \quad (4.5)$$

$$\begin{bmatrix} x \\ y \end{bmatrix} = \begin{bmatrix} 9.33 & 20.24 \\ 18.45 & -38.97 \end{bmatrix}^{-1} \begin{bmatrix} -40.93 \\ -44.09 \end{bmatrix} = \begin{bmatrix} -3.36 \\ -0.45 \end{bmatrix} \quad (4.6)$$

$$(-3.36, -0.45, 0) \quad (4.7)$$

Third, obtain the directional vector of the intersection using cross product of the normal vector of the two planes. Then, the parameter equation of intersection is obtained using direction vector and a point on the intersection.

$$\begin{aligned} \mathbf{u} &= (9.33, 20.24, -1), \quad \mathbf{v} = (18.45, -38.97, -1) \\ \mathbf{u} \times \mathbf{v} &= \begin{vmatrix} 20.24 & -1 \\ -38.97 & -1 \end{vmatrix} \mathbf{i} - \begin{vmatrix} 9.33 & -1 \\ 18.45 & -1 \end{vmatrix} \mathbf{j} + \begin{vmatrix} 9.33 & 20.24 \\ 18.45 & -38.97 \end{vmatrix} \mathbf{k} \\ &= (-59.21, -9.12, -737.02) \end{aligned} \quad (4.8)$$

$$\begin{cases} x = -59.21t - 3.36 \\ y = -9.12t - 0.45 \\ z = -737.02t \end{cases} \quad (4.9)$$

Ch. 4. Advisable UHPC-CNT Composite Material Production Method

Finally, obtain intersection by applying the constraints set by ozone concentration and CNTs proportion variable. The concentration of ozone water (variable x) is set from 0 to 1.3 g/ml and the CNTs proportion (variable y) from 0 to 0.2% in this experiment. Then, apply the obtained intersection to each variables and earn each interval of ozone, CNTs and compressive strength in accordance.

$$\begin{cases} 0 \leq -59.21t - 3.36 \leq 1.3 \\ 0 \leq -9.12t - 0.45 \leq 0.2 \end{cases}$$

$$\therefore -0.07 \leq t \leq -0.056 \quad (4.10)$$

$$\begin{aligned} -0.044 &\leq x \leq 0.785 \\ 0.061 &\leq y \leq 0.188 \\ 41.27 &\leq z \leq 51.59 \end{aligned} \quad (4.11)$$

The above series of calculations show that if the concentration of ozone water is 0.785 g/ml and the CNT mixture is 0.188%, the compressive strength of O3-CNT, one day after room temperature curing, is expressed 51.59 MPa.

When this calculation process is applied to 28th day group and steam curing group, the results are shown in equation (4.12).

(Calculation process is shown in appendix.)

$$\begin{aligned} -0.004 &\leq x \leq 0.033 \\ 0.188 &\leq y \leq 0.195 \\ 109.46 &\leq z \leq 109.47 \\ \\ 0.108 &\leq x \leq 0.408 \\ -0.002 &\leq y \leq 0.197 \\ 120.38 &\leq z \leq 151.59 \end{aligned} \quad (4.12)$$

Chapter 4. Advisable UHPC-CNT Composite Material Production Method

Note that the effective periods represented by each of the three groups of experiments have a common resolution of about 0.2% for CNTs, while for the ozone concentration, results for room temperature curing and steam curing are independent.

This can be attributed to properties of the ozone water. As the results of the experiments on the ozone water itself in Chapter 3, low concentration of ozone water (0.03 g/ml) was calculated as the maximum effective concentration. because the ozone inside the ozone water evaporates and becomes similar to the general UHPC.

On the other hand, steam curing can have positive effect on ozone due to short period of time to curing. It can be inferred that the minimum concentration of ozone water is higher (0.108 g/ml) than the maximum effective concentration at room temperature curing.

Therefore, considering the common part of the concentration zone and the CNT mixture calculated in equation 4.11 and 4.12, it can be inferred that compressive strength of the UHPC is maximized when the concentration of ozone is 0.4 g/ml and proportion of CNTs is approximately 0.2%.

In particular, when steam curing process is applied, expected compressive strength of O₃-CNT composite is close to 150 MPa, indicating that an appropriate amount of ozone and CNTs can express compressive strength to satisfy UHPC standards.

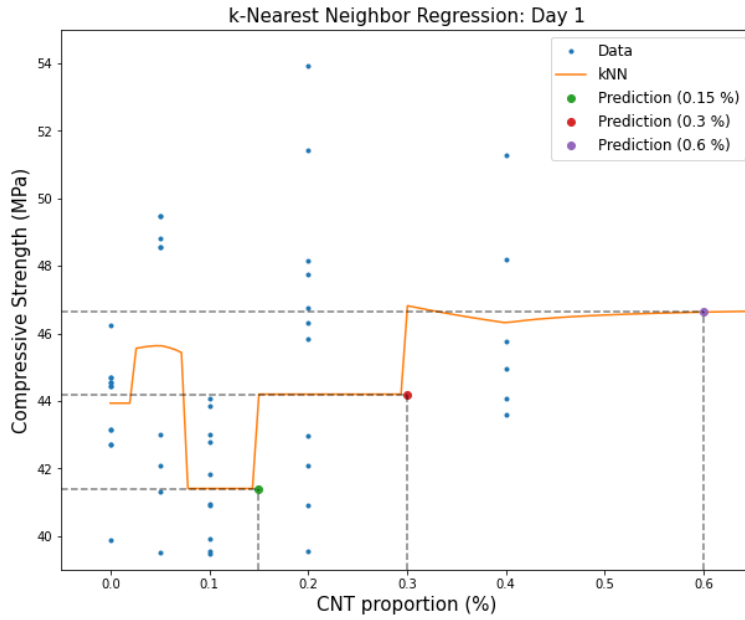
- *k*-NN Regression

To validate the results of the polynomial regression, *k*-NN regression was conducted focusing on the local results of the peripheral data instead of the distribution of the overall data set itself.

To fully reflect the relationship with locally distributed experimental data, 10 neighboring experimental data were set up as populations and then re-analyzed. Based on this analysis, the compressive strength of UHPC produced by CNTs at a specific concentration (0.15, 0.3 and 0.6 %) was predicted.

Ch. 4. Advisable UHPC-CNT Composite Material Production Method

Prediction (0.15 %) = 41.4 MPa
Prediction (0.3 %) = 44.2 MPa
Prediction (0.6 %) = 46.63 MPa



Prediction (0.15 %) = 111.88 MPa
Prediction (0.3 %) = 116.3 MPa
Prediction (0.6 %) = 119.27 MPa

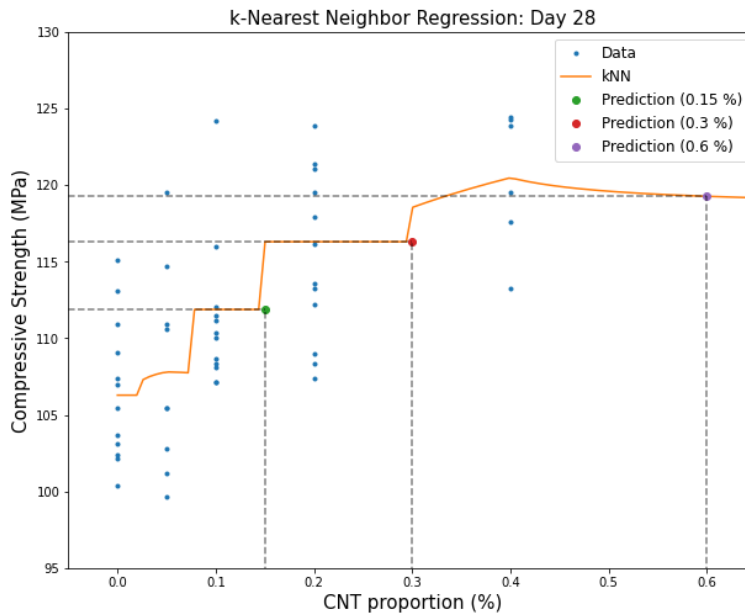


Figure 4-9. *k*-NN regression results of UHPC-CNT composite compressive strength

Prediction (0.15 %) = 143.05 MPa
Prediction (0.3 %) = 157.32 MPa
Prediction (0.6 %) = 155.72 MPa

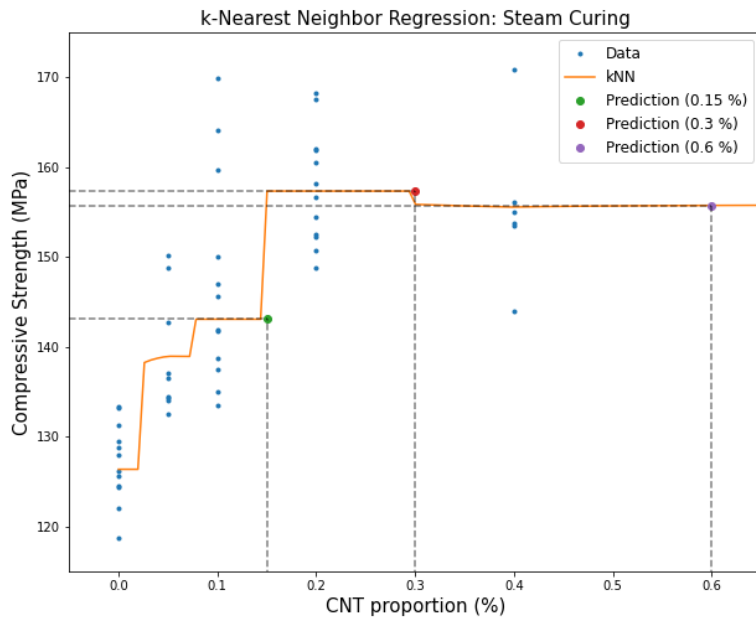


Figure 4-9. (Continued) k -NN regression results of UHPC-CNT composite compressive strength

k -NN regression shows that UHPC-CNT composite in areas without experimental data shows that the higher proportion of CNTs, regardless of the curing method, the compressive strength unchanged or increase significantly.

In particular, it can be seen that the compressive strength greatly increases when CNT is mixed with both the 28th day room temperature curing and the high temperature curing experimental group.

- Decision Tree Method

This method was used to check boundaries of the compressive strength in certain CNTs proportion period. The index for dividing sections was based on the MSE used in k -NN regression, and the proportion ratio was subdivided in four stages.

Ch. 4. Advisable UHPC-CNT Composite Material Production Method

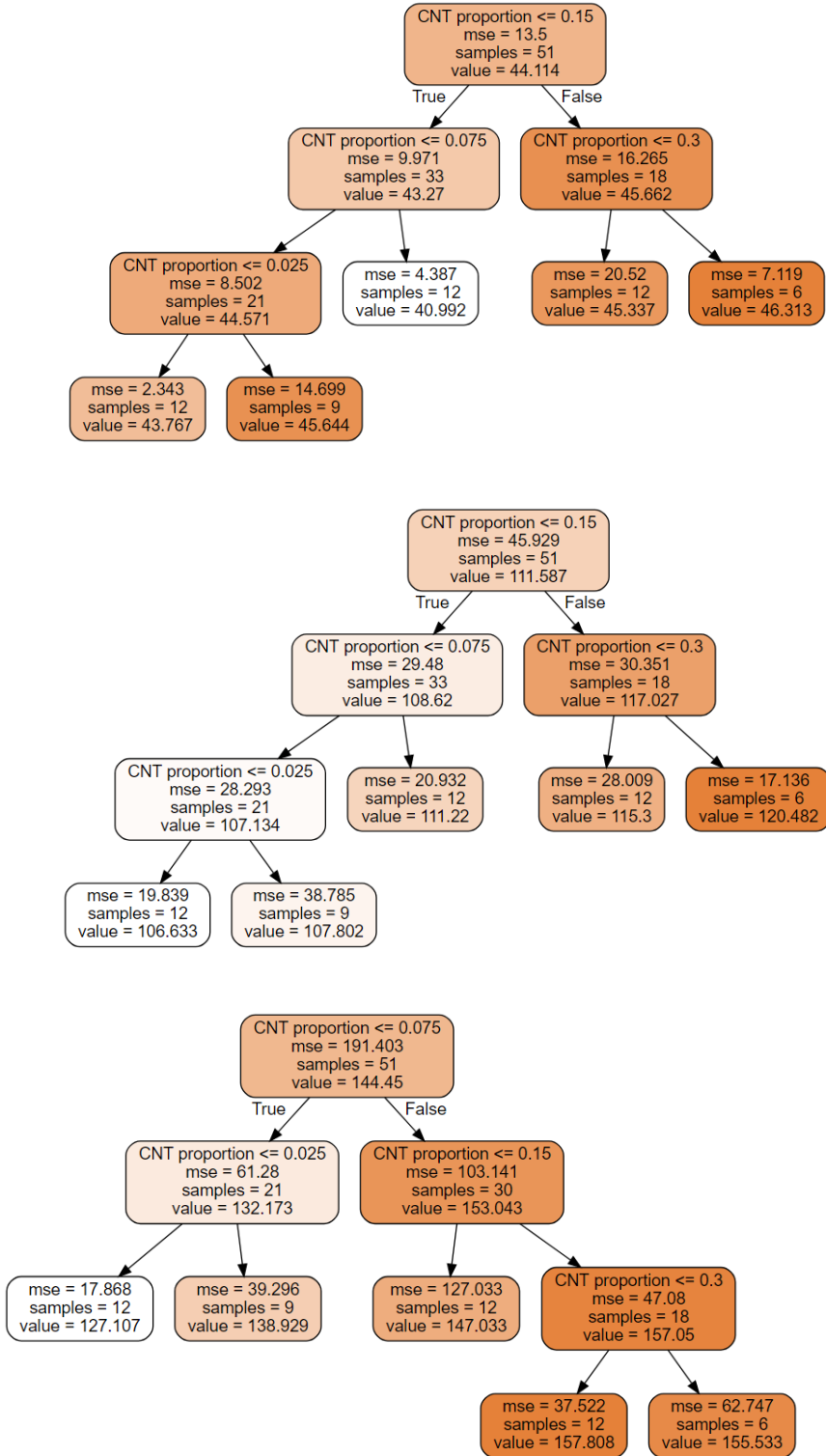


Figure 4-10. Decision tree results of UHPC-CNT composite

Chapter 4. Advisable UHPC-CNT Composite Material Production Method

As a result of performing decision tree method, the leaf nodes in the decision tree of all experimental groups represents same group sizes and decision tree form of all experimental groups is skewed in one direction according to CNTs proportion.

On the other hand, leaf nodes with MSE greater than half the predicted compressive strength value were created in steam cured UHPC-CNT composite specimens. This means that the interval included an outlier, which cause MSE to rise significantly. To address this, the data belonging to that section should be classified in a more granular step.

In finalizing the analysis of the compressive strength by ozone concentration of UHPC-CNT composite through three machine learning techniques, the following conclusion can be obtained.

- Polynomial regression suggest that CNTs increase the initial intensity of UHPC, also, if steam curing is used, high compressive strength can be achieved without steel fiber.
- Regression plane of O3-CNT composite suggest that regardless of curing method, CNTs have positive effects on intensity of UHPC. To maximize mechanical properties, concentration of ozone is 0.4 g/ml and CNT proportion is approximately 0.2%. Also, it is necessary to finish curing in a short period of time to express ozone water properties.
- According to k -NN regression, compressive strength increases significantly if more than a certain proportion of CNTs is added. Overall, since the regression model takes the form of stairs, this can be seen as an immediate response to the CNT proportion in the UHPC.
- By decision tree method, parameters of each concentration period where compressive strength is expressed can confirmed. Based on this result, If the concentration of CNT is mixed in at a rate of 0.025% or higher, it can be inferred that compressive strength increases significantly and is a reliable model because it has less MSE than ozone water.

4.6.2 Cement Paste Fluidity

To easily distinguish the fluidity of cement paste with concentrations of ozone water, O3-UHPC made from ozone water with concentrations of 0.03, 0.1, and 1.3 g/ml were compared. Flow rate of UHPC cement paste for each experimental group is shown in **Table 4-4** and **Figure 4-11**. In addition, the area of the ellipse was calculated in the same way as the O3-UHPC experiment to identify the fluidity of the experimental group and compared relatively.

Experiments show that if the proportion of CNTs increases, the flow rate of cement paste has decreased. It contrasts with the benefits of improving strength. Especially if more than 0.2% of CNT is mixed, the mixing process will consume a lot of energy and fluidity will begin to drop sharply, suggesting that caution is needed in site construction.

Table 4-4. Flow test result and comparison with general UHPC

Experimental Group	Major axis length (cm)	Minor axis length (cm)	Area (cm²)	Relative ratio
UHPC (Ref.)	24.32	23.95	1829.86	1
UHPC-CNT (0.05%)	21.52	21.19	1432.59	0.78
UHPC-CNT (0.1%)	20.55	20.55	1326.7	0.73
UHPC-CNT (0.2%)	19.33	18.84	1144.1	0.63
UHPC-CNT (0.4%)	16.4	16.29	839.3	0.46

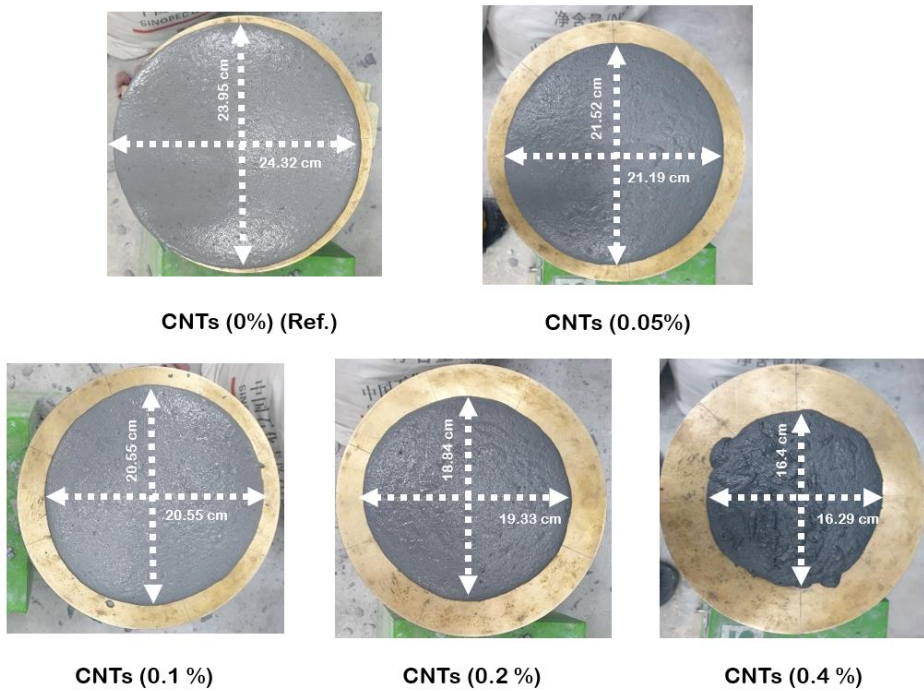


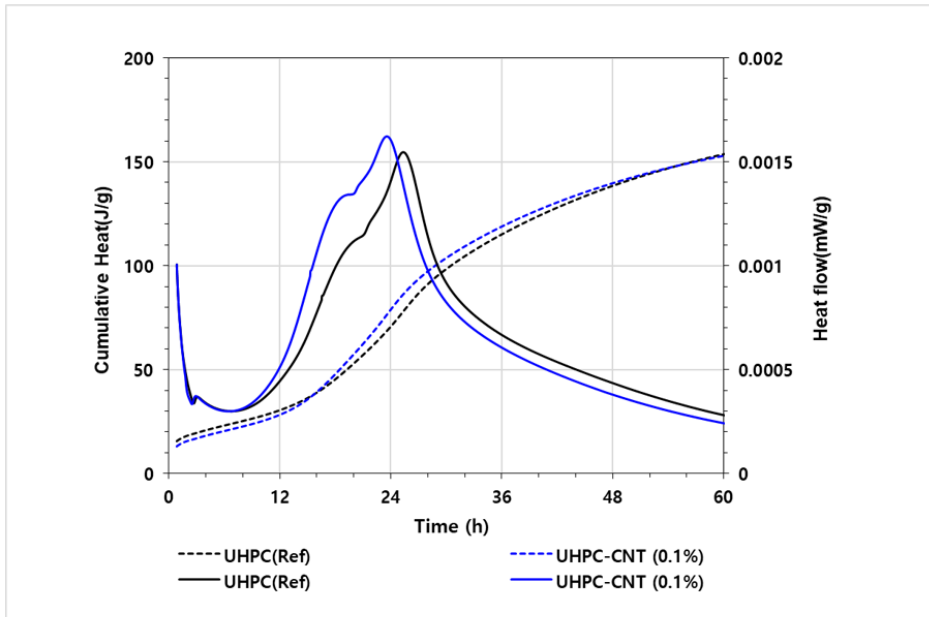
Figure 4-11. Results of flow test of general, UHPC-CNT composite

4.6.3 Hydration reaction at initial period

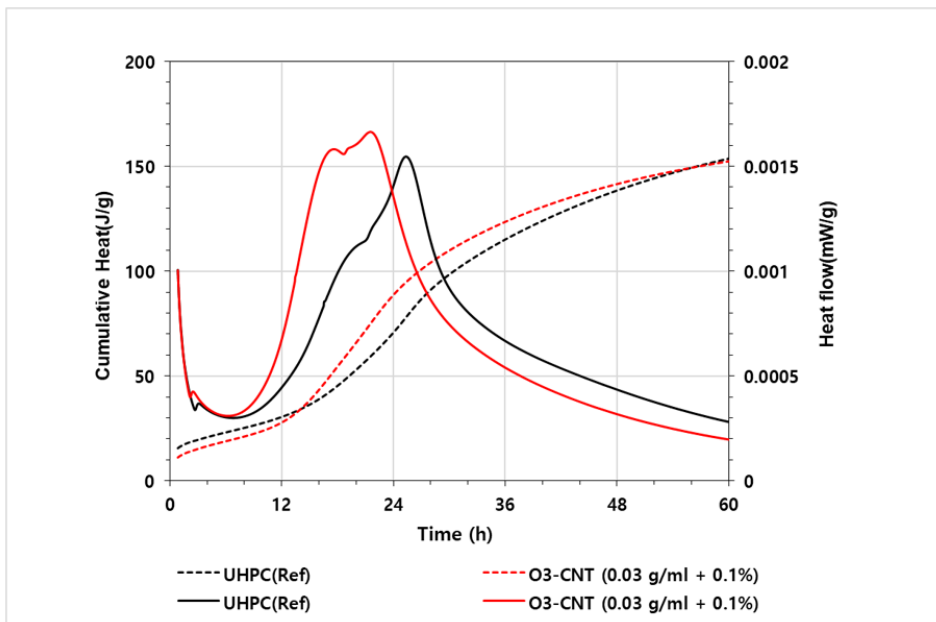
The results of isothermal calorimetry and the numerical values from heat flow curves are presented in **Fig. 4-12** and **Table 4-5**. Experimental methods and precautions are same as O3-UHPC experiment.

As a result, the hydration reactions of general UHPC and UHPC-CNT proportion produced with 0.1 g/ml concentrated water show that neither experimental group had significant differences. Also, O3-CNT, produced from ozone water with 0.1 g/ml, and CNTs proportion with 0.1% and 0.2% also shows almost the same heat flow as a normal UHPC.

The reason for this phenomenon is that the hydration reaction test is performed at a relatively high temperature (20 °C). Due to the nature of ozone water, it can be dissolved in water for longer periods of time at low temperatures (4°C). Therefore, if the experiment continues at room temperature (more than 4°C) for more than a few hours, the material properties of ozone water UHPC can easily disappear.



(a)

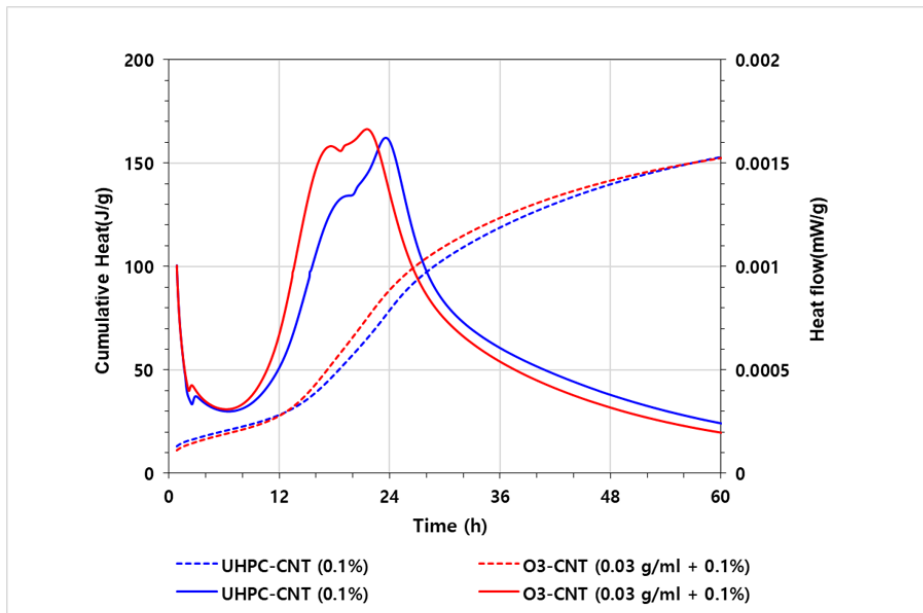


(b)

Figure 4-12. Cumulative heat and heat flow curve comparison (CNTs, O3-CNT)

((a): UHPC-CNT composite with CNTs 0.1%)

((b): UHPC with O3-CNT (ozone 0.03 g/ml and CNTs with 0.1%)



(c)

Figure 4-12. Cumulative heat and heat flow curve comparison (CNTs, O3-CNT)

(Continued) ((c): UHPC-CNT with 0.1% with O3-CNT))

Table 4-5. Numerical values from heat curve of experimental groups

Experimental Group	Minimum heat flow (W/g)	Initial period of acceleration (h)	Slope (W/g · h)
UHPC (Ref.)	0.0002998	6.842	4.38×10^{-5}
UHPC-CNT (0.1 %)	0.0002896	6.814	4.25×10^{-5}
O3-CNT (0.1 g/ml + 0.1%)	0.0002993	6.435	4.65×10^{-5}

4.6.4 Chemical Component Analysis

The chemical component test with CNTs used room temperature curing method for 28 days to check the progress of hydration reactions of cement compounds. Also, matching the peak of the XRD experimental results, the more accurate the amount of compounds can be compared.

As TG analysis results only partially (30g) after shredding the suspended samples, many experiments need to be carried out on the same group of subjects to avoid bias in the analysis. In addition, it may be difficult to compare the exact amount of cement compounds if the slope of the curve occurs in the temperature period where there should be no response in the DTG curve results.

4.6.4.1 XRD Results

The result of XRD of each experimental group with suspension of hydration reaction on 28th day after manufacture is shown in **Figure 4-13**. To accurately compare the cement hydration products of each experimental group, experiment was repeated by matching the quartz peak.

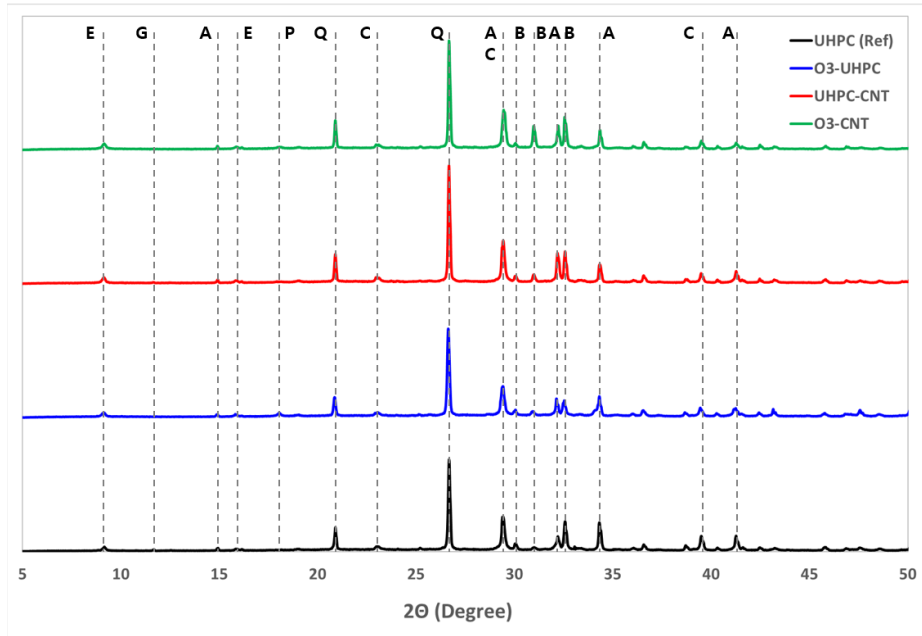


Figure 4-13. XRD Results of hydration suspended samples after 28 days (A : alite,; B : belite; C : calcite; E : ettringite; G : gypsum; P : portlandite; Q : quartz).

Chapter 4. Advisable UHPC-CNT Composite Material Production Method

Experimental results show that the amount of compounds (ettringite at angle 8° and portlandite at angle 18°) produced by hydration reactions in cement represents the same production as general UHPC when only ozone water or CNTs is applied. In particular, O3-UHPC can be found to have about the same chemical composition as typical UHPC, while for UHPC-CNT, the amount of compounds affecting strength (alite and belite at angle $32\sim 33^\circ$) due to CNT has mixed.

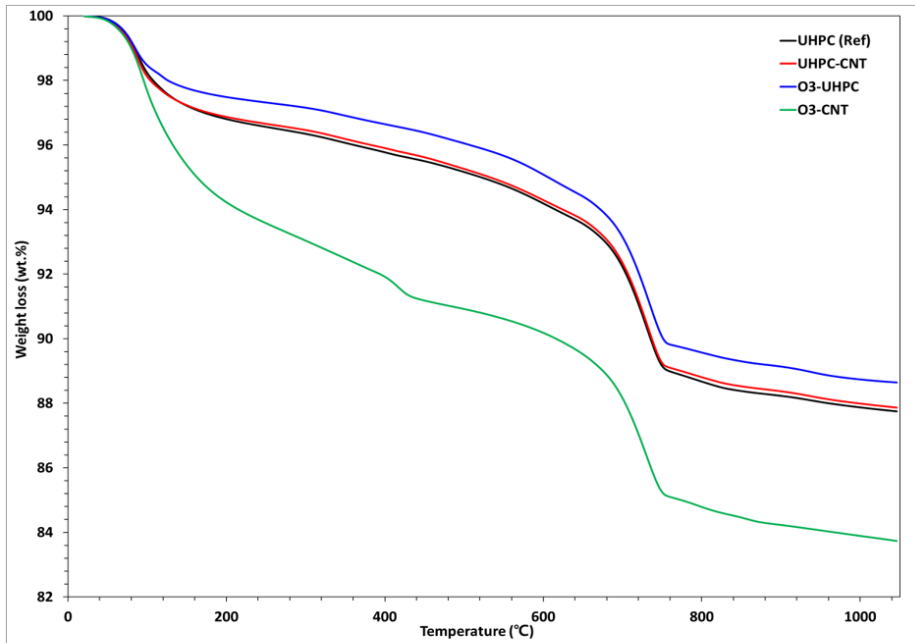
Consequently, the higher proportion of CNTs, the more cement compound(alite) produced which affects initial strength expression are detected. However, ozone did not change the rate of generation of compounds produced by cement hydration. This is because of rapid vaporization of ozone due to generated heat caused by mixing process and ozone properties itself.

4.6.4.2 TG Analysis

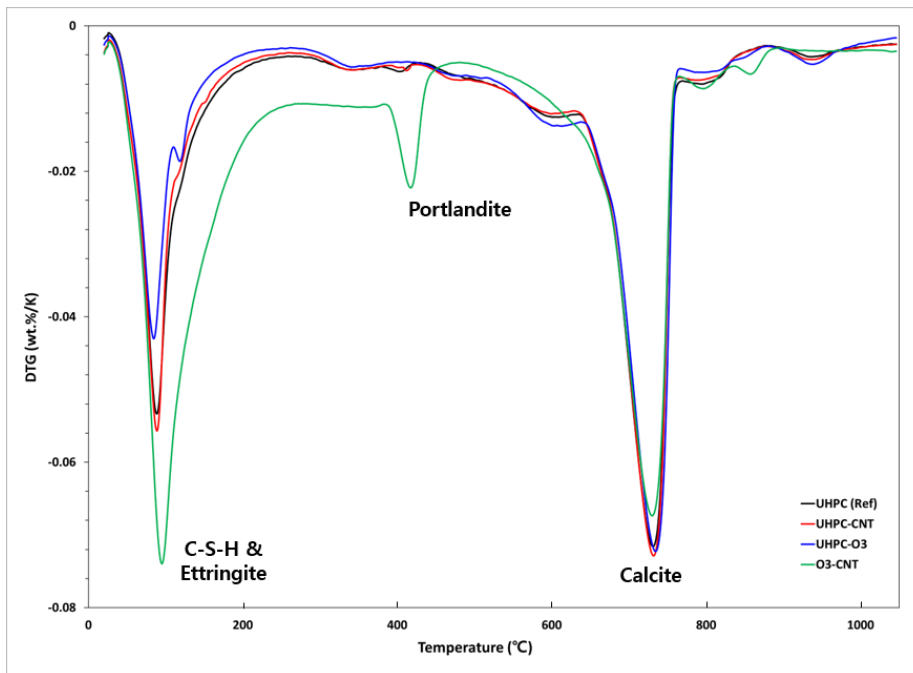
The result of TG analysis of each experimental group with suspension of hydration reaction on 28th day after manufacture is shown in **Figure 4-14**. The concentration of ozone water used in the experiment was 0.03 g/ml and the amount of CNT was mixed with 0.1% of the weight of cement.

According to TG curve, for composite materials produced by adding only ozone water or CNTs to UHPC, it can be found that the reduction in weight by heat is similar to or slightly less than general UHPC. However, for O3-CNT produced by applying both ozone and CNT, the reduction in weight by heat is noticeably reduced. It can be inferred that two materials are helping the hydration of UHPC if used at the same time.

Ch. 4. Advisable UHPC-CNT Composite Material Production Method



(a)



(b)

Figure 4-14. TG analysis of hydration suspended samples after 28 days

((a) : TG curve; (b) : DTG curve)

4.7 Summary

The results of experiments are summarized as follows:

1. The use of CNTs as a mixture of UHPCs may improve compressive strength but decrease fluidity of cement paste. Therefore, an appropriate amount of CNTs should be mixed to balance the compressive strength and flow rate.
2. O₃-CNT composite suggest that regardless of curing method, CNTs have positive effects on intensity of UHPC. In particular, curing period needs to be shortened for compatibility of ozone water and CNTs, and manufacture of O₃-CNT composite at an appropriate rate can produce compressive strength similar to general UHPC, including steel fibers.
3. According to the machine learning methods, If UHPC-CNT composites produced with a certain proportion (0.025%), the compressive strength expressed significantly than general UHPC.
4. By hydration reaction test, XRD, and TG analysis, the chemical composition of O₃-UHPC, UHPC-CNT composite and O₃-CNT UHPC, which is 28 days after casted, confirm that strength can be improved by facilitating the UHPC's hydration reaction when using ozone and CNT at the same time.

When UHPC-CNT composite is applied to the site, it is difficult to achieve effects by low fluidity within mixing process. Therefore, it is necessary to slow the vaporization of ozone in the mixed water by cooling the materials needed for making UHPC.

In case of in-site application, when producing cement materials using CNTs, it is necessary to prepare fluidizer to case properly in construction site. Therefore, further research should be proceeding to develop techniques to maintain the material properties of CNTs itself by keeping certain concentration of ozone water.

Chapter 5. Concluding Remarks

The aim of this research can be divided into two main objectives, which is identifying the effects of ozone water on UHPC and UHPC-based composite materials. To achieve this, three different UHPCs made with ozone water or CNTs were produced and check physical and chemical properties.

Firstly, Comparing the physical and chemical properties of ozone-UHPC (O3-UHPC) and general UHPC by functional water produced by dissolved ozone. The main purpose of this comparison is to identify and differentiate the changed properties of UHPC produced with ozone water and to establish the overall material characteristics from the production to usability.

As a result, using ozone water as a mixture of UHPCs may improve physical properties, including initial compressive strength and fluidity. But due to the nature of ozone, the effects of ozone water are lost when exposed to room temperature environments for a long time or when heat is applied to cementitious material.

This phenomenon can depict by ML techniques. By decision tree method and k-NN regression, if O3-UHPC is produced using ozone water with a certain concentration (0.55g/ml), the compressive strength may be less expressed than general UHPC. In line with, hydration reaction test, XRD, and TG analysis, the chemical composition of O3-UHPC, which is 28 days after casted, confirm that there is no difference from the general UHPC.

Consequently, when producing cement materials using ozone water, it is necessary to prevent the vaporization of ozone present in ozone water. Therefore, it is necessary to develop techniques to maintain the material properties of ozone water itself by keeping the temperature of the surrounding environment low or by producing high concentrations of ozone water initially.

Secondly, proposing an effective CNTs proportion of UHPC-CNT composite produced by mixing powder-type MWCNTs in UHPC and further analyzed the properties of UHPC-CNT composite produced by dissolving ozone into them using machine learning methods.

Since CNT's own structure were strongly attracted each other and cause cohesion within cement paste, it produces composite materials with different timing of adding CNTs and proportion of CNTs should low by weight ratio of cement.

As a result of ML technique, CNTs increase the initial intensity of UHPC, also, if steam curing is used, high compressive strength can be achieved without steel fiber. But appropriate amount of CNTs should be mixed due to the fluidity of composite decreases drastically.

Regression plane of O₃-CNT composite suggest that CNTs have positive effects on strength of UHPC. To maximize mechanical properties, concentration of ozone is 0.4 g/ml and CNT proportion is approximately 0.2%. Also, it is necessary to finish curing in a short period of time to characterize ozone water properties.

Ch. 5. Concluding Remarks

In case of chemical component test, it can be inferred that the amount of hydration compounds in cementitious material represents the same production as typical UHPC when only ozone water or CNTs is applied. However, for O3-CNT produced by applying both ozone and CNT, the reduction in weight by heat is noticeably reduced. It can be inferred that two materials are facilitating the hydration of UHPC and improve initial and long-term strength.

When UHPC-CNT composite is applied to the site, it is difficult to achieve effects by low fluidity within mixing process. Therefore, it is necessary to slow the vaporization of ozone in the mixed water by cooling the materials needed for making UHPC.

In conclusion, when producing cement materials using CNTs, it is necessary to prepare fluidizer to case properly in construction site. Therefore, it is necessary to develop techniques to maintain the material properties of CNTs itself by keeping certain concentration of ozone water.

References

- [1] Research, Development, and Technology Turner-Fairbank Highway Research Center, Ultra-High Performance Concrete: A State-of-the-Art Report for the Bridge Community (2013), 1-6.
- [2] A.C. 239, ACI 239R-18 Ultra-High-Performance Concrete: An Emerging Technology Report, American Concrete Institute (2018), 3-5.
- [3] Gallard, Hervé; Gunten, Urs von, Chlorination of natural organic matter: kinetics of chlorination and of THM formation, *Water Research*. 36 (2002), 65–74.
- [4] Kwak Kyu-Sung, Seo Hyun-Jae, Miyauchi Hiroyuki, Kim Gyu-Yong, Oh Sang-Keun, A Study on Suggestion of the Evaluation Method of Deterioration of Waterproofing and Corrosion Prevention Materials in Concrete Facility for Advanced Water Treatment Using Ozone(O) Sterilization, *Journal of the Architectural Institute of Korea Structure & Construction* (2010), 79-86.
- [5] Bethune, D. S.; Kiang, C. H.; De Vries, M. S.; Gorman, G.; Savoy, R.; Vazquez, J.; Beyers, R., Cobalt-catalyzed growth of carbon nanotubes with single-atomic-layer walls, *Nature*. 363 (1993), 605–607.
- [6] Iijima, Sumio, Helical microtubules of graphitic carbon, *Nature*. 354 (1991), 56–58.
- [7] B Ribeiro, EC Botelho, ML Costa, CF Bandeira, Carbon nanotube buckypaper reinforced polymer composites: a review, *Polímeros*, (2017).

References

- [8] Yu, M.-F.; Lourie, O; Dyer, MJ; Moloni, K; Kelly, TF; Ruoff, RS, Strength and Breaking Mechanism of Multiwalled Carbon Nanotubes Under Tensile Load, *Science*. 287 (2000), 637–640.
- [9] H Li, X Lu, D Yuan, J Sun, F Erden, F Wang, Lightweight flexible carbon nanotube/polyaniline films with outstanding EMI shielding properties, *Journal of Materials Chemistry C*. 34 (2017).
- [10] JJ Park, ST Kang, KT Koh, SW Kim, Influence of the ingredients on the compressive strength of UHPC as a fundamental study to optimize the mixing proportion, *Ultra High Performance Concrete: (UHPC); Proceedings of the Second International Symposium on Ultra High Performance Concrete, Kassel, Germany, March 05 - 07 (2008)*, 108-109.
- [11] M Alkaysi, S El-Tawil, Effects of variations in the mix constituents of ultra-high performance concrete (UHPC) on cost and performance, *Materials and Structures* volume 49 (2016), 4185-4200.
- [12] R Yang, R Yu, Z Shui, X Gao, X Xiao, Feasibility analysis of treating recycled rock dust as an environmentally friendly alternative material in Ultra-High Performance Concrete (UHPC), *Journal of Cleaner Production*, Vol. 258 (2020).
- [13] J Lee, K Lee, Changes of Adsorption Capacity and Structural Properties during in situ Regeneration of Activated Carbon Bed Using Ozonated Water, *Applied Chemistry for Engineering* Vol. 31 (2020), 341-345.
- [14] B. Del, I. Martin, settings, The Effect of Different Oxygen Surface Functionalization of Carbon Nanotubes on the Electrical Resistivity and Strain Sensing Function of Cement Pastes, *Nanomaterials* Vol.10 (2020).
- [15] M Jung, S Hong, J Moon, Ozone treatment on the dispersion of carbon nanotubes in ultra-high performance concrete, *Materials & Design* Vol.193 (2020).

- [16] W Pu, D Fu, Z Wang, Realizing crack diagnosing and self-healing by electricity with a dynamic crosslinked flexible polyurethane composite, *Advanced Science* Vol.5 (2018).
- [17] EM Gartner, JF Young, Hydration of Portland cement, *Structure and Performance of Cements*, Second Edition (2002).
- [18] SH Kang, Y Jeong, J Moon, The use of limestone to replace physical filler of quartz powder in UHPFRC, *Cement and Concrete Composite* Vol.94 (2018), 238-247.
- [19] P Ziolkowski, M Niedostatkiewicz, Machine learning techniques in concrete mix design, *Materials* Vol.12(8) (2002).
- [20] ASTM C109, Standard Test Method for Compressive Strength of Hydraulic Cement Mortars (2020).
- [21] ASTM C348-20, Standard Test Method for Compressive Strength of Hydraulic Cement Mortars (2020).
- [22] ASTM C1856, Standard Practice for Fabricating and Testing Specimens of Ultra-High Performance Concrete (2017).

Appendix

Appendix. A-1 Polynomial Regression dataset, python codes

```
%matplotlib inline
import matplotlib as mpl
import matplotlib.pyplot as plt
mpl.rc('axes', labelsz=14)
mpl.rc('xtick', labelsz=12)
mpl.rc('ytick', labelsz=12)

import numpy as np
import numpy.random as rnd

m = 200
X = 3 * np.random.rand(m, 1) - 1
y = 2 * X**3 + 0.2 * X**2 + X - 4 + np.random.randn(m, 1)

from sklearn.preprocessing import PolynomialFeatures
poly_features = PolynomialFeatures(degree=2, include_bias=False)
X_poly = poly_features.fit_transform(X)

from sklearn.linear_model import LinearRegression
lin_reg = LinearRegression()
lin_reg.fit(X_poly, y)

X_new=np.linspace(-3, 3, 200).reshape(200, 1)
X_new_poly = poly_features.transform(X_new)
y_new = lin_reg.predict(X_new_poly)

from sklearn.preprocessing import StandardScaler
from sklearn.pipeline import Pipeline

for style, width, degree in (('g-', 1, 10), ('b--', 2, 2), ('r+', 2, 1)):
    polybig_features = PolynomialFeatures(degree=degree, include_bias=False)
    std_scaler = StandardScaler()
    lin_reg = LinearRegression()
    polynomial_regression = Pipeline([
        ("poly_features", polybig_features),
        ("std_scaler", std_scaler),
        ("lin_reg", lin_reg),
    ])
    polynomial_regression.fit(X, y)
    y_newbig = polynomial_regression.predict(X_new)
    plt.plot(X_new, y_newbig, style, label=str(degree), linewidth=width)

plt.title("Polynomial Regression", fontsize=18)
plt.plot(X, y, "b.", linewidth=3)
plt.legend(loc="best")
plt.xlabel("$x_1$", fontsize=18)
plt.ylabel("$y$", rotation=0, fontsize=18)
plt.axis([-1.5, 2.5, -10, 10])
plt.show()
```

Result of the regression calculation using the 2nd order polynomial after generating the data of the 3rd order polynomial:

```
lin_reg.intercept_, lin_reg.coef_
(array([-0.74344944]), array([[1.74835376, 3.75258767]]))
```

$$\hat{y} = 3.75x_1^2 + 1.75x_1 - 0.74$$

```
from sklearn.metrics import mean_squared_error
from sklearn.model_selection import train_test_split

def plot_learning_curves(model, X, y):
    X_train, X_val, y_train, y_val = train_test_split(X, y, test_size=0.2)
    train_errors, val_errors = [], []
    for m in range(1, len(X_train)):
        model.fit(X_train[:m], y_train[:m])
        y_train_predict = model.predict(X_train[:m])
        y_val_predict = model.predict(X_val)
        train_errors.append(mean_squared_error(y_train[:m], y_train_predict))
        val_errors.append(mean_squared_error(y_val, y_val_predict))

    plt.plot(np.sqrt(train_errors), "r--", linewidth=2, label="train")
    plt.plot(np.sqrt(val_errors), "b-", linewidth=3, label="val")
    plt.legend(loc="upper right", fontsize=14)
    plt.xlabel("Training set size", fontsize=14)
    plt.ylabel("RMSE", fontsize=14)

lin_reg = LinearRegression()
plot_learning_curves(lin_reg, X, y)
plt.axis([0, 80, 0, 6])
plt.show()
```

Appendix. A-2 Example of k -NN Regression applied in biased datasets, python codes

```
import numpy as np
import matplotlib.pyplot as plt
%matplotlib inline

G0 = np.random.multivariate_normal([1,1], np.eye(2), 40)
G1 = np.random.multivariate_normal([10,10], np.eye(2), 20)
G2 = np.random.multivariate_normal([20,20], np.eye(2), 40)

X2 = np.vstack([G0,G1,G2])
X2 = np.asmatrix(X2)
print(X2.shape)

from sklearn import neighbors
reg1 = neighbors.KNeighborsRegressor(n_neighbors = 2, p = 2, weights='distance')
reg1.fit(X2[:,0], X2[:,1])

reg2 = neighbors.KNeighborsRegressor(n_neighbors = 10, p = 2, weights='distance')
reg2.fit(X2[:,0], X2[:,1])

(300, 2)
KNeighborsRegressor(algorithm='auto', leaf_size=30, metric='minkowski',
                    metric_params=None, n_jobs=None, n_neighbors=10, p=2,
                    weights='distance')

x_new = np.array([[15]])
pred1 = reg1.predict(x_new)[0,0]
pred2 = reg2.predict(x_new)[0,0]
print(pred1)
print(pred2)

10.569216249306415
15.897201399708559
```

Similar to the actual experimental results, k -NN regression was applied after differences in the number of peripheral data (n_{neighbor}) considered for a particular set of results biased data.

```
x1p = np.linspace(-10, 30, 50).reshape(-1,1)
y1p = reg1.predict(x1p)

x2p = np.linspace(-10, 30, 50).reshape(-1,1)
y2p = reg2.predict(x2p)

fig, axes = plt.subplots(ncols=2, figsize=(20, 8), sharey=False)

plt.sca(axes[0])
plt.title('k-Nearest Neighbor Regression (n_neighbors = 2)', fontsize = 15)
plt.plot(X2[:,0], X2[:,1], '.', label = 'Data')
plt.plot(x1p, y1p, label = 'kNN')
plt.plot(x_new, pred1, 'o', label = 'Prediction')
plt.plot([x_new[0,0], x_new[0,0]], [-30, pred1], 'k--', alpha=0.5)
plt.plot([-30, x_new[0,0]], [pred1, pred1], 'k--', alpha=0.5)
plt.xlabel('X', fontsize=15)
plt.ylabel('Y', fontsize=15)
plt.legend(fontsize=12)
plt.axis([-5,25,-5,25])

plt.sca(axes[1])
plt.title('k-Nearest Neighbor Regression (n_neighbors = 10)', fontsize = 15)
plt.plot(X2[:,0], X2[:,1], '.', label = 'Data')
plt.plot(x2p, y2p, label = 'kNN')
plt.plot(x_new, pred2, 'o', label = 'Prediction')
plt.plot([x_new[0,0], x_new[0,0]], [-30, pred2], 'k--', alpha=0.5)
plt.plot([-30, x_new[0,0]], [pred2, pred2], 'k--', alpha=0.5)
plt.xlabel('X', fontsize=15)
plt.ylabel('Y', fontsize=15)
plt.legend(fontsize=12)
plt.axis([-5, 25, -5, 25])

plt.show()
```

Appendix. A-3 Decision tree regression of sample dataset, python codes

```

np.random.seed(42)
m = 100
X = np.random.rand(m, 1)
y = -0.5 * (X-1) ** 3 + X ** 2 - 1 * X + 3
y = y + np.random.randn(m, 1) / 10

tree_reg1 = DecisionTreeRegressor(random_state=42, max_depth=2)
tree_reg2 = DecisionTreeRegressor(random_state=42, max_depth=3)
tree_reg3 = DecisionTreeRegressor(random_state=42, max_depth=4)
tree_reg1.fit(X, y)
tree_reg2.fit(X, y)
tree_reg3.fit(X, y)

def plot_regression_predictions(tree_reg, X, y, axes=[-0.1, 1.1, 2.5, 3.5], ylabel="$y$"):
    x1 = np.linspace(axes[0], axes[1], 150).reshape(-1, 1)
    y_pred = tree_reg.predict(x1)
    plt.axis(axes)
    plt.xlabel("$x_1$", fontsize=18)
    if ylabel:
        plt.ylabel(ylabel, fontsize=18, rotation=0)
    plt.plot(X, y, "b.")
    plt.plot(x1, y_pred, "r.-", label=r"$\hat{y}$")

fig, axes = plt.subplots(ncols=3, figsize=(18, 6), sharey=True)
plt.sca(axes[0])
plot_regression_predictions(tree_reg1, X, y)
for split, style in ((0.197, "k-"), (0.112, "k--"), (0.328, "k--")):
    plt.plot([split, split], [2.5, 3.5], style, linewidth=2)
plt.legend(loc="best", fontsize=18)
plt.title("max_depth=2", fontsize=14)

plt.sca(axes[1])
plot_regression_predictions(tree_reg2, X, y, ylabel=None)
for split, style in ((0.197, "k-"), (0.112, "k--"), (0.328, "k--")):
    plt.plot([split, split], [2.5, 3.5], style, linewidth=2)
for split in (0.04, 0.14, 0.265, 0.812):
    plt.plot([split, split], [2.5, 3.5], "k:", linewidth=1)
plt.legend(loc="best", fontsize=18)
plt.title("max_depth=3", fontsize=14)

plt.sca(axes[2])
plot_regression_predictions(tree_reg3, X, y, ylabel=None)
for split, style in ((0.197, "k-"), (0.112, "k--"), (0.328, "k--")):
    plt.plot([split, split], [2.5, 3.5], style, linewidth=2)
for split in (0.04, 0.14, 0.265, 0.812):
    plt.plot([split, split], [2.5, 3.5], "k:", linewidth=1)
for split in (0.023, 0.064, 0.118, 0.148, 0.199, 0.311, 0.448, 0.97):
    plt.plot([split, split], [2.5, 3.5], "k:", linewidth=1)
plt.legend(loc="best", fontsize=18)
plt.title("max_depth=4", fontsize=14)

plt.show()

```

```
from graphviz import Source
from sklearn.tree import export_graphviz
import os
PROJECT_ROOT_DIR = "."
CHAPTER_ID = "decision_trees"
IMAGES_PATH = os.path.join(PROJECT_ROOT_DIR, "images", CHAPTER_ID)
os.makedirs(IMAGES_PATH, exist_ok=True)

export_graphviz(
    tree_reg3,
    out_file=os.path.join(IMAGES_PATH, "regression_tree.dot"),
    feature_names=["x1"],
    rounded=True,
    filled=True
)

Source.from_file(os.path.join(IMAGES_PATH, "regression_tree.dot"))
```

Appendix. A-4 Python codes written for regression by experimental group in O3-UHPC.

[Importing Data: importing openpyxl]

```
%matplotlib inline
import matplotlib as mpl
import matplotlib.pyplot as plt

import numpy as np

from openpyxl import workbook
import re
import sys

def cleanText(readData):
    p = re.compile("[^0-9]")
    return"".join(p.findall(readData))

def Excel():
    wb1 = load_workbook('CS Data (Ozone Day 1).xlsx')

    ws1 = wb1.active
    chk = "0123456789"
    pre = ws1.rows

    for r in ws1.rows:
        ty = r[0].value
        data=r[1].value

def Excel():
    wb2 = load_workbook('CS Data (Ozone Day 28).xlsx')

    ws2 = wb2.active
    chk = "0123456789"
    pre = ws2.rows

    for r in ws2.rows:
        ty = r[0].value
        data=r[1].value

def Excel():
    wb3 = load_workbook('CS Data (Ozone Steam Curing).xlsx')

    ws3 = wb3.active
    chk = "0123456789"
    pre = ws3.rows

    for r in ws3.rows:
        ty = r[0].value
        data=r[1].value

X1=np.asmatrix(X1)
X2=np.asmatrix(X2)
X3=np.asmatrix(X3)
```

```

plt.figure(figsize=(10,8))
plt.title("03-UHPC compressive strength test data (n=153)", fontsize=18)
plt.plot(X1[:,0], X1[:,1], 'ro', label='Day 1')
plt.plot(X2[:,0], X2[:,1], 'bo', label='Day 28')
plt.plot(X3[:,0], X3[:,1], 'go', label='Steam Curing')
plt.xlabel('Ozone Concentration (g/ml)',fontsize=15)
plt.ylabel('Compressive Strength (MPa)',fontsize=15)
plt.legend(loc='lower center',fontsize=12)
plt.axis([-0.05,1.35,38,156])
plt.show()

```

[Polynomial regression python codes]

```

from sklearn.preprocessing import PolynomialFeatures
poly_features = PolynomialFeatures(degree=1, include_bias=False)
X_poly = poly_features.fit_transform(X1[:,0])

from sklearn.linear_model import LinearRegression
lin_reg = LinearRegression()
lin_reg.fit(X_poly, X1[:,1])

X_new=np.linspace(-3, 3, 200).reshape(-1, 1)
X_new_poly = poly_features.transform(X_new)
y_new = lin_reg.predict(X_new_poly)

from sklearn.preprocessing import StandardScaler
from sklearn.pipeline import Pipeline

for style, width, degree in (("g", 1, 1), ("b", 1, 2), ("r", 1, 3), ("y", 1, 4)):
    polybig_features = PolynomialFeatures(degree=degree, include_bias=False)
    std_scaler = StandardScaler()
    lin_reg = LinearRegression()
    polynomial_regression = Pipeline([
        ("poly_features", polybig_features),
        ("std_scaler", std_scaler),
        ("lin_reg", lin_reg),
    ])
    polynomial_regression.fit(X1[:,0], X1[:,1])
    y_newbig = polynomial_regression.predict(X_new)
    plt.plot(X_new, y_newbig, style, label=str(degree), linewidth=width)

plt.title("Polynomial Regression: Day 1", fontsize=15)
plt.plot(X1[:,0], X1[:,1], ".", linewidth=3, label='Data')
plt.legend(loc="upper left", fontsize=7)
plt.xlabel("Ozone Concentration (g/ml)", fontsize=12)
plt.ylabel("Compressive Strength (MPa)", rotation=90, fontsize=12)
plt.axis([-0.25,1.5,38,56])
plt.show()

```

Appendix

```
from sklearn.preprocessing import PolynomialFeatures
poly_features1 = PolynomialFeatures(degree=1, include_bias=False)
X_poly1 = poly_features1.fit_transform(X1[:,0])
poly_features2 = PolynomialFeatures(degree=2, include_bias=False)
X_poly2 = poly_features2.fit_transform(X1[:,0])
poly_features3 = PolynomialFeatures(degree=3, include_bias=False)
X_poly3 = poly_features3.fit_transform(X1[:,0])
poly_features4 = PolynomialFeatures(degree=4, include_bias=False)
X_poly4 = poly_features4.fit_transform(X1[:,0])

lin_reg1 = LinearRegression()
lin_reg1.fit(X_poly1, X1[:,1])
lin_reg2 = LinearRegression()
lin_reg2.fit(X_poly2, X1[:,1])
lin_reg3 = LinearRegression()
lin_reg3.fit(X_poly3, X1[:,1])
lin_reg4 = LinearRegression()
lin_reg4.fit(X_poly4, X1[:,1])

print(lin_reg1.intercept_, lin_reg1.coef_)
print(lin_reg2.intercept_, lin_reg2.coef_)
print(lin_reg3.intercept_, lin_reg3.coef_)
print(lin_reg4.intercept_, lin_reg4.coef_)

[45.75244007] [[2.69721212]]
[45.59866305] [[ 6.21739904 -2.79693641]]
[43.97920286] [[ 55.21305142 -93.46043372  41.75514583]]
[43.80758261] [[ 74.84189902 -325.02957084  405.62572892 -151.75224746]]
```

Equation of linear Regression : $\hat{y} = 2.70x + 45.75$

Equation of 2nd order polynomial Regression : $\hat{y} = -2.80x^2 + 6.22x + 45.6$

Equation of 3rd order polynomial Regression :

$$\hat{y} = 41.76x^3 - 93.46x^2 + 55.21x + 43.98$$

Equation of 4th order polynomial Regression :

$$\hat{y} = -151.75x^4 + 405.63x^3 - 325.03x^2 + 74.84x + 43.81$$

Starting with more than three-order polynomial regression models, it can be over-fitting by certain experimental data Except for overfit model, regression models for intervals (0.2 to 1 g/ml) without experimental data tend to increase.

```

%matplotlib inline
import matplotlib as mpl
import matplotlib.pyplot as plt

import numpy as np
import numpy.random as rnd

from sklearn.preprocessing import PolynomialFeatures
poly_features = PolynomialFeatures(degree=1, include_bias=False)
X_poly = poly_features.fit_transform(X2[:,0])

from sklearn.linear_model import LinearRegression
lin_reg = LinearRegression()
lin_reg.fit(X_poly, X2[:,1])

X_new=np.linspace(-3, 3, 200).reshape(-1, 1)
X_new_poly = poly_features.transform(X_new)
y_new = lin_reg.predict(X_new_poly)

from sklearn.preprocessing import StandardScaler
from sklearn.pipeline import Pipeline

for style, width, degree in (("g", 1, 1), ("b", 1, 2), ("r", 1, 3), ("y", 1, 4)):
    polybig_features = PolynomialFeatures(degree=degree, include_bias=False)
    std_scaler = StandardScaler()
    lin_reg = LinearRegression()
    polynomial_regression = Pipeline([
        ("poly_features", polybig_features),
        ("std_scaler", std_scaler),
        ("lin_reg", lin_reg),
    ])
    polynomial_regression.fit(X2[:,0], X2[:,1])
    y_newbig = polynomial_regression.predict(X_new)
    plt.plot(X_new, y_newbig, style, label=str(degree), linewidth=width)

plt.title("Polynomial Regression: Day 28", fontsize=15)
plt.plot(X2[:,0], X2[:,1], ".", linewidth=3, label='Data')
plt.legend(loc="lower center", fontsize=7)
plt.xlabel("Ozone Concentration (g/ml)", fontsize=12)
plt.ylabel("Compressive Strength (MPa)", rotation=90, fontsize=12)
plt.axis([-0.25,1.5,90,130])
plt.show()

```

Appendix

```
from sklearn.preprocessing import PolynomialFeatures
poly_features1 = PolynomialFeatures(degree=1, include_bias=False)
X_poly1 = poly_features1.fit_transform(X2[:,0])
poly_features2 = PolynomialFeatures(degree=2, include_bias=False)
X_poly2 = poly_features2.fit_transform(X2[:,0])
poly_features3 = PolynomialFeatures(degree=3, include_bias=False)
X_poly3 = poly_features3.fit_transform(X2[:,0])
poly_features4 = PolynomialFeatures(degree=4, include_bias=False)
X_poly4 = poly_features4.fit_transform(X2[:,0])

lin_reg1 = LinearRegression()
lin_reg1.fit(X_poly1, X2[:,1])
lin_reg2 = LinearRegression()
lin_reg2.fit(X_poly2, X2[:,1])
lin_reg3 = LinearRegression()
lin_reg3.fit(X_poly3, X2[:,1])
lin_reg4 = LinearRegression()
lin_reg4.fit(X_poly4, X2[:,1])

print(lin_reg1.intercept_, lin_reg1.coef_)
print(lin_reg2.intercept_, lin_reg2.coef_)
print(lin_reg3.intercept_, lin_reg3.coef_)
print(lin_reg4.intercept_, lin_reg4.coef_)

[108.48738673] [[-3.34776855]]
[108.62202241] [[-6.42978143  2.44878874]]
[108.396471] [[ 0.39412113 -10.17843106  5.81547612]]
[109.6446952] [[ -142.36992953  1674.06451083 -2640.6790825  1103.72070685]]
```

Equation of linear Regression : $\hat{y} = -3.35x + 108.49$

Equation of 2nd order polynomial Regression : $\hat{y} = 2.45x^2 - 6.43x + 108.62$

Equation of 3rd order polynomial Regression :

$$\hat{y} = 5.82x^3 - 10.18x^2 + 0.39x + 108.4$$

Equation of 4th order polynomial Regression :

$$\hat{y} = 1103.72x^4 - 2640.68x^3 + 1674.06x^2 - 142.37x + 109.64$$

Starting with more than fourth-order polynomial regression models, it can be over-fitting by certain experimental data Except for overfit model, regression models for intervals (0.2 to 1 g/ml) without experimental data tend to decrease.

```
%matplotlib inline
import matplotlib as mpl
import matplotlib.pyplot as plt

import numpy as np
import numpy.random as rnd

from sklearn.preprocessing import PolynomialFeatures
poly_features = PolynomialFeatures(degree=1, include_bias=False)
X_poly = poly_features.fit_transform(X3[:,0])

from sklearn.linear_model import LinearRegression
lin_reg = LinearRegression()
lin_reg.fit(X_poly, X3[:,1])

X_new=np.linspace(-3, 3, 200).reshape(-1, 1)
X_new_poly = poly_features.transform(X_new)
y_new = lin_reg.predict(X_new_poly)

from sklearn.preprocessing import StandardScaler
from sklearn.pipeline import Pipeline

for style, width, degree in (("g", 1, 1), ("b", 1, 2), ("r", 1, 3), ("y", 1, 4)):
    polybig_features = PolynomialFeatures(degree=degree, include_bias=False)
    std_scaler = StandardScaler()
    lin_reg = LinearRegression()
    polynomial_regression = Pipeline([
        ("poly_features", polybig_features),
        ("std_scaler", std_scaler),
        ("lin_reg", lin_reg),
    ])
    polynomial_regression.fit(X3[:,0], X3[:,1])
    y_newbig = polynomial_regression.predict(X_new)
    plt.plot(X_new, y_newbig, style, label=str(degree), linewidth=width)

plt.title("Polynomial Regression: Steam Curing", fontsize=15)
plt.plot(X3[:,0], X3[:,1], ".", linewidth=3, label='Data')
plt.legend(loc="lower center", fontsize=7)
plt.xlabel("Ozone Concentration (g/ml)", fontsize=12)
plt.ylabel("Compressive Strength (MPa)", rotation=90, fontsize=12)
plt.axis([-0.25,1.5,105,155])
plt.show()
```

Appendix

```
from sklearn.preprocessing import PolynomialFeatures
poly_features1 = PolynomialFeatures(degree=1, include_bias=False)
X_poly1 = poly_features1.fit_transform(X3[:,0])
poly_features2 = PolynomialFeatures(degree=2, include_bias=False)
X_poly2 = poly_features2.fit_transform(X3[:,0])
poly_features3 = PolynomialFeatures(degree=3, include_bias=False)
X_poly3 = poly_features3.fit_transform(X3[:,0])
poly_features4 = PolynomialFeatures(degree=4, include_bias=False)
X_poly4 = poly_features4.fit_transform(X3[:,0])

lin_reg1 = LinearRegression()
lin_reg1.fit(X_poly1, X3[:,1])
lin_reg2 = LinearRegression()
lin_reg2.fit(X_poly2, X3[:,1])
lin_reg3 = LinearRegression()
lin_reg3.fit(X_poly3, X3[:,1])
lin_reg4 = LinearRegression()
lin_reg4.fit(X_poly4, X3[:,1])

print(lin_reg1.intercept_, lin_reg1.coef_)
print(lin_reg2.intercept_, lin_reg2.coef_)
print(lin_reg3.intercept_, lin_reg3.coef_)
print(lin_reg4.intercept_, lin_reg4.coef_)

[130.41693294] [[5.09640481]]
[130.44788585] [[4.38984625 0.56297954]]
[127.39336804] [[ 96.80217844 -170.44046306  78.75577156]]
[128.54084994] [[ -34.43959958 1377.86975431 -2354.14417621 1014.64106219]]
```

Equation of linear Regression : $\hat{y} = 5.1x + 130.42$

Equation of 2nd order polynomial Regression : $\hat{y} = 0.56x^2 - 4.39x + 130.45$

Equation of 3rd order polynomial Regression :

$$\hat{y} = 78.76x^3 - 170.44x^2 + 96.8x + 127.39$$

Equation of 4th order polynomial Regression :

$$\hat{y} = 1014.64x^4 - 2354.14x^3 + 1377.87x^2 - 34.44x + 128.54$$

Starting with more than third-order polynomial regression models, it can be over-fitting by certain experimental data Except for overfit model, regression models for intervals (0.2 to 1 g/ml) without experimental data tend to increase.

[*k*-NN regression python codes]

```

from sklearn import neighbors

X1=np.asmatrix(X1)

reg = neighbors.KNeighborsRegressor(n_neighbors = 10, p = 2, weights = 'distance')
reg.fit(X1[:,0], X1[:,1])

KNeighborsRegressor(algorithm='auto', leaf_size=30, metric='minkowski',
                    metric_params=None, n_jobs=None, n_neighbors=10, p=2,
                    weights='distance')

x_new1 = np.array([[0.4]])
pred1 = reg.predict(x_new1)[0,0]

x_new2 = np.array([[0.6]])
pred2 = reg.predict(x_new2)[0,0]

x_new3 = np.array([[0.8]])
pred3 = reg.predict(x_new3)[0,0]

xp = np.linspace(0, 1.3, 200).reshape(-1,1)
yp = reg.predict(xp)

plt.figure(figsize=(10,8))
plt.title('k-Nearest Neighbor Regression: Day 1', fontsize = 15)
plt.plot(X1[:,0], X1[:,1], '.', label = 'Data')
plt.plot(xp, yp, label = 'kNN')

plt.plot(x_new1, pred1, 'o', label = 'Prediction (0.4 g/ml)')
plt.plot([x_new1[0,0], x_new1[0,0]], [39, pred1], 'k--', alpha=0.5)
plt.plot([-0.05, x_new1[0,0]], [pred1, pred1], 'k--', alpha=0.5)

plt.plot(x_new2, pred2, 'o', label = 'Prediction (0.6 g/ml)')
plt.plot([x_new2[0,0], x_new2[0,0]], [39, pred2], 'k--', alpha=0.5)
plt.plot([-0.05, x_new2[0,0]], [pred2, pred2], 'k--', alpha=0.5)

plt.plot(x_new3, pred3, 'o', label = 'Prediction (0.8 g/ml)')
plt.plot([x_new3[0,0], x_new3[0,0]], [39, pred3], 'k--', alpha=0.5)
plt.plot([-0.05, x_new3[0,0]], [pred3, pred3], 'k--', alpha=0.5)

print("Prediction (0.4 g/ml) = {} MPa".format(round(pred1,2)))
print("Prediction (0.6 g/ml) = {} MPa".format(round(pred2,2)))
print("Prediction (0.8 g/ml) = {} MPa".format(round(pred3,2)))
plt.xlabel('Ozone Concentration (g/ml)', fontsize=15)
plt.ylabel('Compressive Strength (MPa)', fontsize=15)
plt.legend(fontsize=12)
plt.axis([-0.05, 1.35, 39, 55])
plt.show()

```

Appendix

```
from sklearn import neighbors

X2=np.asmatrix(X2)

reg = neighbors.KNeighborsRegressor(n_neighbors = 10, p = 2, weights = 'distance')
reg.fit(X2[:,0], X2[:,1])

KNeighborsRegressor(algorithm='auto', leaf_size=30, metric='minkowski',
                    metric_params=None, n_jobs=None, n_neighbors=10, p=2,
                    weights='distance')

x_new1 = np.array([[0.4]])
pred1 = reg.predict(x_new1)[0,0]

x_new2 = np.array([[0.6]])
pred2 = reg.predict(x_new2)[0,0]

x_new3 = np.array([[0.8]])
pred3 = reg.predict(x_new3)[0,0]

xp = np.linspace(0, 1.3, 200).reshape(-1,1)
yp = reg.predict(xp)

plt.figure(figsize=(10,8))
plt.title('k-Nearest Neighbor Regression: Day 28', fontsize = 15)
plt.plot(X2[:,0], X2[:,1], '.', label = 'Data')
plt.plot(xp, yp, label = 'kNN')

plt.plot(x_new1, pred1, 'o', label = 'Prediction (0.4 g/ml)')
plt.plot([x_new1[0,0], x_new1[0,0]], [90, pred1], 'k--', alpha=0.5)
plt.plot([-0.05, x_new1[0,0]], [pred1, pred1], 'k--', alpha=0.5)

plt.plot(x_new2, pred2, 'o', label = 'Prediction (0.6 g/ml)')
plt.plot([x_new2[0,0], x_new2[0,0]], [90, pred2], 'k--', alpha=0.5)
plt.plot([-0.05, x_new2[0,0]], [pred2, pred2], 'k--', alpha=0.5)

plt.plot(x_new3, pred3, 'o', label = 'Prediction (0.8 g/ml)')
plt.plot([x_new3[0,0], x_new3[0,0]], [90, pred3], 'k--', alpha=0.5)
plt.plot([-0.05, x_new3[0,0]], [pred3, pred3], 'k--', alpha=0.5)

print("Prediction (0.4 g/ml) = {} MPa".format(round(pred1,2)))
print("Prediction (0.6 g/ml) = {} MPa".format(round(pred2,2)))
print("Prediction (0.8 g/ml) = {} MPa".format(round(pred3,2)))
plt.xlabel('Ozone Concentration (g/ml)', fontsize=15)
plt.ylabel('Compressive Strength (MPa)', fontsize=15)
plt.legend(fontsize=12)
plt.axis([-0.05, 1.35, 90, 130])
plt.show()
```

```

from sklearn import neighbors

X3=np.asmatrix(X3)

reg = neighbors.KNeighborsRegressor(n_neighbors = 10, p = 2, weights = 'distance')
reg.fit(X3[:,0], X3[:,1])

KNeighborsRegressor(algorithm='auto', leaf_size=30, metric='minkowski',
                    metric_params=None, n_jobs=None, n_neighbors=10, p=2,
                    weights='distance')

x_new1 = np.array([[0.4]])
pred1 = reg.predict(x_new1)[0,0]

x_new2 = np.array([[0.6]])
pred2 = reg.predict(x_new2)[0,0]

x_new3 = np.array([[0.8]])
pred3 = reg.predict(x_new3)[0,0]

xp = np.linspace(0, 1.3, 200).reshape(-1,1)
yp = reg.predict(xp)

plt.figure(figsize=(10,8))
plt.title('k-Nearest Neighbor Regression: Steam Curing', fontsize = 15)
plt.plot(X3[:,0], X3[:,1], '.', label = 'Data')
plt.plot(xp, yp, label = 'kNN')

plt.plot(x_new1, pred1, 'o', label = 'Prediction (0.4 g/ml)')
plt.plot([x_new1[0,0], x_new1[0,0]], [90, pred1], 'k--', alpha=0.5)
plt.plot([-0.05, x_new1[0,0]], [pred1, pred1], 'k--', alpha=0.5)

plt.plot(x_new2, pred2, 'o', label = 'Prediction (0.6 g/ml)')
plt.plot([x_new2[0,0], x_new2[0,0]], [90, pred2], 'k--', alpha=0.5)
plt.plot([-0.05, x_new2[0,0]], [pred2, pred2], 'k--', alpha=0.5)

plt.plot(x_new3, pred3, 'o', label = 'Prediction (0.8 g/ml)')
plt.plot([x_new3[0,0], x_new3[0,0]], [90, pred3], 'k--', alpha=0.5)
plt.plot([-0.05, x_new3[0,0]], [pred3, pred3], 'k--', alpha=0.5)

print("Prediction (0.4 g/ml) = {} MPa".format(round(pred1,2)))
print("Prediction (0.6 g/ml) = {} MPa".format(round(pred2,2)))
print("Prediction (0.8 g/ml) = {} MPa".format(round(pred3,2)))
plt.xlabel('Ozone Concentration (g/ml)', fontsize=15)
plt.ylabel('Compressive Strength (MPa)', fontsize=15)
plt.legend(fontsize=12)
plt.axis([-0.05,1.35,105,155])
plt.show()

```

Appendix

[Decision tree method python codes]

```
from sklearn.tree import DecisionTreeRegressor

tree_reg1 = DecisionTreeRegressor(max_depth=2)
tree_reg2 = DecisionTreeRegressor(max_depth=3)
tree_reg3 = DecisionTreeRegressor(max_depth=4)
tree_reg1.fit(X1[:,0], X1[:,1])
tree_reg2.fit(X1[:,0], X1[:,1])
tree_reg3.fit(X1[:,0], X1[:,1])

DecisionTreeRegressor(ccp_alpha=0.0, criterion='mse', max_depth=4,
                      max_features=None, max_leaf_nodes=None,
                      min_impurity_decrease=0.0, min_impurity_split=None,
                      min_samples_leaf=1, min_samples_split=2,
                      min_weight_fraction_leaf=0.0, presort='deprecated',
                      random_state=None, splitter='best')

def plot_regression_predictions(tree_reg, X, y, axes=[-0.05, 1.35, 38, 56], ylabel="Compressive Strength (MPa)":
    x1 = np.linspace(axes[0], axes[1], 500).reshape(-1, 1)
    y_pred = tree_reg.predict(x1)
    plt.axis(axes)
    plt.xlabel("Ozone (g/ml)", fontsize=15)
    if ylabel:
        plt.ylabel(ylabel, fontsize=15, rotation=90)
    plt.plot(X1[:,0], X1[:,1], "b.")
    plt.plot(x1, y_pred, "r.-", label=r"Decision Boundary",)

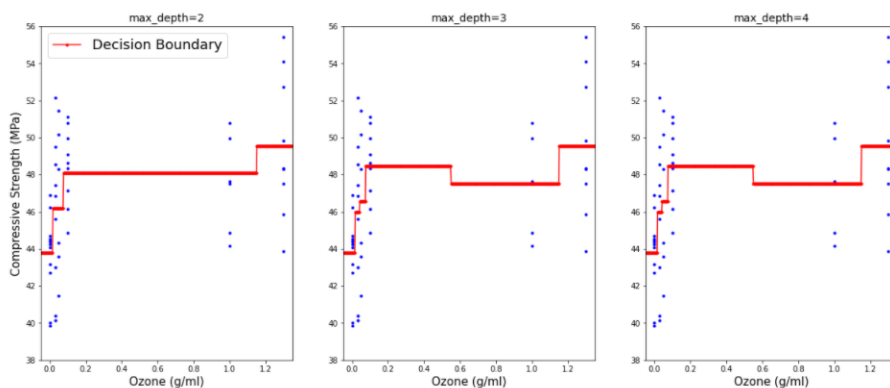
fig, axes = plt.subplots(ncols=3, figsize=(20, 8), sharey=False)
plt.sca(axes[0])
plot_regression_predictions(tree_reg1, X1[:,0], X1[:,1])
plt.legend(loc="best", fontsize=18)
plt.title("max_depth=2", fontsize=14)

plt.sca(axes[1])
plot_regression_predictions(tree_reg2, X1[:,0], X1[:,1], ylabel=None)
plt.title("max_depth=3", fontsize=14)

plt.sca(axes[2])
plot_regression_predictions(tree_reg3, X1[:,0], X1[:,1], ylabel=None)
plt.title("max_depth=4", fontsize=14)

plt.show()
```

Results of applying the decision tree diagram to scattered data



The above graph shows that the classification of the data has been completed at a decision tree's depth of three.

```

from sklearn.tree import DecisionTreeRegressor

tree_reg1 = DecisionTreeRegressor(max_depth=2)
tree_reg2 = DecisionTreeRegressor(max_depth=3)
tree_reg3 = DecisionTreeRegressor(max_depth=4)
tree_reg1.fit(X2[:,0], X2[:,1])
tree_reg2.fit(X2[:,0], X2[:,1])
tree_reg3.fit(X2[:,0], X2[:,1])

DecisionTreeRegressor(ccp_alpha=0.0, criterion='mse', max_depth=4,
                      max_features=None, max_leaf_nodes=None,
                      min_impurity_decrease=0.0, min_impurity_split=None,
                      min_samples_leaf=1, min_samples_split=2,
                      min_weight_fraction_leaf=0.0, presort='deprecated',
                      random_state=None, splitter='best')

def plot_regression_predictions(tree_reg, X, y, axes=[-0.05, 1.35, 90, 130], ylabel="Compressive Strength (MPa)":
    x2 = np.linspace(axes[0], axes[1], 500).reshape(-1, 1)
    y_pred = tree_reg.predict(x2)
    plt.axis(axes)
    plt.xlabel("Ozone (g/ml)", fontsize=15)
    if ylabel:
        plt.ylabel(ylabel, fontsize=15, rotation=90)
    plt.plot(X2[:,0], X2[:,1], "b.")
    plt.plot(x2, y_pred, "r.-", label="Decision Boundary",)

fig, axes = plt.subplots(ncols=3, figsize=(20, 8), sharey=False)
plt.sca(axes[0])
plot_regression_predictions(tree_reg1, X2[:,0], X2[:,1])
plt.legend(loc="best", fontsize=18)
plt.title("max_depth=2", fontsize=14)

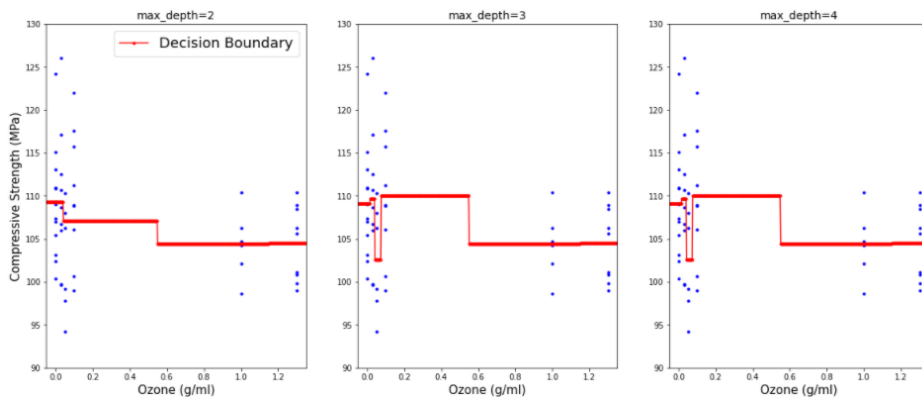
plt.sca(axes[1])
plot_regression_predictions(tree_reg2, X2[:,0], X2[:,1], ylabel=None)
plt.title("max_depth=3", fontsize=14)

plt.sca(axes[2])
plot_regression_predictions(tree_reg3, X2[:,0], X2[:,1], ylabel=None)
plt.title("max_depth=4", fontsize=14)

plt.show()

```

Results of applying the decision tree diagram to scattered data



The above graph shows that the classification of the data has been completed at a decision tree's depth of three.

Appendix

```
from sklearn.tree import DecisionTreeRegressor

tree_reg1 = DecisionTreeRegressor(max_depth=2)
tree_reg2 = DecisionTreeRegressor(max_depth=3)
tree_reg3 = DecisionTreeRegressor(max_depth=4)
tree_reg1.fit(X3[:,0], X3[:,1])
tree_reg2.fit(X3[:,0], X3[:,1])
tree_reg3.fit(X3[:,0], X3[:,1])

DecisionTreeRegressor(ccp_alpha=0.0, criterion='mse', max_depth=4,
                      max_features=None, max_leaf_nodes=None,
                      min_impurity_decrease=0.0, min_impurity_split=None,
                      min_samples_leaf=1, min_samples_split=2,
                      min_weight_fraction_leaf=0.0, presort='deprecated',
                      random_state=None, splitter='best')

def plot_regression_predictions(tree_reg, X, y, axes=[-0.05,1.35,105,155], ylabel="Compressive Strength (MPa)":
    x3 = np.linspace(axes[0], axes[1], 500).reshape(-1, 1)
    y_pred = tree_reg.predict(x3)
    plt.axis(axes)
    plt.xlabel("Ozone (g/ml)", fontsize=15)
    if ylabel:
        plt.ylabel(ylabel, fontsize=15, rotation=90)
    plt.plot(X3[:,0], X3[:,1], "b.")
    plt.plot(x3, y_pred, "r.-", label=r"Decision Boundary",)

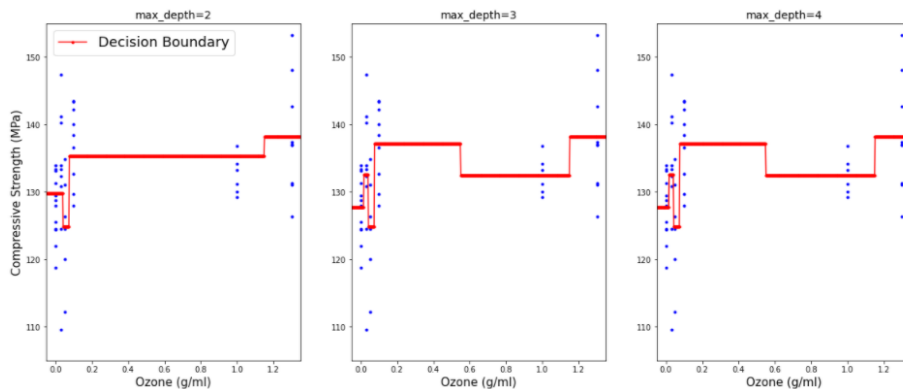
fig, axes = plt.subplots(ncols=3, figsize=(20, 8), sharey=False)
plt.sca(axes[0])
plot_regression_predictions(tree_reg1, X3[:,0], X3[:,1])
plt.legend(loc="best", fontsize=18)
plt.title("max_depth=2", fontsize=14)

plt.sca(axes[1])
plot_regression_predictions(tree_reg2, X3[:,0], X3[:,1], ylabel=None)
plt.title("max_depth=3", fontsize=14)

plt.sca(axes[2])
plot_regression_predictions(tree_reg3, X3[:,0], X3[:,1], ylabel=None)
plt.title("max_depth=4", fontsize=14)

plt.show()
```

Results of applying the decision tree diagram to scattered data



The above graph shows that the classification of the data has been completed at a decision tree's depth of three.

[Python code of decision tree diagram]

```

from graphviz import Source
from sklearn.tree import export_graphviz
import os
PROJECT_ROOT_DIR = "."
CHAPTER_ID = "decision_trees"
IMAGES_PATH = os.path.join(PROJECT_ROOT_DIR, "images", CHAPTER_ID)
os.makedirs(IMAGES_PATH, exist_ok=True)

export_graphviz(
    tree_reg3,
    out_file=os.path.join(IMAGES_PATH, "regression_tree.dot"),
    feature_names=["Ozone Concentration"],
    rounded=True,
    filled=True
)

Source.from_file(os.path.join(IMAGES_PATH, "regression_tree.dot"))

```

Appendix. A-5 Python codes written for regression by experimental group in O3-CNT composite.

[Python code of Regression plane]

```

x1=np.array([0,0,0,0,1,0,1,0,1,0,23,0,23,0,23,1,1,1,0,0,0,0,1,0,1,0,1,0,23,0,23,0,23,0,0,0,0,1,0,1,0,1,0,23,0,23,0,23]).reshape(-1,1)
x2=np.array([0,0,0,0,0,0,0,0,0,0,0,0,0,1,0,1,0,1,0,1,0,1,0,1,0,1,0,1,0,1,0,1,0,2,0,2,0,2,0,2,0,2,0,2,0,2,0,2,0,2]).reshape(-1,1)

y1=np.array([42,72,43,16,44,08,40,16,45,6,43,43,56,44,32,48,28,48,28,55,4,47,52,43,84,40,96,40,92,38,96,36,76,37,4,41,4,39,86,40,
32,48,16,42,98,46,3,49,96,50,24,51,44,54,16,57,52,52,52]).reshape(-1,1)
y2=np.array([124,16,113,08,109,04,106,76,110,72,99,68,110,28,108,99,16,99,8,100,68,108,96,110,108,32,112,08,103,4,106,6,
108,12,107,12,110,32,108,68,121,36,108,96,117,92,111,12,115,6,
114,64,108,92,119,52,108,96]).reshape(-1,1)
y3=np.array([139,12,128,72,129,48,140,32,147,44,130,8,126,32,131,08,124,52,131,08,126,32,136,96,133,48,126,12,150,08,121,36,
140,24,133,48,138,04,134,84,137,04,164,04,169,84,161,96,163,32,156,12,161,8,169,84,170,88,167,04]).reshape(-1,1)

A=np.hstack([x1**0, x1, x2])
A=np.asmatrix(A)

theta1=(A.T*A).I+A.T*y1
theta2=(A.T*A).I+A.T*y2
theta3=(A.T*A).I+A.T*y3

X1,X2=np.meshgrid(np.arange(np.min(x1), np.max(x1), 0.001),
np.arange(np.min(x2), np.max(x2), 0.001))

YP1=theta1[0,0]+theta1[1,0]*X1+theta1[2,0]*X2
YP2=theta2[0,0]+theta2[1,0]*X1+theta2[2,0]*X2
YP3=theta3[0,0]+theta3[1,0]*X1+theta3[2,0]*X2
|
fig, axes = plt.subplots(nrows = 2, ncols=2, sharex=False, sharey=False)

plt.sca(axes[0,0])
fig=plt.figure(figsize=(10,8))
ax=fig.add_subplot(1,1,1,projection='3d')
ax.set_title('Regression Plane', fontsize=14)
ax.set_xlabel('Ozone (g/ml)', fontsize=12)
ax.set_ylabel('CNT Proportion (ppm)', fontsize=12)
ax.set_zlabel('Compressive Strength (MPa)', fontsize=12)
ax.scatter(x1, x2, y1, 'ro', label='Day 1')
ax.plot_wireframe(X1,X2,YP1,color='blue',alpha=0.3,label='Regression Plane (Day 1)')
plt.legend(loc="best", fontsize=10)

```

Appendix

```

plt.sca(axes[0,1])
fig=plt.figure(figsize=(10,8))
ax=fig.add_subplot(1,1,1,projection='3d')
ax.set_title('Regression Plane', fontsize=14)
ax.set_xlabel('Ozone (g/ml)', fontsize=12)
ax.set_ylabel('CNT Proportion (ppm)', fontsize=12)
ax.set_zlabel('Compressive Strength (MPa)', fontsize=12)
ax.scatter(x1, x2, y2, 'bo', label='Day 28')
ax.plot_wireframe(X1,X2,YP2,color='orange',alpha=0.3,label='Regression Plane (Day 28)')
plt.legend(loc="best", fontsize=10)

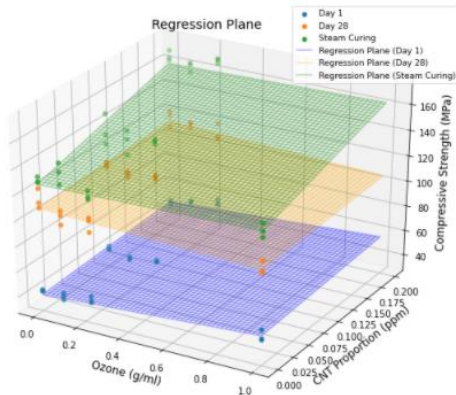
plt.sca(axes[1,0])
fig=plt.figure(figsize=(10,8))
ax=fig.add_subplot(1,1,1,projection='3d')
ax.set_title('Regression Plane', fontsize=14)
ax.set_xlabel('Ozone (g/ml)', fontsize=12)
ax.set_ylabel('CNT Proportion (ppm)', fontsize=12)
ax.set_zlabel('Compressive Strength (MPa)', fontsize=12)
ax.scatter(x1, x2, y3, 'go', label='Steam Curing')
ax.plot_wireframe(X1,X2,YP3,color='green',alpha=0.3,label='Regression Plane (Steam Curing)')
plt.legend(loc="best", fontsize=10)

plt.sca(axes[1,1])
fig=plt.figure(figsize=(10,8))
ax=fig.add_subplot(1,1,1,projection='3d')
ax.set_title('Regression Plane', fontsize=14)
ax.set_xlabel('Ozone (g/ml)', fontsize=12)
ax.set_ylabel('CNT Proportion (ppm)', fontsize=12)
ax.set_zlabel('Compressive Strength (MPa)', fontsize=12)
ax.scatter(x1, x2, y1, 'ro', label='Day 1')
ax.scatter(x1, x2, y2, 'bo', label='Day 28')
ax.scatter(x1, x2, y3, 'go', label='Steam Curing')
ax.plot_wireframe(X1,X2,YP1,color='blue',alpha=0.3,label='Regression Plane (Day 1)')
ax.plot_wireframe(X1,X2,YP2,color='orange',alpha=0.3,label='Regression Plane (Day 28)')
ax.plot_wireframe(X1,X2,YP3,color='green',alpha=0.3,label='Regression Plane (Steam Curing)')

#ax.view_init(0,0)

plt.legend(loc="best", fontsize=9)
plt.show()
print('theta1:\n',theta1)
print('theta2:\n',theta2)
print('theta3:\n',theta3)

```



```

theta1:
[[40.26597685]
 [10.48746883]
 [33.03352058]]
theta2:
[[109.06632963]
 [-7.10108617]
 [22.43096132]]
theta3:
[[127.48642408]
 [ 3.76106679]
 [162.45692922]]

```

[Python code of two regression planes from separated data]

```

%matplotlib inline
import matplotlib as mpl
import matplotlib.pyplot as plt

import numpy as np

x1=np.array([0,0,0,0,1,0,1,0,1,0,23,0,23,0,23,1,1,1,0,0,0,0,1,0,1,0,1,0,23,0,23,0,23,0,0,0,0,1,0,1,0,1,1,1]).reshape(-1,1) #x轴
x2=np.array([0,0,0,0,0,0,0,0,0,0,1,0,1,0,1,0,1,0,1,0,1,0,1,0,1,0,1,0,23,0,23,0,23,0,23,0,23,0,23,1,1,1]).reshape(-1,1) #x轴
x3=np.array([0,0,0,0,0,0,0,0,0,0,0,0,0,1,0,1,0,1,0,1,0,1,0,1,0,1,0,1,0,1,0,2,0,2,0,2,0,2,0,2,0,2,0,2,0,2]).reshape(-1,1) #y轴

y1=np.array([42.72,43.16,44.08,40.16,45.6,43,43,56,44,32,48,28,48,28,55,4,47,52,43,84,40,96,40,92,38,96,36,76,37,4,41,4,39,86,40,32,
48,16,42,98,46,3,49,96,50,24,51,44,54,16,57,52,52,52]).reshape(-1,1) #z轴
y2=np.array([44,36,46,88,44,24,44,08,40,03,46,24,39,86,44,69,44,54,48,36,51,12,50,8,38,96,36,76,37,4,44,08,41,82,43,84,41,4,39,86,
40,32,46,3,42,98,42,08,41,4,39,86,41,24,54,16,57,52,52,52]).reshape(-1,1) #z轴

A=np.hstack([x1+0, x1, x3])
A=np.asmatrix(A)

B=np.hstack([x2+0, x2, x3])
B=np.asmatrix(B)

theta1=(A.T*A).I+A.T*y1
theta2=(B.T*B).I+B.T*y2

X1,X2=np.meshgrid(np.arange(np.min(x1), np.max(x1), 0.001),
np.arange(np.min(x3), np.max(x3), 0.001))

X3,X4=np.meshgrid(np.arange(np.min(x2), np.max(x2), 0.001),
np.arange(np.min(x3), np.max(x3), 0.001))

YP1=theta1[0,0]+theta1[1,0]*X1+theta1[2,0]*X2
YP2=theta2[0,0]+theta2[1,0]*X3+theta2[2,0]*X4

fig=plt.figure(figsize=(10,8))
ax=fig.add_subplot(1,1,1,projection='3d')
ax.set_title('O3-CNT Regression Plane (Day 1)', fontsize=15)
ax.set_xlabel('Ozone Concentration (g/ml)', fontsize=12)
ax.set_ylabel('CNT Proportion (%)', fontsize=12)
ax.set_zlabel('Compressive Strength (MPa)', fontsize=12)
ax.scatter(x1, x3, y1, 'bo', label='Data1 (Day 1)')
ax.scatter(x2, x3, y2, 'bo', label='Data2 (Day 1)')
ax.plot_wireframe(X1,X3,YP1,color='blue',alpha=0.3,label='Regression Plane1 (Day 1)')
ax.plot_wireframe(X2,X3,YP2,color='red',alpha=0.3,label='Regression Plane2 (Day 1)')

#ax.view_init(0,0)

plt.legend(loc="best", fontsize=8.5)
plt.show()
print('theta1:\n',theta1)
print('theta2:\n',theta2)

```

Appendix. A-6 Calculation process of highest performance interval of O3-CNT composite (Experimental group: Day 28, Steam Curing)

1. Check positional relationship between two regression planes.

[Day 28]

$$(-7.1 \times 3.91) - (22.43 \times 14.98) + 1 = -363.9745 \neq 0$$

[Steam curing]

$$(3.76 \times -3.35) - (162.46 \times 151.7) + 1 = 24633.586 \neq 0$$

Dot product result of two normal vector is not zero, so the two planes in both experimental group have intersection.

Appendix

2. Find point of intersection assume $z = 0$.

[Day 28]

$$\begin{cases} -7.1x + 22.43y = -109.07 \\ 3.91x - 14.98y = -110.19 \end{cases}$$

$$\begin{bmatrix} x \\ y \end{bmatrix} = \begin{bmatrix} -7.1 & 22.43 \\ 3.91 & -14.98 \end{bmatrix}^{-1} \begin{bmatrix} -109.07 \\ -110.19 \end{bmatrix} = \begin{bmatrix} 219.48 \\ 64.78 \end{bmatrix}$$

$$\therefore (219.48, 64.78, 0)$$

[Steam curing]

$$\begin{cases} 3.76x + 162.46y = -127.49 \\ -3.35x + 151.7y = -129.53 \end{cases}$$

$$\begin{bmatrix} x \\ y \end{bmatrix} = \begin{bmatrix} 3.76 & 162.46 \\ -3.35 & 151.47 \end{bmatrix}^{-1} \begin{bmatrix} -127.49 \\ -129.53 \end{bmatrix} = \begin{bmatrix} 1.57 \\ -0.77 \end{bmatrix}$$

$$\therefore (1.57, -0.77, 0)$$

3. Obtain directional vector and parameter equation of intersection.

[Day 28]

$$\begin{aligned} \mathbf{u} &= (-7.1, 22.43, -1), \quad \mathbf{v} = (3.91, -14.98, -1) \\ \mathbf{u} \times \mathbf{v} &= \begin{vmatrix} 22.43 & -1 \\ -14.98 & -1 \end{vmatrix} \mathbf{i} - \begin{vmatrix} -7.1 & -1 \\ 3.91 & -1 \end{vmatrix} \mathbf{j} + \begin{vmatrix} -7.1 & 22.43 \\ 3.91 & -14.98 \end{vmatrix} \mathbf{k} \\ &= (-37.41, -11.01, 18.66) \end{aligned}$$

$$\begin{cases} x = -37.41t + 219.48 \\ y = -11.01t + 67.48 \\ z = 18.66t \end{cases}$$

[Steam curing]

$$\begin{aligned} \mathbf{u} &= (3.76, 162.46, -1), \quad \mathbf{v} = (-3.35, 151.7, -1) \\ \mathbf{u} \times \mathbf{v} &= \begin{vmatrix} 162.46 & -1 \\ 151.7 & -1 \end{vmatrix} \mathbf{i} - \begin{vmatrix} 3.76 & -1 \\ -3.35 & -1 \end{vmatrix} \mathbf{j} + \begin{vmatrix} 3.76 & 162.46 \\ -3.35 & 151.7 \end{vmatrix} \mathbf{k} \\ &= (-10.76, 7.11, 1114.63) \end{aligned}$$

$$\begin{cases} x = -10.76t + 1.57 \\ y = 7.11t - 0.77 \\ z = 1114.63t \end{cases}$$

4. Obtain intersection by applying the constraints set by ozone concentration and CNTs proportion variable. Then calculates the range of each variable due to the intersection.

[Day 28]

$$\begin{cases} 0 \leq -37.41t + 219.48 \leq 1.3 \\ 0 \leq -11.01t + 67.48 \leq 0.2 \end{cases}$$

$$\therefore 5.866 \leq t \leq 5.867$$

$$-0.004 \leq x \leq 0.033$$

$$0.188 \leq y \leq 0.195$$

$$109.46 \leq z \leq 109.47$$

[Steam curing]

$$\begin{cases} 0 \leq -10.76t + 1.57 \leq 1.3 \\ 0 \leq 7.11t - 0.77 \leq 0.2 \end{cases}$$

$$\therefore 0.108 \leq t \leq 0.136$$

$$0.108 \leq x \leq 0.408$$

$$-0.002 \leq y \leq 0.197$$

$$120.38 \leq z \leq 151.59$$

The calculations of the above two experimental groups show the properties of ozone water. When room temperature curing has been carried out in O3-CNT, it is difficult to identify changes in UHPC to high ozone concentrations due to vaporization over time after casting. That is, only 0.03 g/ml can affect strength of UHPC. On the other hand, in case of steam curing, strength enhancement by ozone water can be confirmed in a short period of time, which can be expressed up to 0.408 g/ml as calculated.

초 록

오존수는 자체적으로 화학 반응이 활발하며 탄소나노튜브 (CNTs)를 분산시키는 효과가 있다. 분산으로 인하여, CNT는 초고성능 콘크리트 (UHPC)의 자가 감지 능력을 추가로 부여할 수 있으며 동시에 기계적 특성도 개선할 수 있다. 본 논문은 이러한 성능 발현에 초점을 두어 오존수로 제작한 O3-UHPC와 CNT를 첨가하여 제작한 UHPC의 전반적인 재료 특성을 확립하는 것을 목표로 한다.

본 연구의 목적을 달성하기 위해 특수 제작된 오존수 생성기를 이용하여 특정 농도에서의 오존수로 제작한 O3-UHPC의 변화된 물리적, 화학적 재료 특성을 확인하였으며, 압축강도 실험 결과에 대해 기계 학습 기법을 적용하여 오존수의 농도에 따른 압축강도 추세를 분석하였다. 이러한 결과에 입각해 O3-UHPC의 성능 발현이 용이할 수 있도록 이상적인 오존수 농도 구간을 소개하였다.

압축강도 시험 결과, 오존수 농도가 0.55 g/ml 이상일 때, UHPC의 압축 강도의 변화가 없거나 충분히 발현되지 않음을 확인할 수 있으며, 0.03 g/ml 이하일 경우 유동성이 소폭 향상되지만 그 수치보다 더할 경우 유동성의 변화가 미비하였다. 또한 수화 반응 시험, XRD, TG 결과를 통해 몇 분 이상 경과한 O3-UHPC 시료는 오존수의 영향이 사라졌으며 일반 UHPC와 거의 동일한 화학 구조를 가지고 있음을 유추할 수 있다.

CNT의 경우, 일정 비율의 CNT를 혼입하여 제작한 각 복합재료의 기계적, 화학적 특성을 정리하였으며, 복합재료의 성능 발현 및 현장 시공성이 용이할 수 있도록 적합한 CNT 혼입률을 제안하였다.

UHPC에 CNT가 혼입되어 제작된 복합재료의 압축강도 실험 결과 기계 학습 (Machine Learning) 기법을 적용한 결과, CNT를 시멘트 중량 대비 0.1% 이상 혼합하였을 때 복합재료의 물리적 성능이 현저히 감소하였으며, 화학적 구성도 CNT가 일정 농도를 초과하여 혼합될 경우 시멘트성 재료의 특성이 발현되지 않음을 확인할 수 있다.

마지막으로, 오존수와 CNT가 UHPC에 미치는 긍정적인 효과를 동시에 발생시키기 위해 UHPC-CNT 복합재료 제작 시 오존수를 이용하였으며 오존수의 농도와 CNT 혼입률에 대한 변수의 차이를 두는 것으로 실험군을 추가로 설정하여 실험을 수행하였다.

오존수의 농도와 CNT 배합율을 변수로 설정하여 제작한 UHPC의 압축강도 결과를 3차원으로 매핑한 결과, 오존수의 농도가 0.4 g/ml, CNT 혼입률이 시멘트 중량 대비 약 0.2%로 조절한 후 증기 양생을 실시하였을 때, 복합재료의 압축 강도가 최대로 발생되었으며, 이는 강섬유를 혼입하여 제작한 일반 UHPC와 비슷한 강도를 발현하는 것을 확인할 수 있다.

이는 UHPC 복합 재료가 특정한 오존수의 농도와 CNT의 비율로 고온 증기 양생을 통해 생산될 경우 일반 UHPC보다 유사한 기계적 성능을 발현하면서 전자파 차폐 기능을 비롯한 다양한 추가 성능을 부여할 수 있음을 시사한다.

주요어 : 초고성능 콘크리트, 오존수, O₃-UHPC, 기계 학습, 탄소나노튜브, UHPC-CNT 복합재료

학 번 : 2019-22286